nagra.

Arbeitsbericht NAB 16-20

FEBEX-DP Post-mortem analysis: Sensors

May 2016

M. Rey, F-J. Sanz, J-L. García-Siñeriz

AITEMIN

National Cooperative
for the Disposal of
Radioactive Waste

Hardstrasse 73
P.O. Box 280
5430 Wettingen
Switzerland
Tel. +41 56 437 11 11

www.nagra.ch

nagra.

Arbeitsbericht NAB 16-20

FEBEX-DP Post-mortem analysis: Sensors

May 2016

M. Rey, F-J. Sanz, J-L. García-Siñeriz

AITEMIN

KEYWORDS

FEBEX, FEBEX-DP, postmortem sensor validation

National Cooperative
for the Disposal of
Radioactive Waste

Hardstrasse 73
P.O. Box 280
5430 Wettingen
Switzerland
Tel. +41 56 437 11 11

www.nagra.ch

Nagra Arbeitsberichte ("Working Reports") present the results of work in progress that have not necessarily been subject to a comprehensive review. They are intended to provide rapid dissemination of current information.
This report was prepared on behalf of Nagra. The viewpoints presented and conclusions reached are those of the author(s) and do not necessarily represent those of Nagra.

"Copyright © 2016 by Nagra, Wettingen (Switzerland) / All rights reserved.
All parts of this work are protected by copyright. Any utilisation outwith the remit of the copyright law is unlawful and liable to prosecution. This applies in particular to translations, storage and processing in electronic systems and programs, microfilms, reproductions, etc."

FEBEX-DP Post-mortem analysis: Sensors

NAB 16-020

Authors: Rey M., Sanz F-J. and García-Siñeriz J-L. (AITEMIN)

Date: May 2016

AITEMIN c/ Margarita Salas, 14. Parque Leganés Tecnológico. 28918, Leganés -MADRID- Spain

INDEX

LIST OF FIGURES

LIST OF TABLES

1 INTRODUCTION

1.1 THE FEBEX PROJECT

FEBEX (Full-scale Engineered Barrier Experiment in Crystalline Host Rock) is a research and demonstration project that was initiated by Enresa (Spain).

The aim of the project is to study the behaviour of near-field components in a repository for high-level radioactive waste in granite formations. The main objectives of the project may be grouped in two areas:

- Demonstration of the feasibility of constructing the engineered barrier system in a horizontal configuration according to the Spanish concept for deep geological storage (AGP), and analysis of the technical problems to be solved for this type of disposal method
- Better understanding of the thermo-hydro-mechanical (THM) and thermo-hydro-geochemical (THG) processes in the near field, and development and validation of the modelling tools required for interpretation and prediction of the evolution of such processes

The project consists of two large-scale tests (see Figure 1. Overall layout of FEBEX "in situ" test (left) and "mock-up" test (right)

) – "in situ" and "mock-up" (the latter is managed by CIEMAT in Spain) – a series of laboratory tests, and THM and THG modelling tasks.

The full-scale heating test ("in situ" test), to which this document refers, was performed at the Grimsel underground laboratory in Switzerland, also known as Grimsel Test Site (GTS) or Felslabor Grimsel (FLG in German). A complete description of the FEBEX project objectives and test program may be found in the "FEBEX Full-scale Engineered Barriers Experiment in Crystalline Host Rock. Pre-operational stage summary report" (Fuentes-Cantillana et al. 1998a).

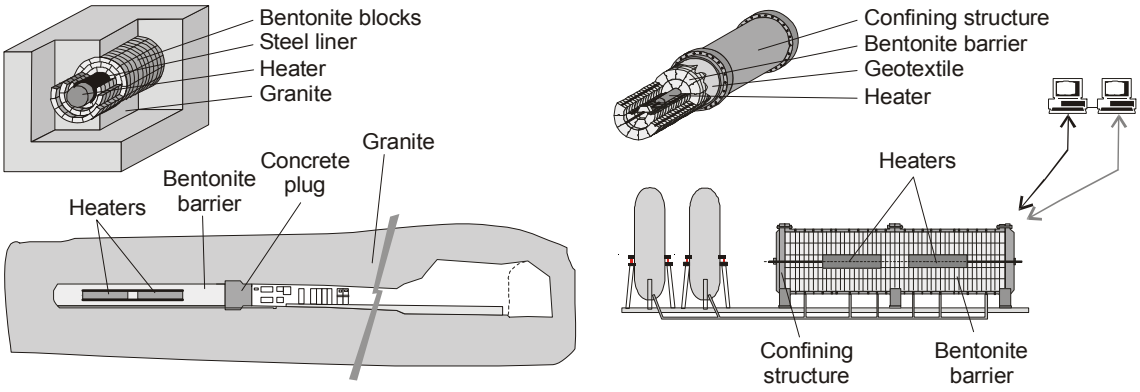

Figure 1. Overall layout of FEBEX "in situ" test (left) and "mock-up" test (right)

The project started in 1994, and has been supported by the European Commission through consecutive contracts, identified as FEBEX I (contract nº FI4W-CT-95-0006) for the period January 1996 to June 1999, and FEBEX II (contract nº FIKW-CT-2000-

00016), from September 2000 to December 2004. Afterwards, NF-PRO took place from January 2005 to December 2007. Finally, in January 2008 the "in situ" test was transferred from Enresa to a consortium composed by SKB (Sweden), POSIVA (Finland), CIEMAT (Spain), Nagra (Switzerland) and more recently KAERI (South Korea), the FEBEXe Consortium, which supports it currently.

The "in situ" experiment excavation was carried out in 2015 and new partners, interested in taking part in the planned sampling and analysis operations, have been incorporated to the Consortium (now called FEBEX-DP) for that purpose, namely US DOE (USA), Obayashi (Japan), RWM (UK), Andra (France), BGR (Germany) and SURAO (Check Republic).

1.2 TEST CONFIGURATION DURING FEBEX I

The installation of the "in situ" test was carried out at the GTS. A horizontal drift with a diameter of 2.28 m was excavated in the Grimsel granodiorite especially for this experiment using a TBM (a tunnel boring machine). Two electrical heaters, of the same size and of a similar weight as the reference canisters, were placed in the axis of the drift. The gap between the heaters and the rock was backfilled with compacted bentonite blocks, up to a length of 17.40 m, this requiring a total 115'716 kg of bentonite. The backfilled area was sealed with a plain concrete plug placed into a recess excavated in the rock and having a length of 2.70 m and a volume of 17.8 m^3. Figure 2 shows schematically the dimensions and layout of the test components.

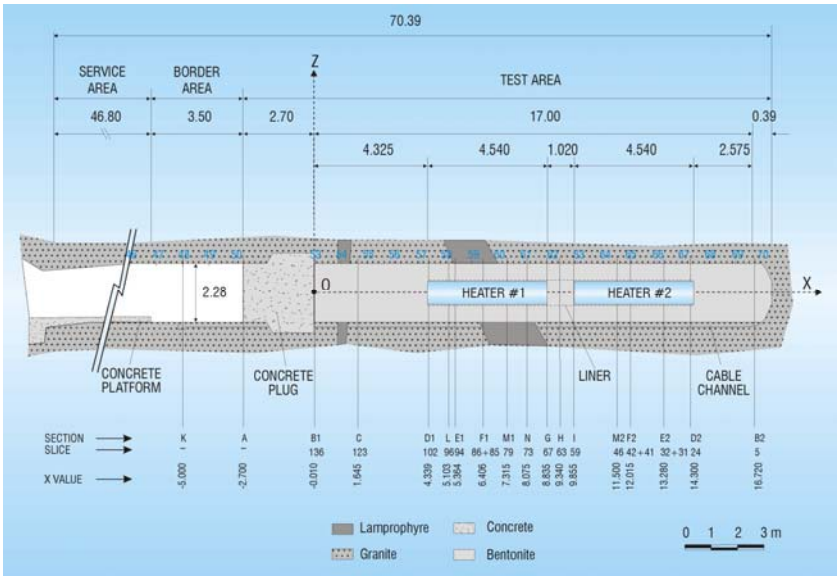

Figure 2. General layout of the FEBEX "in situ" test (FEBEX I configuration)

A total of 632 instruments were placed in the system along a number of instrumented sections, both in the bentonite buffer and in the host rock, to monitor relevant parameters such as temperature, humidity, total and pore pressure, displacements, ... etc. The instruments were of many different kinds and their characteristics and positions are fully described in the report titled "FEBEX Full-scale Engineered Barriers Experiment in Crystalline Host Rock. Final design and installation of the in-situ test at Grimsel" (Fuentes-Cantillana & García-Siñeriz 1998b).

A Data Acquisition and Control System (DACS) located in the service area of the FEBEX drift collected the data provided by the instruments. This system recorded and stored information from the sensors and also controlled the power applied to the electrical heaters, in order to maintain a constant temperature at the heaters/bentonite interface. The DACS allowed the experiment to be run in an automated mode, with remote supervision from Madrid. Data stored at the local DACS were periodically downloaded in Madrid and used to build the experimental Master Data Base.

The construction of the concrete plug was completed in October 1996, and the heating operation started on 28 February 1997. A constant temperature of 100 °C was maintained at the heaters/bentonite interface, while the bentonite buffer has been slowly hydrating with the water naturally issuing from the rock. A complete report that includes both the installation of the test and the results gathered after two years of operation is given in "FEBEX full-scale engineered barriers experiment for a deep geological repository for high level radioactive waste in crystalline host rock Final Report" (Fuentes-Cantillana et al. 2000).

1.3 DISMANTLING OF HEATER 1 AND TEST CONFIGURATION AFTERWARDS (FEBEX II)

A partial dismantling of the FEBEX "in situ" test was carried out during the summer of 2002, after 5 years of continuous heating. The operation included the demolition of the concrete plug, the removal of the section of the test corresponding to the first heater, and the sealing with a new shotcrete plug. A large number of samples from all types of materials were taken for analysis. A number of instruments were subsequently dismantled, as well as a few new ones were installed. Accordingly, system design was adapted, and the physical layout was changed in order to ease the partial dismantling operation.

The buffer and all components were removed up to a distance of 2 metres from heater #2 to minimize disturbance of the non-dismantled area. A dummy steel cylinder with a length of 1 m was inserted in the void left by heater #1 in the centre of the buffer. Some new sensors were installed in that one additional metre of bentonite buffer.

Additional sensors were introduced in boreholes drilled in the buffer parallel to the drift. To simplify this operation, the new concrete plug was constructed in two phases: an initial temporary plug measuring just 1 m in length, which was built immediately after dismantling, and a second section to complete the plug length to the 3 m planned in the design of the experiment. Unlike FEBEX I, the new plug was a parallel plug, without a recess excavated in the rock, constructed by shotcreting.

The description of the partial dismantling operation is given by the report titled "Dismantling of the Heater 1 at the FEBEX "in situ" test. Description of operations" (Bárcena et al. 2003). The configuration of the test, after completing the partial dismantling operation and construction of the full plug length, is shown in Figure 3.

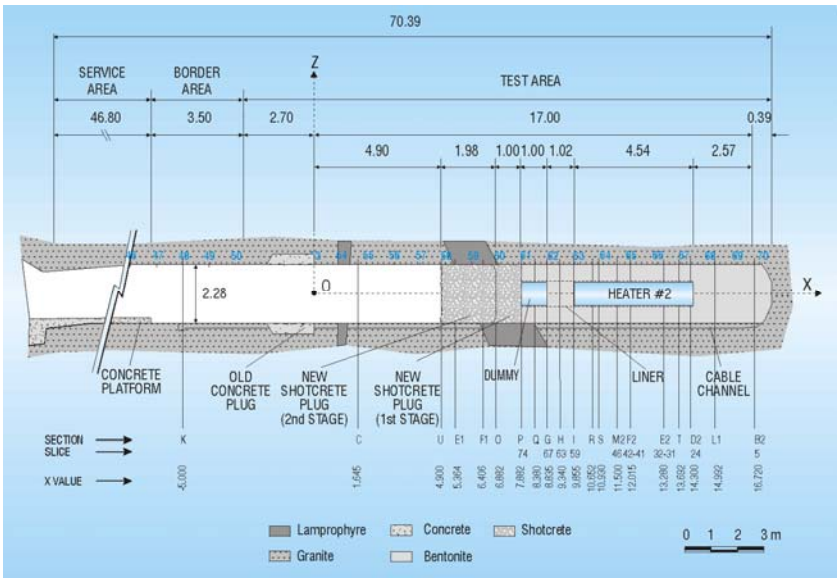

Figure 3. Status of the FEBEX "in situ" test after the partial dismantling (FEBEX II configuration)

A more complete report that describes the test from the conception up to two years of operation after the partial dismantling is given in the document titled "FEBEX Full-scale Engineered Barriers Experiment. UPDATED FINAL REPORT 1994 – 2004" (Huertas et al. 2006).

FEBEX (Full-scale Engineered Barrier Experiment in Crystalline Host Rock) is a research and demonstration project that was carried out by an international consortium. The aim of the project was to study the behaviour of the near-field components in a repository for high-level radioactive waste in granite formations.

The project consisted of two large-scale tests –“in situ” and “mock-up”–, a series of laboratory tests and THM and THG modelling tasks. The full-scale heating test (“in situ” test) was performed at the Grimsel underground laboratory in Switzerland. A complete description may be found in the “FEBEX Full-scale Engineered Barriers Experiment in Crystalline Host Rock. PRE-OPERATIONAL STAGE SUMMARY REPORT” (Fuentes-Cantillana et al. 1998).

The project started in 1994, and benefited from different financial supports over the years; it was supported by the European Commission through consecutive contracts, identified as FEBEX I (contract nº FI4W-CT-95-0006) for the period January 1996 to June 1999, and FEBEX II (contract nº FIKW-CT-2000-00016), from September 2000 to December 2004. Afterwards, NF-PRO took place from January 2005 to December 2007. Finally, the final FEBEX-e consortium started in January 2008 and lasted until the final excavation. In 2014, several new partners joined for the dismantling operation, called FEBEX-DP, the continuation of the project.

The installation of the “in-situ” test was carried out in 1996 in the Grimsel underground laboratory (Switzerland). The operational phase started in February 1997. Two electrical heaters, of the same size and of a similar weight as the reference canisters, were placed in the axis of a horizontal drift excavated in the Grimsel granodiorite. The

report that includes both the installation of the test and the results gathered after two years of operation is given in “FEBEX full-scale engineered barriers experiment for a deep geological repository for high level radioactive waste in crystalline host rock FINAL REPORT” (Fuentes-Cantillana et al. 2000).

A partial dismantling of the FEBEX “in-situ” test was carried out during the summer of 2002, after 5 years of continuous heating. The operation included the demolition of the concrete plug, the removal of the section of the test corresponding to the first heater, and the sealing with a new shotcrete plug; more details can be found in the report describing the test from the conception up to two years of operation after the partial dismantling: “FEBEX Full-scale Engineered Barriers Experiment. UPDATED FINAL REPORT 1994-2004” (Huertas et al. 2006).

The dismantling of the “in-situ” experiment started at the beginning of 2015. The plan “FEBEX-DP (GTS) Full Dismantling Test Plan” (Bárcena and García-Siñeriz 2015b), was to remove all the remaining parts of the “in-situ” test, including the remaining heater. It also included a sampling campaign of the bentonite, rock, relevant interfaces, sensors, metallic components and tracers allowing the analysis of the barriers’ conditions after more than 18 years of heating and natural hydration (see “FEBEX-DP (GTS) Full Dismantling Sampling Plan” (Bárcena and García-Siñeriz 2015a) and its update (Rey et al. 2015) for more details).

2 SCOPE

This document relates the post-mortem analysis of the sensors recovered during the dismantling operations (García-Siñeriz, J.L. et al. 2016); only sensors installed in the buffer were analysed because those in the rock walls were left in place. The list includes total pressure cells, pore pressure and displacement sensors, thermocouples, psychrometers and a crackmeter.

The checks and verifications carried out depended on the state of the sensors after dismantling. The data evolution provided by these sensors can be seen in the final data report (Martínez, V. et al. 2016).

Chapter 3 provides a general overview of the sensor distribution in the experiment, the number of sensors sampled and their operational status at the moment of dismantling. Chapter 4 details the observations during the dismantling operation, mostly regarding the state of sensors. Chapter 5 describes the analysis of the sensors once they were received at the laboratory, chapter 6 is focused on the results obtained from the verification of the surviving sensors and chapter 7 summarises the results and provides conclusions and recommendations. References used are found in chapter 8 and the detailed technical description of the dismantled sensors can be found in chapter 9.

3 GENERAL LAYOUT

The general layout of the sampling sections for the dismantling of the FEBEX experiment is shown in Figure 4 (Rey, M. et al. 2015); sensors' sections are in purple colour and correspond to dismantling sections (numbers) as well as to instrumented section (letters)

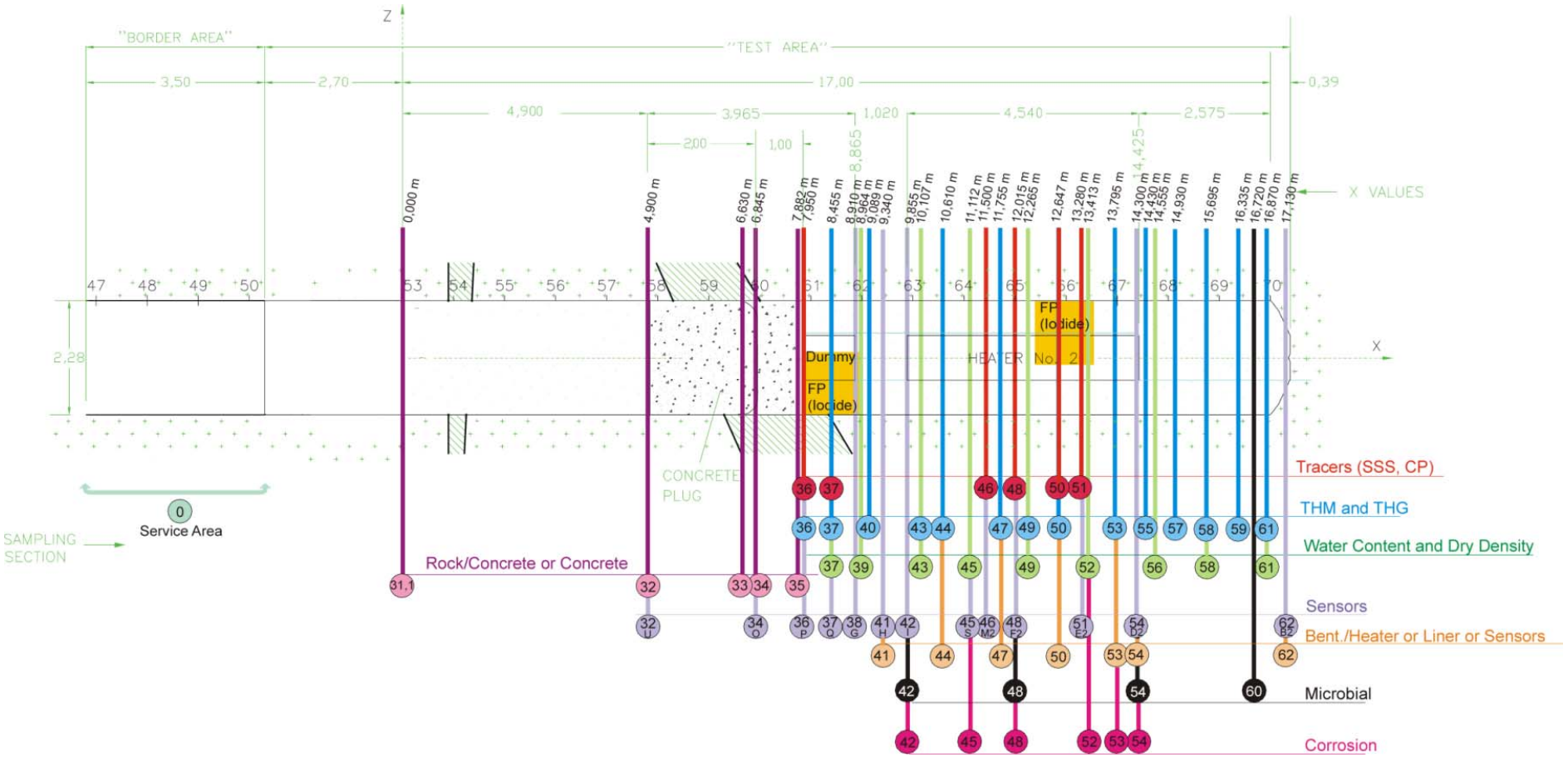

Figure 4. Sampling sections, general view

3.1 SENSORS CODIFICATION

Originally, all installed sensors were coded according to their type and location in the experiment. This code was called the installation code and it was different to the one assigned as sample for the dismantling (Rey, M. et al. 2015) and called dismantling code. The installation code for all sensors can be seen in chapter 9 (complete table) while only those sensors of interest for the dismantling are included below (simplified table).

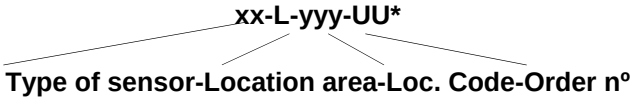

*Hyphen used to separate the codes could be removed to simplify the sensor description.

"xx" - TYPE OF SENSORS

T	Temperature thermocouple
P	Total pressure
Q	Pore Pressure (bentonite)
SH	Heater displacement
SB	Bentonite block displacement
S	Displacement (general)
3S	Crackmeter/fissurometer
WC	Water content (capacitive)
WP	Water content (psychrometer)
WT	Water content (TDR)

"L" - TYPE OF LOCATION

S	Section (bentonite)
H	Heaters

"yyy" - LOCATION CODE. This code specifies the instrumented section in the FEBEX drift where the sensor was placed, sections U, O, P, Q, G, H, I, R, S, M2, F2, E2, T, D2, L1 and B2 (updated after the partial dismantling made in 2002).

"UU" - ORDER NUMBER. This code was given according to the sequence of installation of the sensors of each type of sensor in each specific section.

3.2 LIST OF SAMPLED SENSORS

The complete list of the sensors sampled during the dismantling operation is given in Table 1 with the corresponding date of dismantling. All thermocouples (shown *) were left in place for further calibration. Table 1 lists both the dismantling code and the installation code.

Table 1. List of sampled sensors

Dismantling section	Dismantling code	Installation code	Dismantling date	Date of failure during operation	Damaged during dismantling*
32	S-S-32-1	SPSU-1	09/02/2015	-	-
	S-S-32-2	SPSU-2	09/02/2015	-	-
	S-S-32-3	SPSU-3	09/02/2015	-	-
	S-S-32-4	SPSU-4	09/02/2015	-	-
34	S-S-34-1	PSO-01	14/04/2015	03/04/2009	-
	S-S-34-2	PSO-02	14/04/2015	04/08/2008	-
36	S-S-36-1	PSP-1	05/05/2015	-	Yes
	S-S-36-2	PSP-2	07/05/2015	-	Yes
37	S-S-37-1	WCSQ-1	20/05/2015	12/06/2003	-
	S-S-37-2	WCSQ-2	19/05/2015	12/06/2003	-
	S-S-37-3	WCSQ-3	19/05/2015	12/06/2003	-
38	S-S-38-1	SHSG-01	22/05/2015	18/03/2002	-
	S-S-38-2	SHSG-02	22/05/2015	31/05/1997	-
	S-S-38-3	T-SG-01	21/05/2015*	-	Yes
	S-S-38-4	T-SG-02	21/05/2015*	-	Probably
	S-S-38-5	T-SG-03	21/05/2015*	-	Lost in dismantling
	S-S-38-6	T-SG-04	21/05/2015*	06/06/2003	-
	S-S-38-7	T-SG-05	21/05/2015*	10/06/2003	-
	S-S-38-8	T-SG-06	21/05/2015*	10/02/2008	
	S-S-38-9	T-SG-07	21/05/2015*	-	Probably
	S-S-38-10	T-SG-08	21/05/2015*	23/04/2004	-
	S-S-38-11	T-SG-09	21/05/2015*	-	-
	S-S-38-12	T-SG-10	21/05/2015*	-	-
	S-S-38-13	T-SG-11	21/05/2015*	-	-
	S-S-38-14	T-SG-12	21/05/2015*	12/06/2003	-
	S-S-38-15	T-SG-13	21/05/2015*	-	Probably
	S-S-38-16	P-SG-01	21/05/2015	-	-
41	S-S-41-1	QSH-01	29/05/2015	05/07/1999	-
	S-S-41-2	QSH-02	29/05/2015	-	-
	S-S-41-3	QSH-03	29/05/2015	-	-
	S-S-41-4	QSH-04	28/05/2015	-	-
	S-S-41-5	QSH-05	28/05/2015	08/03/2001	-
	S-S-41-6	QSH-06	28/05/2015	-	Yes
	S-S-41-7	QSH-07	28/05/2015	-	-
	S-S-41-8	QSH-08	29/05/2015	-	-
	S-S-41-9	QSH-09	29/05/2015	-	-

Dismantling section	Dismantling code	Installation code	Dismantling date	Date of failure during operation	Damaged during dismantling*
41	S-S-41-10	QSH-10	29/05/2015	-	-
	S-S-41-11	QSH-11	29/05/2015	-	-
	S-S-41-12	QSH-12	29/05/2015	-	-
	S-S-41-13	WCSH-01	29/05/2015	18/07/1998	-
	S-S-41-14	WCSH-02	29/05/2015	22/05/2003	-
	S-S-41-15	WCSH-03	29/05/2015	01/01/2002	-
	S-S-41-16	WCSH-04	28/05/2015	26/06/2003	-
	S-S-41-17	WCSH-05	28/05/2015	25/06/2003	Yes
	S-S-41-18	WCSH-06	28/05/2015	05/04/2001	-
	S-S-41-19	WCSH-07	28/05/2015	12/06/2003	-
	S-S-41-20	WCSH-08	28/05/2015	12/11/1998	-
	S-S-41-21	WCSH-09	29/05/2015	25/02/2000	
	S-S-41-22	WCSH-10	29/05/2015	22/01/2000	-
	S-S-41-23	WCSH-11	29/05/2015	28/02/2002	
	S-S-41-24	WCSH-12	29/05/2015	25/06/2003	-
	S-S-41-25	WCSH-13	29/05/2015	16/06/2002	-
	S-S-41-26	WPSH-01	29/05/2015	17/03/1998	Yes
	S-S-41-27	WPSH-02	29/05/2015	-	-
	S-S-41-28	WPSH-03	29/05/2015	08/07/1997	-
	S-S-41-29	WPSH-04	28/05/2015	-	Yes
	S-S-41-30	WPSH-05	29/05/2015	14/07/1997	-
	S-S-41-31	WPSH-06	29/05/2015	09/10/1997	Yes
	S-S-41-32	WPSH-07	29/05/2015	02/06/1997	-
	S-S-41-33	WPSH-08	29/05/2015	Beginning	-
42	S-S-42-1	SHSI-01	10/06/2015	23/05/2008	-
	S-S-42-2	SHSI-02	10/06/2015	20/04/2000	-
	S-S-42-3	TSI-01	10/06/2015*	-	Yes
	S-S-42-4	TSI-02	10/06/2015*	-	Yes
	S-S-42-5	TSI-03	10/06/2015*	-	Yes
	S-S-42-6	TSI-04	10/06/2015*	19/12/1996	-
	S-S-42-7	TSI-05	10/06/2015*	-	Probably
	S-S-42-8	TSI-06	10/06/2015*	-	Probably
	S-S-42-9	TSI-07	10/06/2015*	-	-
	S-S-42-10	TSI-08	10/06/2015*	-	-
	S-S-42-11	TSI-09	10/06/2015*	-	-
	S-S-42-12	TSI-10	10/06/2015*	-	-
	S-S-42-13	TSI-11	10/06/2015*	11/06/2003	-
	S-S-42-14	TSI-12	10/06/2015*	-	-
	S-S-42-15	TSI-13	10/06/2015*	-	-
	S-S-42-16	P-SI-01	04/06/2015	19/01/2009	-
46	S-S-46-01	WTSM2-03	02/07/2015	-	Yes
	S-S-46-02	WTSM2-04	01/07/2015	-	Yes
	S-S-46-03	WTSM2-05	01/07/2015	-	Yes

Dismantling section	Dismantling code	Installation code	Dismantling date	Date of failure during operation	Damaged during dismantling*
46	S-S-46-04	WTSM2-06	01/07/2015	-	Yes
	S-S-46-05	WTSM2-07	01/07/2015	-	Yes
	S-S-46-06	WTSM2-08	30/06/2015	-	Yes
	S-S-46-07	WTSM2-09	30/06/2015	-	Yes
	S-S-46-08	WTSM2-10	30/06/2015	-	Yes
	S-S-46-09	WTSM2-11	30/06/2015	01/10/2008	-
	S-S-46-10	WTSM2-12	30/06/2015	-	Yes
47	S-S-47-1	3SEF2-01-F1	03/07/2015	13/07/1999	-
	S-S-47-2	3SEF2-01-F2	03/07/2015	13/07/1999	-
	S-S-47-3	3SEF2-01-F3	03/07/2015	13/07/1999	-
48	S-S-48-1	WCSF2-01	06/07/2015	16/01/1997	-
	S-S-48-2	WCSF2-02	06/07/2015	26/11/2001	Yes
	S-S-48-3	WCSF2-03	06/07/2015	26/06/2003	-
	S-S-48-4	WCSF2-04	06/07/2015	05/04/2003	Yes
	S-S-48-5	WCSF2-05	06/07/2015	15/10/1997	-
	S-S-48-6	WCSF2-06	06/07/2015	15/11/2005	-
	S-S-48-7	WCSF2-07	06/07/2015	26/03/2003	-
	S-S-48-8	WCSF2-08	06/07/2015	19/06/1999	-
	S-S-48-9	QSF2-01	07/07/2015	-	-
	S-S-48-10	QSF2-02	07/07/2015	-	Yes
	S-S-48-11	QSF2-03	07/07/2015	05/05/2005	-
	S-S-48-12	QSF2-04	07/07/2015	31/03/2009	-
	S-S-48-13	QSF2-05	06/07/2015	05/05/2006	-
	S-S-48-14	QSF2-06	06/07/2015	22/09/2004	-
	S-S-48-15	QSF2-07	03/07/2015	-	-
	S-S-48-16	QSF2-08	03/07/2015	18/06/2003	Yes
	S-S-48-17	WPSF2-01	06/07/2015	-	-
	S-S-48-18	WPSF2-02	06/07/2015	15/10/1997	-
	S-S-48-19	WPSF2-03	06/07/2015	12/07/2002	-
	S-S-48-20	WPSF2-04	06/07/2015	29/06/1998	-
	S-S-48-21	WPSF2-05	06/07/2015	23/06/1997	-
	S-S-48-22	WPSF2-06	06/07/2015	-	-
	S-S-48-23	WPSF2-07	03/07/2015	05/08/1997	-
	S-S-48-24	WPSF2-08	06/07/2015	-	-
	S-S-48-25	TSF2-01	02/07/2015*	-	Yes
	S-S-48-26	TSF2-02	02/07/2015*	-	-
	S-S-48-27	TSF2-03	02/07/2015*	31/08/2002	-
	S-S-48-28	TSF2-04	02/07/2015*	18/06/2002	-
	S-S-48-29	SBSF2-01	10/07/2015	22/02/1998	-
	S-S-48-30	SBSF2-02	10/07/2015	-	-
51	S-S-51-1	WCSE2-01	13/07/2015	16/01/1997	-
	S-S-51-2	WCSE2-02	13/07/2015	16/01/1997	-
	S-S-51-3	WCSE2-03	09/07/2015	04/05/1997	-

Dismantling section	Dismantling code	Installation code	Dismantling date	Date of failure during operation	Damaged during dismantling*
51	S-S-51-4	WCSE2-04	13/07/2015	25/07/1997	-
	S-S-51-5	WCSE2-05	10/07/2015	31/10/1997	-
	S-S-51-6	WCSE2-06	13/07/2015	16/03/1997	-
	S-S-51-7	WCSE2-07	10/07/2015	14/07/1999	-
	S-S-51-8	WCSE2-08	13/07/2015	14/10/2000	-
	S-S-51-9	WCSE2-09	10/07/2015	22/03/1999	-
	S-S-51-10	WCSE2-10	10/07/2015	28/01/2001	-
	S-S-51-11	QSE2-01	13/07/2015	-	-
	S-S-51-12	QSE2-02	13/07/2015	26/09/2014	-
	S-S-51-13	QSE2-03	10/07/2015	12/08/2009	-
	S-S-51-14	QSE2-04	13/07/2015	16/04/1999	-
	S-S-51-15	QSE2-05	13/07/2015	-	-
	S-S-51-16	QSE2-06	13/07/2015	09/11/2007	-
	S-S-51-17	QSE2-07	13/07/2015	-	-
	S-S-51-18	QSE2-08	13/07/2015	-	-
	S-S-51-19	WPSE2-01	13/07/2015	30/09/2000	-
	S-S-51-20	WPSE2-02	13/07/2015	01/04/1998	-
	S-S-51-21	WPSE2-03	13/07/2015	03/05/1997	-
	S-S-51-22	WPSE2-04	13/07/2015	01/01/1999	-
	S-S-51-23	WPSE2-05	13/07/2015	20/07/2002	-
	S-S-51-24	WPSE2-06	13/07/2015	17/07/1998	-
	S-S-51-25	WPSE2-07	10/07/2015	18/05/1997	-
	S-S-51-26	WPSE2-08	10/07/2015	04/04/2001	-
	S-S-51-27	TSE2-01	13/07/2015	-	Lost in dismantling
	S-S-51-28	TSE2-02	13/07/2015	19/12/1996	Lost in dismantling
	S-S-51-29	PSE2-02	13/07/2015	24/02/2005	-
	S-S-51-30	PSE2-05	13/07/2015	27/03/1997	-
	S-S-51-31	SBSE2-01	13/07/2015	13/12/1999	-
	S-S-51-32	SBSE2-02	13/07/2015	26/08/2009	-
54	S-S-54-1	TSD2-01	17/07/2015*	-	-
	S-S-54-2	TSD2-02	17/07/2015*	-	-
	S-S-54-3	TSD2-03	17/07/2015*	11/08/2013	Probably
	S-S-54-4	TSD2-04	17/07/2015*	12/08/2000	-
	S-S-54-5	TSD2-05	17/07/2015*	-	-
	S-S-54-6	TSD2-06	17/07/2015*	-	Probably
	S-S-54-7	TSD2-07	17/07/2015*		-
	S-S-54-8	TSD2-08	17/07/2015*	-	-
	S-S-54-9	TSD2-09	17/07/2015*	-	-
	S-S-54-10	TSD2-10	17/07/2015*	-	-
	S-S-54-11	TSD2-11	17/07/2015*	-	-
	S-S-54-12	TSD2-12	17/07/2015*	16/06/2003	-
	S-S-54-13	TSD2-13	17/07/2015*	-	Probably
	S-S-54-14	SHSD2-01	20/07/2015	17/01/2005	-

Dismantling section	Dismantling code	Installation code	Dismantling date	Date of failure during operation	Damaged during dismantling*
54	S-S-54-15	SHSD2-02	20/07/2015	-	-
	S-S-54-16	SHSD2-03	21/07/2015	18/06/2001	-
62	S-S-62-1	TSB2-01	04/08/2015*	-	-
	S-S-62-2	TSB2-02	04/08/2015*	-	-
	S-S-62-3	TSB2-03	04/08/2015*	-	-
	S-S-62-4	TSB2-04	04/08/2015*	-	-
	S-S-62-5	TSB2-05	04/08/2015*	19/12/1996	-
	S-S-62-6	TSB2-06	04/08/2015*	-	-
	S-S-62-7	TSB2-07	04/08/2015*	-	-
	S-S-62-8	TSB2-08	04/08/2015*	-	Probably
	S-S-62-9	TSB2-09	04/08/2015*	-	-

*"Probably" was indicated in the table when the sensor provided wrong data during checking and there was a chance the sensor was damaged, but not clearly, during dismantling. This applies to corroded sensors or those with clear signs of mechanical defects.

All information and details regarding the dates and sampling of sensors are included in García-Siñeriz, J.L. et al. 2016, Annex I: Updated sampling section logs.

Except for the drawings/figures of the sampling sections, the sensors' name/code used hereafter for identification is the one assigned at the installation, as well as the reference used in the dismantling operation.

4 DISMANTLING OF SENSORS

4.1 SAMPLING SECTION 32/INSTRUMENTED SECTION U

Section 32 corresponds to the front part of the concrete plug, four displacement sensors (S-S-32-1 to 4/ SPSU-1 to 4) were previously installed on the surface (instrumented section U). The technical characteristics of these sensors are included in section 9.3.6.

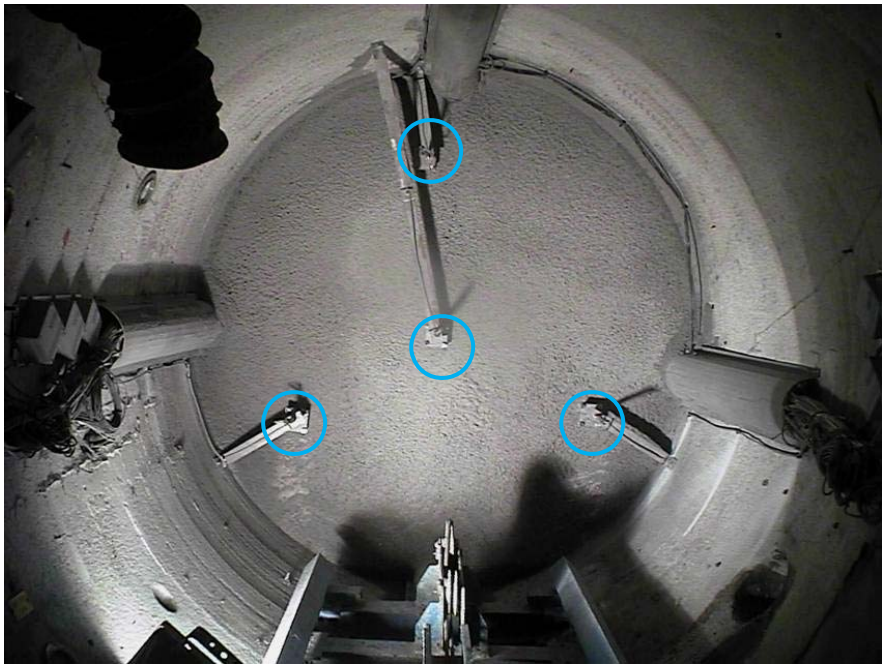

Figure 5. Sampling section 32/instrumented section U, view after installation (Sensors are shown inside a blue circle)

Table 2. Sensors retrieved sampling section 32 / Instrumented section U

Dismantling section	Layer	GM (m)	Dismantling code	Installation code	Dismantling date	Date of failure	Damaged during dismantling
32	-	Plug	S-S-32-1	SPSU-1	09/02/2015	-	-
			S-S-32-2	SPSU-2	09/02/2015	-	-
			S-S-32-3	SPSU-3	09/02/2015	-	-
			S-S-32-4	SPSU-4	09/02/2015	-	-

These sensors were operative at the moment of dismantling; they had good external appearance due to the favourable environmental conditions in the gallery. However, the internal springs had lost their elasticity due to rusting as a consequence of humidity; their functioning did not seem significantly affected by this as proven by the verification analysis (see chapter 5.1.1).

Figure 6. Detail of retrieved displacement sensor

4.2 SAMPLING SECTION 34/INSTRUMENTED SECTION O

This section corresponds to instrumented section O and is located in the contact zone of the two sections of the plug. The concrete plug was made in two parts, as described in Huertas F. et al. 2006, with a waterproof membrane installed between them to increase the water tightness.

Figure 7. Section 34/Instrumented section O, after installation

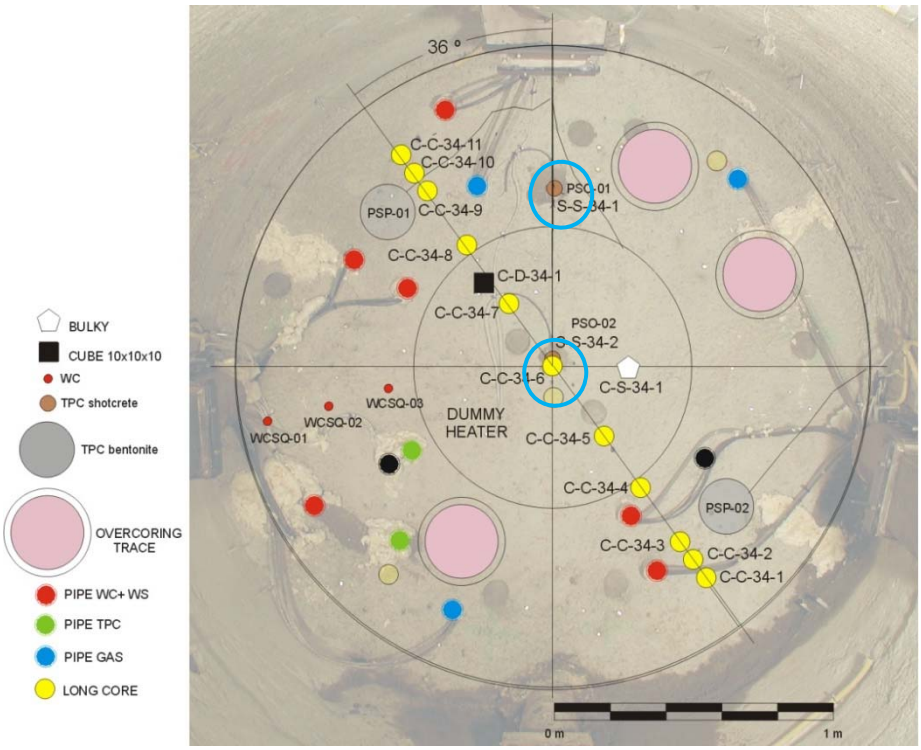

Figure 8. Sensors in sampling section 34 (circled in blue)

Figure 9. Overall view of sampling section 34 during dismantling (red circles indicate the expected location of total pressure cells)

Two total pressure cells were recovered, PSO-01 and PSO-02, which were out of order (see Table 3) well before dismantling on the 14th April 2015. The technical characteristics of these sensors are included in section 9.3.2 (KULITE ones).

Table 3. Sensors retrieved sampling section 34 / Instrumented section O

Dismantling section	Layer	GM (m)	Dismantling code	Installation code	Dismantling date	Date of failure	Damaged during dismantling
34	-	6.85	S-S-34-1	PSO-01	14/04/2015	03/04/2009	-
			S-S-34-2	PSO-02	14/04/2015	04/08/2008	-

The first total pressure cell (PSO-01) was apparently in quite good conditions (see Figure 10). The sensor's body, the cable gland and the cable were in a good state; the protection rubber was separated from the membrane, but the sensor was not mechanically damaged. The conductors were clean without any traces of rust.

Figure 10. Detail of state of total pressure cell PSO-01

The second total pressure cell (PSO-02) was found very much damaged; the protection membrane was completely separated from the joint, the measuring area was pierced and no oil remained. The body of the sensor was quite corroded and water had entered the electronics, the conducting wires appeared rusty; see Figure 11.

Figure 11. Detail of state of total pressure cell PSO-02

There is no clear explanation of why the second pressure cell was much more damaged than the first one.

4.3 SAMPLING SECTION 36/INSTRUMENTED SECTION P

This section corresponds to instrumented section P, located at the interface plug-bentonite buffer. The two total pressure cells, PSP-01 and PSP-02, were operative –see Table 4– until their dismantling between the 5th and 7th of May 2015. PSP-01 went out of order during the dismantling of the concrete plug, see García-Siñeriz, J.L. et al. 2016 and Martínez, V. et al. 2016. The technical characteristics of these sensors are included in section 9.3.2 (GEOKON model 4810-7).

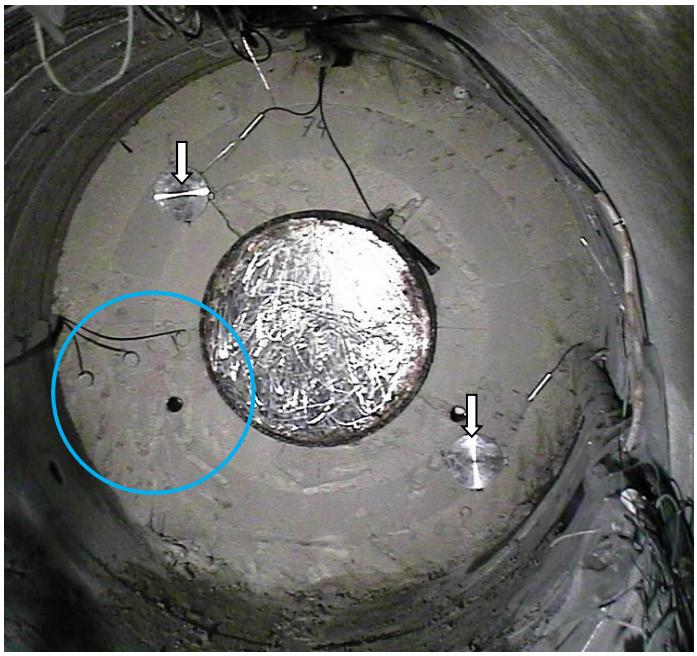

Figure 12. Sensors in sampling section 36/instrumented section P, after installation[1]

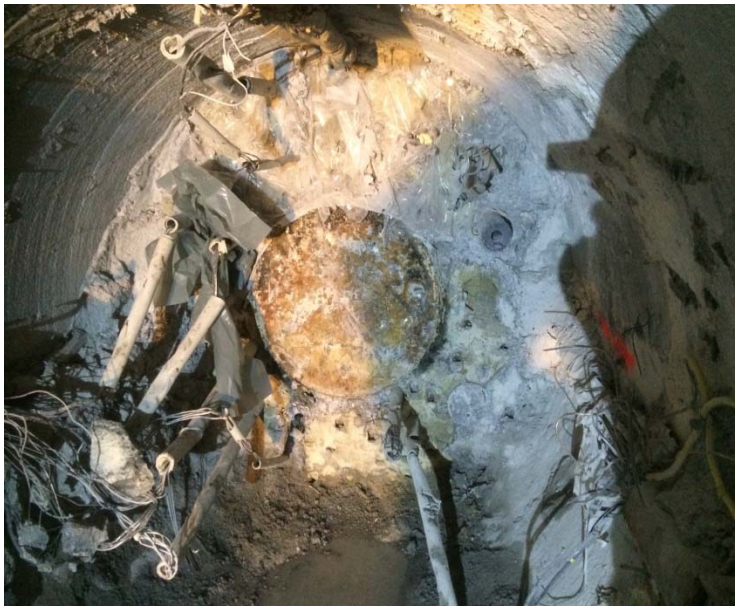

Figure 13. Sampling section 36 during dismantling

[1] Total pressure cells are clearly visible at the surface of the blocks. The location of the thermo hygrometers in the instrumented section Q can be seen hidden below circular bentonite blocks at the left hand side of the dummy canister (circled in blue).

Table 4. Sensors retrieved sampling section 36 / Instrumented section P

Dismantling section	Layer	GM (m)	Dismantling code	Installation code	Dismantling date	Date of failure	Damaged during dismantling
36	74	7.9	S-S-36-1	PSP-1	05/05/2015	-	Yes
			S-S-36-2	PSP-2	07/05/2015	-	Yes

The two total pressure cells were slightly damaged during their extraction, showing some hits of the robot that had dismantled the plug, although their general state of conservation was good; they did not reveal any signs of external corrosion (see Figure 14). The cable was slightly damaged in the vicinity of the sensors, but there was no internal rusting of the wires, indicating they had remained watertight or that the presence of water had not been significant in the section; see Figure 15.

Figure 14. Detail of sensors PSP-01 (left) and PSP-02 (right)

Figure 15. Detail of final estate of cable, sensors PSP-01 and PSP-02

4.4 SAMPLING SECTION 37/INSTRUMENTED SECTION Q

This section corresponds to instrumented section Q. The sensors (three thermohygrometers S-S-37-1 to 3/ WCSQ-1 to 3 of the capacitive type from Vaisala, see location in Figure 17 and Figure 12, inside the blue circle) failed during the operational phase due to the accidental cut of the cables –see Table 5– and they were dismantled between the 19th and 20th of May 2015. The technical data of these sensors are given in section 9.3.7 (VAISALA HMP237).

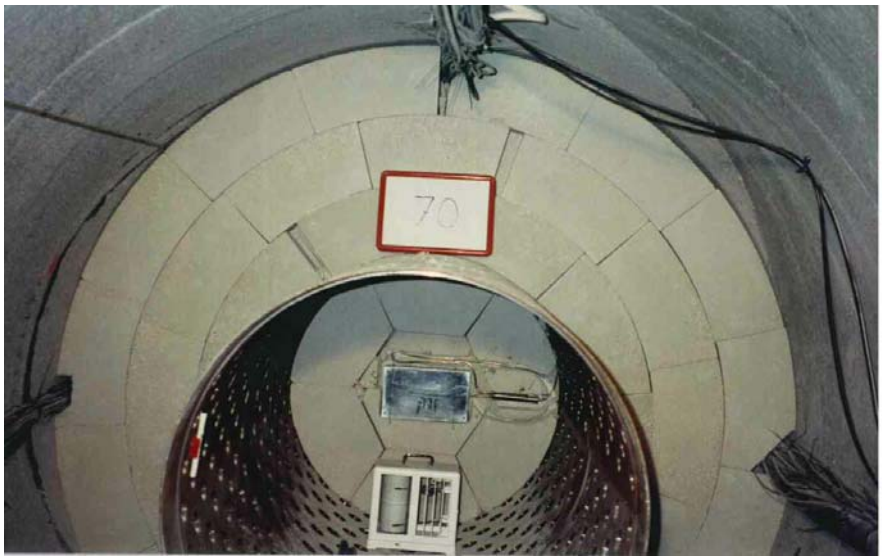

Figure 16. Section 37 / instrumented section Q after construction of the buffer. The instrumented pipes and the thermohygrometers are not shown because they were installed during the partial dismantling

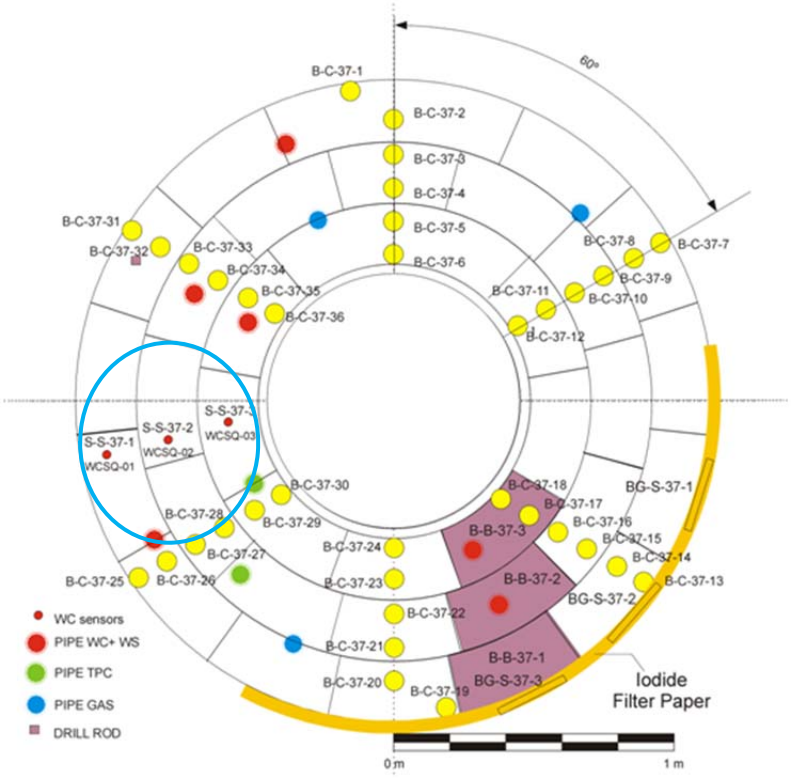

Figure 17. Sensors in sampling section 37 (circled in blue)

Figure 18. Sampling section 37 after dismantling

Table 5. Sensors retrieved sampling section 37 / Instrumented section Q

Dismantling section	Layer	GM (m)	Dismantling code	Installation code	Dismantling date	Date of failure	Damaged during dismantling
37	70	8.41	S-S-37-1	WCSQ-1	20/05/2015	12/06/2003	-
			S-S-37-2	WCSQ-2	19/05/2015	12/06/2003	-
			S-S-37-3	WCSQ-3	19/05/2015	12/06/2003	-

The three sensors (WCSQ-01, WCSQ-02 and WCSQ-03) were in good conditions; they had not been significantly damaged by bentonite during the operation.

In the case of WCSQ-02, there were some bentonite traces at the filter surface (see Figure 19).The internal part of the three thermohygrometers (filter and sensing element) showed some rusty parts/traces of rust and evidence of contact with water, see Figure 20.

Figure 19. Detail of external aspect of WCSQ-01

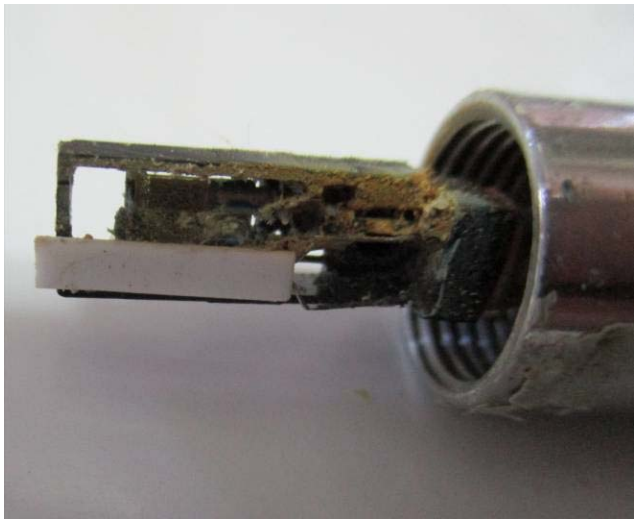

Figure 20. Detail of internal aspect of WCSQ-02

The plastic jacket of the cables of these sensors appeared quite deteriorated. The external shield of the cable had a bad smell and a *malleable* texture. The internal shield and wires were very rusty, evidence of their contact with water, see Figure 21.

Figure 21. Detail of internal shield, WCSQ-03

4.5 SAMPLING SECTION 38/INSTRUMENTED SECTION G

This section corresponds to instrumentation section G. The sensors (two extensometers S-S-38-1 and 2/ SHSG-1 and 2, thirteen thermocouples S-S-38-3 to 15/T-SG-01 to 13 and a total pressure cell S-S-38-16/P-SG-01) were all dismantled on the 21st May 2015, and more than half were -in principle- operative at the time of dismantling (see Table 6).

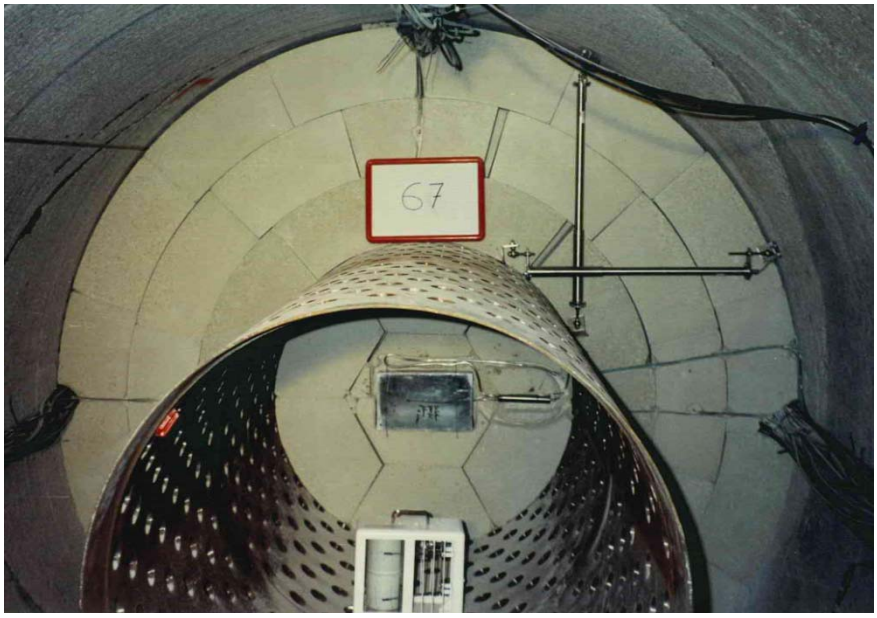

Figure 22. Sampling section 38 after installation

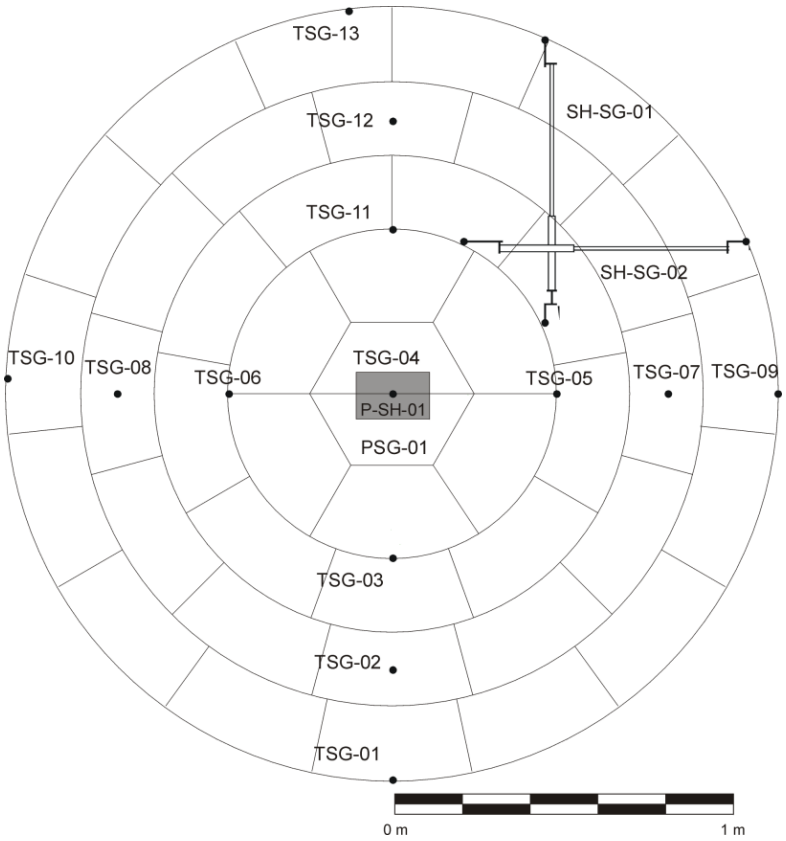

Figure 23. Sensors in sampling section 38

Table 6. Sensors retrieved sampling section 38 / Instrumented section G

Dismantling section	Layer	GM (m)	Dismantling code	Installation code	Dismantling date	Date of failure	Damaged during dismantling
38	67	8.83	S-S-38-1	SHSG-01	22/05/2015	18/03/2002-	-
			S-S-38-2	SHSG-02	22/05/2015	31/051997-	-
			S-S-38-3	T-SG-01	21/05/2015*	-	Yes
			S-S-38-4	T-SG-02	21/05/2015*	-	Probably
			S-S-38-5	T-SG-03	21/05/2015*	-	Lost
			S-S-38-6	T-SG-04	21/05/2015*	06/06/2003	-
			S-S-38-7	T-SG-05	21/05/2015*	10/06/2003	-
			S-S-38-8	T-SG-06	21/05/2015*	Not reliable from 10/02/2008	-
			S-S-38-9	T-SG-07	21/05/2015*	-	Probably
			S-S-38-10	T-SG-08	21/05/2015*	23/04/2004	-
			S-S-38-11	T-SG-09	21/05/2015*	-	-
			S-S-38-12	T-SG-10	21/05/2015*	-	-
			S-S-38-13	T-SG-11	21/05/2015*	-	-
			S-S-38-14	T-SG-12	21/05/2015*	12/06/2003	-
			S-S-38-15	T-SG-13	21/05/2015*	-	Probably
			S-S-38-16	P-SG-01	21/05/2015	-	Not analysed

The two extensometers (SH-SG-01 and 02) were found blocked[2], showed some external scratches from the dismantling operation and were slightly deformed as a consequence of the bentonite's swelling. The technical data of these sensors is given in section 9.3.4.

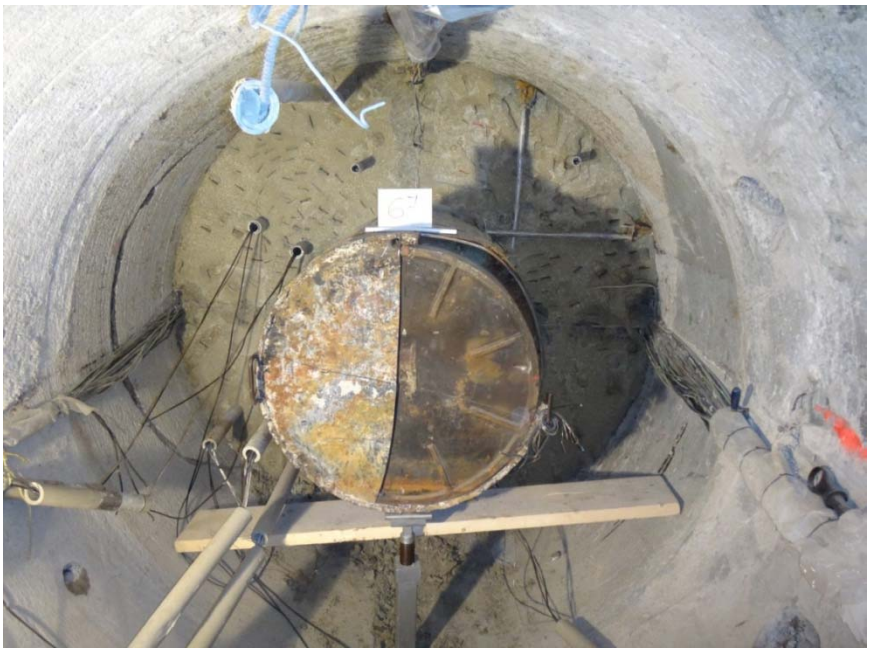

Figure 24. Sampling section 38 during dismantling

[2] No movement of the sensor's sliding elements was possible.

Figure 25. Detail of extensometers in sampling section 38 during dismantling

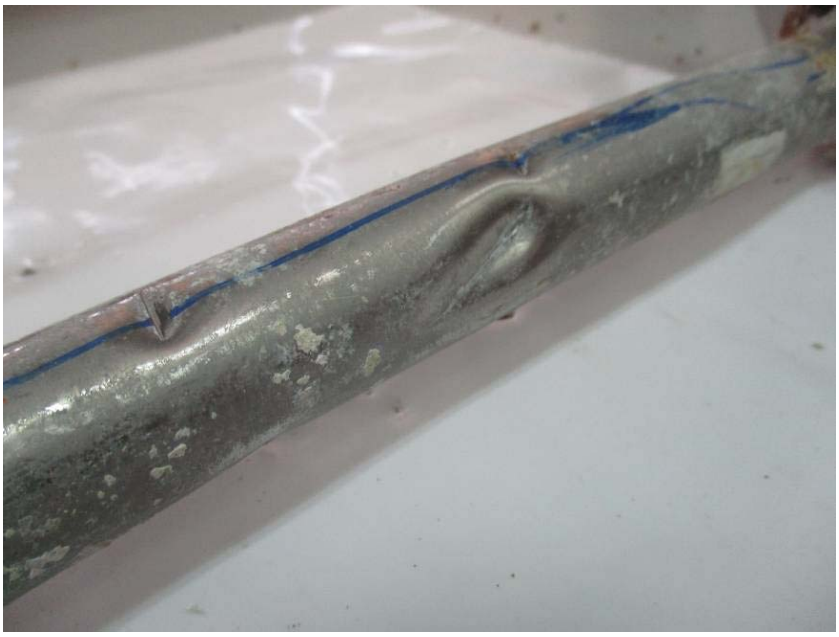

Figure 26. Detail sensor SH-SG-02, slight deformation
(Dents were caused by dismantling works)

The thermocouples were left in place (collected and protected close to the rock walls, see Figure 27 and Figure 28) in order to be checked at the end of the dismantling phase (see 5.4). The technical data of the thermocouples can be found in section 9.3.1.

Figure 27. Thermocouples in place before being collected

Figure 28. Thermocouples moved to the rock walls to continue with the dismantling.

The total pressure cell P-SG-01 was not retrieved as expected. The “dummy canister” and the surrounding liner section were extracted together with the bentonite layer at the rear part (see Garcia-Siñeriz J.L. et al. 2016), which was inside the liner section too (see photo below); therefore, it remained hidden and included in the complete sample package that was left at the Grimsel Test Site. The technical data of the total pressure cell are given in section 9.3.2 (GEOKON 4580-2-6MPa NATM type).

Figure 29. View of the back part of the dummy canister inside the liner section showing the layer of bentonite that covers the total pressure cell P-SG-01 (approximate location is indicated by the red circle)

4.6 SAMPLING SECTION 41/INSTRUMENTED SECTION H

This section corresponds to instrumented section H. The sensors (twelve pore pressure sensors (S-S-41-1 to S-S-41-12/QSH-01 to 12), thirteen thermohygrometers (S-S-41-13 to S-S-41-25/WCSH-01 to WCSH-13) of the capacitive type, eight psychrometers (S-S-41-26 to S-S-41-33/WPSH-01 to WPSH-08) and a gas pressure sensor were dismantled between the 28th and 29th of May 2015. Some of the sensors were still operative before dismantling, see Table 7.

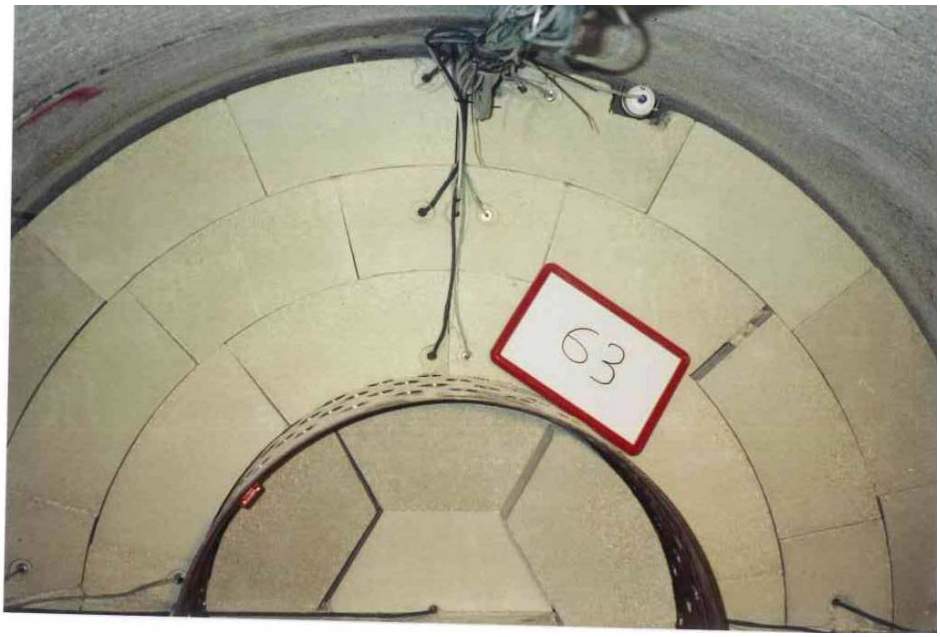

Figure 30. Sampling section 41 after installation

Figure 31. Sampling section 41 after dismantling

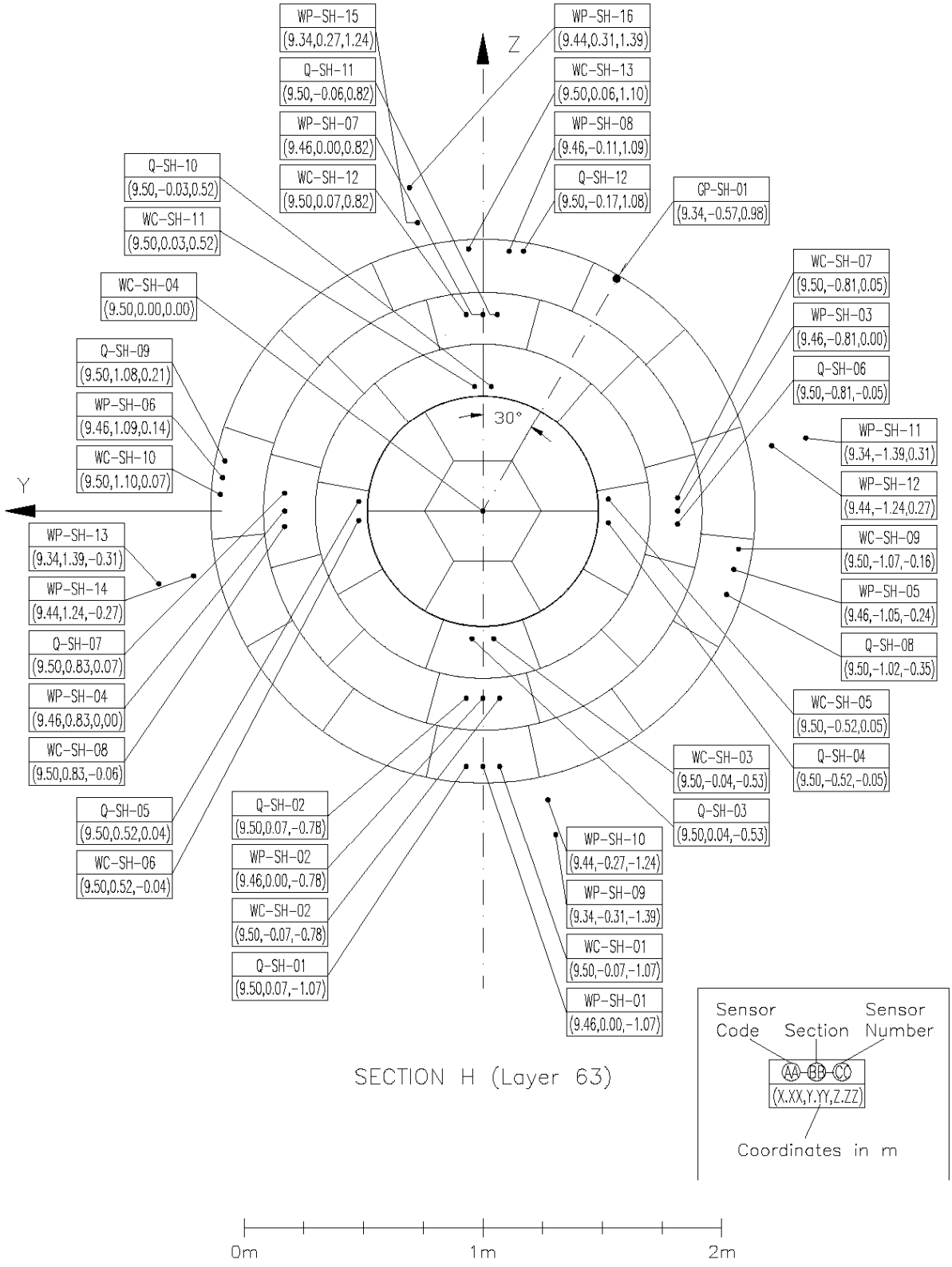

Figure 32. Sensors in sampling section 41

Table 7. Sensors retrieved sampling section 41 / Instrumented section H

Dismantling section	Layer	GM (m)	Dismantling code	Installation code	Dismantling date	Date of failure	Damaged during dismantling
41	63	9.3-9.5	S-S-41-1	QSH-01	29/05/2015	05/07/1999	-
			S-S-41-2	QSH-02	29/05/2015	-	-
			S-S-41-3	QSH-03	29/05/2015	-	-
			S-S-41-4	QSH-04	28/05/2015	-	-
			S-S-41-5	QSH-05	28/05/2015	08/03/2001	-
			S-S-41-6	QSH-06	28/05/2015	-	Yes
			S-S-41-7	QSH-07	28/05/2015	-	-
			S-S-41-8	QSH-08	29/05/2015	-	-
			S-S-41-9	QSH-09	29/05/2015	-	-
			S-S-41-10	QSH-10	29/05/2015	-	-
			S-S-41-11	QSH-11	29/05/2015	-	-
			S-S-41-12	QSH-12	29/05/2015	-	-
			S-S-41-13	WCSH-01	29/05/2015	18/07/1998	-
			S-S-41-14	WCSH-02	29/05/2015	22/05/2003	-
			S-S-41-15	WCSH-03	29/05/2015	01/01/2002	-
			S-S-41-16	WCSH-04	28/05/2015	26/06/2003	-
			S-S-41-17	WCSH-05	28/05/2015	25/06/2003	-
			S-S-41-18	WCSH-06	28/05/2015	05/04/2001	-
			S-S-41-19	WCSH-07	28/05/2015	12/06/2003	-
			S-S-41-20	WCSH-08	28/05/2015	12/11/1998	-
			S-S-41-21	WCSH-09	29/05/2015	25/02/2000	
			S-S-41-22	WCSH-10	29/05/2015	22/01/2000	-
			S-S-41-23	WCSH-11	29/05/2015	28/02/2002	
			S-S-41-24	WCSH-12	29/05/2015	25/06/2003	-
			S-S-41-25	WCSH-13	29/05/2015	16/06/2002	-
			S-S-41-26	WPSH-01	29/05/2015	17/03/1998	Yes
			S-S-41-27	WPSH-02	29/05/2015	-	-
			S-S-41-28	WPSH-03	29/05/2015	08/07/1997	Yes
			S-S-41-29	WPSH-04	28/05/2015	-	Yes
			S-S-41-30	WPSH-05	29/05/2015	14/07/1997	-
			S-S-41-31	WPSH-06	29/05/2015	09/10/1997	Yes
			S-S-41-32	WPSH-07	29/05/2015	02/06/1997	-
			S-S-41-33	WPSH-08	29/05/2015	Beginning	Yes

In general, the sensors were in good conditions, except for the psychrometers.

Most of the pore pressure sensors –Q-SH-01 to 12 except Q-SH-05 and Q-SH-06– were operative; they showed very small signs of rusting. Some of them had small deformations caused by the swelling of bentonite (Q-SH-03, Q-SH-04, Q-SH-10, Q-SH-11 and Q-SH-12), probably because they were installed either between joints or between layers.

Sensors Q-SH-01 and Q-SH-04 were quite damaged, they were found separated from the filter and with bentonite inside the measuring chamber. The technical data of these sensors can be found in section 9.3.3.

Of all sensors, those in the vicinity of the liner (Q-SH-03, Q-SH-04, Q-SH-05 and Q-SH-10) were in the worst conditions after dismantling, and those in the upper part (Q-SH-10, Q-SH-11 and Q-SH-12) were the most deformed; see Figure 33.

Figure 33. Detail of deformation sensors Q-SH-04 and Q-SH-10

In all cases, the cable of the pore pressure sensors was quite difficult to manipulate, it had lost its initial flexibility and appeared very rigid; in some sensors the jacket was broken just at the output of the sensor body, causing water to enter the inner part of the cable; see Figure 34.

Figure 34. Detail of broken cable shield sensor Q-SH-04

All capacitive thermohygrometers (WC-SH-01 to 13) went out of order during the operation but showed a good state of conservation, except for the cables and the plastic jackets that protected them, which were quite damaged in all sensors and squashed in some of them (WC-SH-07, WC-SH-08, WC-SH-09 and WC-SH-10); see Figure 35. The technical data of the thermohygrometers are included in section 9.3.7. (ROTRONIC ones).

Figure 35. Detail of squashed plastic jacket in thermohygrometers

Evidence of the presence of water/humidity inside the sensors was seen, affecting both the filter and sensing element inside the measuring chamber. This was especially the case of thermohygrometers in the central and lower part of the section (WC-SH-01 to WC-SH-06 and WC-SH-11), where the sensing elements (capacitive film and temperature sensor) appeared corroded and/or destroyed, see Figure 36 and Figure 37.

Figure 36. Detail state of sensing element, capacitive thermohygrometers

Figure 37. Detail state of sensor WC-SH-11, close to the liner

Regarding the psychrometers (WP-SH-01 to 08), the swelling of bentonite caused a deformation of the Teflon® body in most of them. In some sensors the ceramic filter was broken (WP-SH-02, 04, 05, 06, 07 and 08) and in WP-SH-03 the cable was separated from the body. The technical characteristics of these sensors are included in section 9.3.8.

Figure 38. Detail of state of Teflon® protection, sensor WP-SH-02

The cables and their protection tubes appeared quite damaged, squashed and broken. The cable was degraded and a change of colour was also noticed; see Figure 39 and Figure 40.

Figure 39. Detail state of cable and protection tube, psychrometers section 41

Figure 40. Detail of cable with colour changes, psychrometers section 41

It can be stated that all the sensors located in the lower part of the section were in direct contact with free water[3]. They did not suffer significant mechanical damages but the sensitive parts –sensing element– were seriously damaged by corrosion.

On the other hand, the effect of bentonite swelling was particularly observed in the central area of the section, and it was clearer in the intermediate ring, where the sensors and especially the cables, suffered more mechanical effects (by pulling or compression).

Finally, the sensors in the upper part were quite rusty, although this effect was less important in the vertical direction towards the rock, in the outer sections of the buffer.

The gas pressure sensor (GP-SH-01) was found complete but clearly deformed due to the bentonite swelling, see Figure 41.

[3] Positive pore pressure was measured in almost all the sections and, in particular, at the bottom first and then at the right hand side looking from the gallery entry (Martínez, V. et al. 2016), so the porosity of the bentonite was saturated.

Figure 41. Gas pressure sensor GP-SH-01 after dismantling

4.7 SAMPLING SECTION 42/INSTRUMENTED SECTION I

This section corresponds to instrumented section I. The sensors (two extensometers S-S-42-1 and 22/ SHSI-01 and 02, thirteen thermocouples S-S-42-3 to S-S-42-15/TSI-01 to TSI-13) and 1 total pressure cell S-S-42-16/P-SI-01) were dismantled on the 10th of June 2015; the thermocouples were left in place for further calibration. Many sensors were in principle operative before the dismantling operation (see Table 8). The total pressure cell was kept on the heater's surface until it was transported to AITEMIN's facilities at Toledo (Spain)

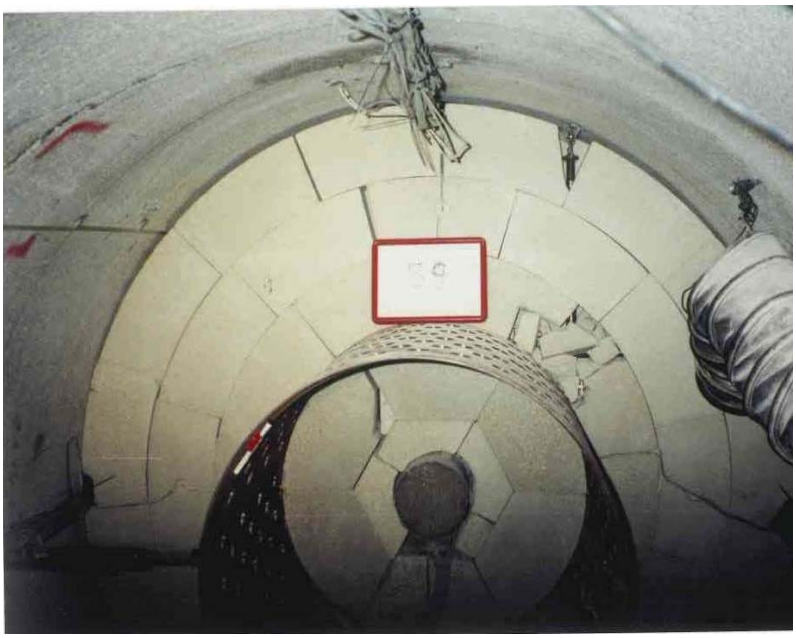

Figure 42. Sampling section 42 after installation

Table 8. Sensors retrieved sampling section 42 / Instrumented section I

Dismantling section	Layer	GM (m)	Dismantling code	Installation code	Dismantling date	Date of failure	Damaged during dismantling
42	59, 58	9.85	S-S-42-1	SHSI-01	10/06/2015	23/05/2008	-
			S-S-42-2	SHSI-02	10/06/2015	20/04/2000	-
			S-S-42-3	TSI-01	10/06/2015*	-	Yes
			S-S-42-4	TSI-02	10/06/2015*	-	Yes
			S-S-42-5	TSI-03	10/06/2015*	-	Yes
			S-S-42-6	TSI-04	10/06/2015*	19/12/1996	-
			S-S-42-7	TSI-05	10/06/2015*	-	Probably
			S-S-42-8	TSI-06	10/06/2015*	-	Probably
			S-S-42-9	TSI-07	10/06/2015*	-	-
			S-S-42-10	TSI-08	10/06/2015*	-	-
			S-S-42-11	TSI-09	10/06/2015*	-	-
			S-S-42-12	TSI-10	10/06/2015*	-	-
			S-S-42-13	TSI-11	10/06/2015*	11/06/2003	-
			S-S-42-14	TSI-12	10/06/2015*	-	-
			S-S-42-15	TSI-13	10/06/2015*	-	-
			S-S-42-16	P-SI-01	04/06/2015	19/01/2009	-

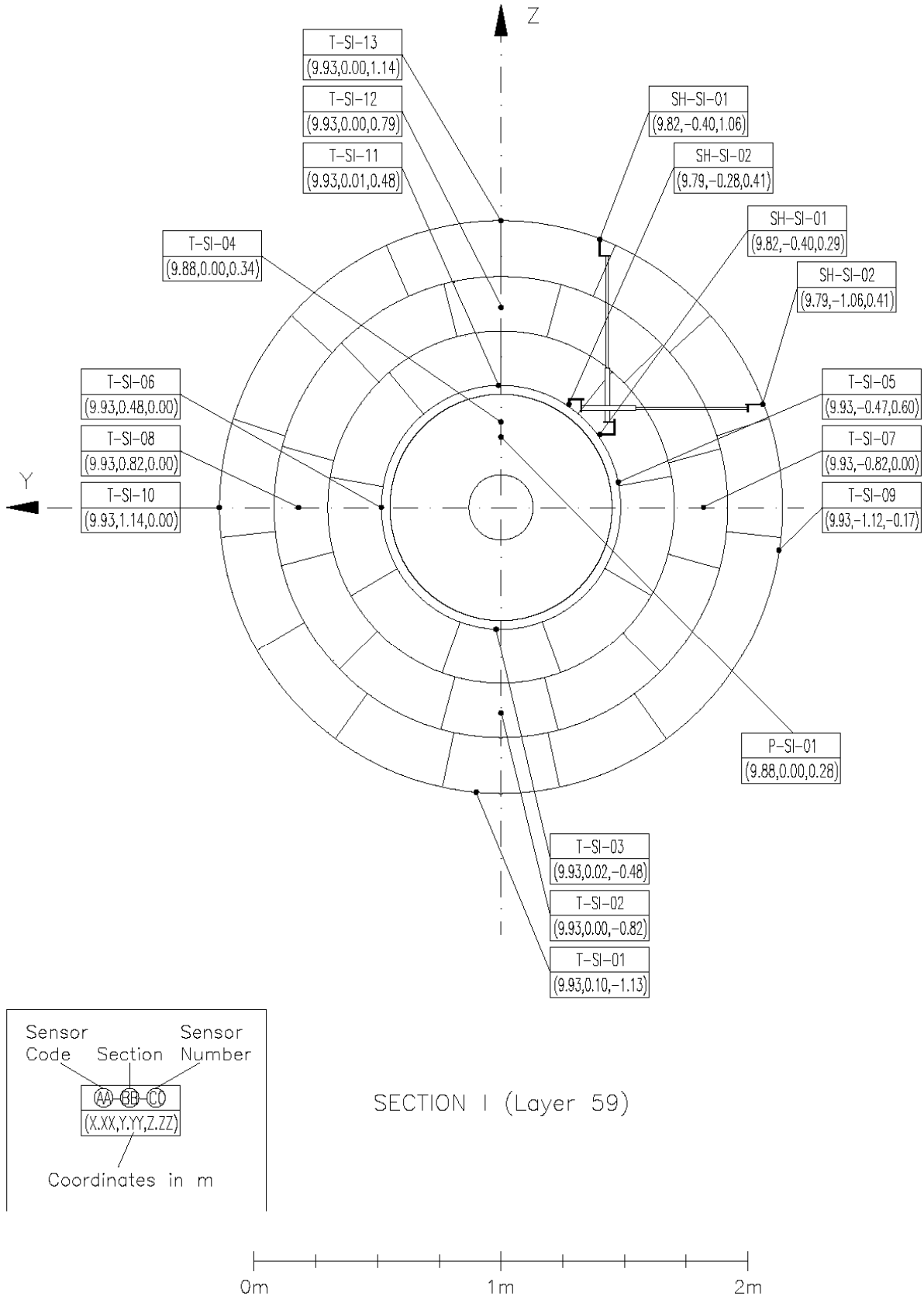

Figure 43. Sensors in sampling section 42

Figure 44. Sampling section 42 during dismantling

Figure 45. Sensors in sampling section 42 during dismantling

The heater displacement sensors (SHSI-01 and SHSI-02, see characteristic at section 9.3.4.) were found slightly deformed as a consequence of bentonite swelling. The body of the sensor was in good condition, but this was not the case of the coupling parts, screws…, which were quite rusty. The cable was not externally damaged but it seemed to have lost some of its properties and was very rigid, as it had previously happened with the same type of sensors in other sections (Geokon ones). There were no signs of water presence inside of the cable or the wires.

The technical data of the thermocouples can be found in section 9.3.1. and that of the total pressure cell in section 9.3.2. (GEOKON 4580-2-6MPa NATM type).

4.8 SAMPLING SECTION 46/INSTRUMENTED SECTION M2

Figure 47 shows the position of the sensors in sampling section 46 from which ten bentonite TDR probes (S-S-46-01 to 10/WTSM2-03 to 12) and ten temperature sensors were retrieved (see Table 9).

Figure 46. Sampling section 46 after installation

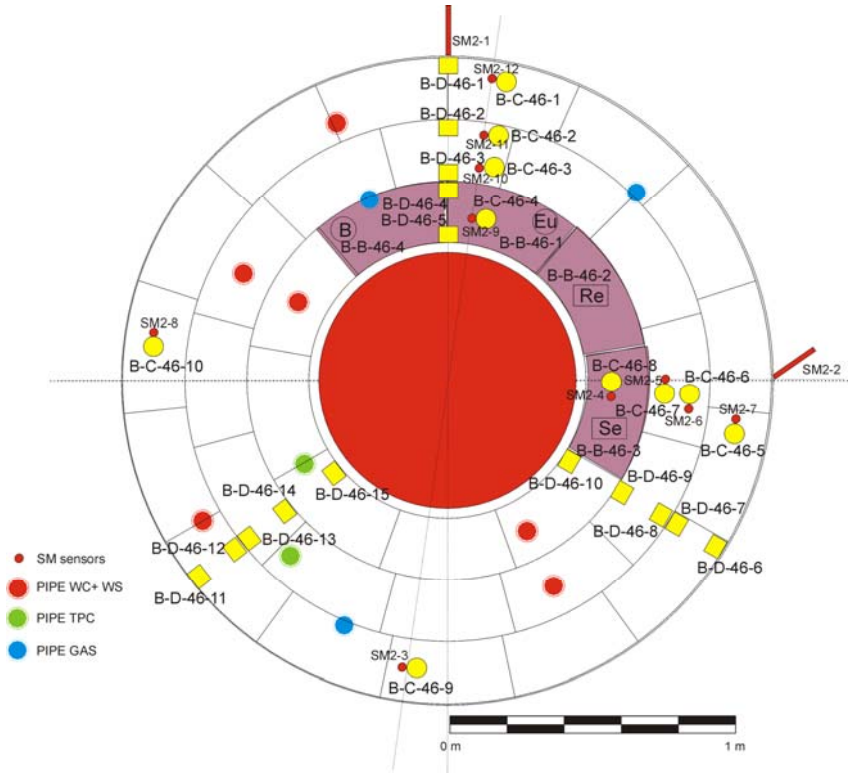

Figure 47. Sensors in sampling section 46
Bentonite TDR probes (50 cm long) extend over bentonite slices 46, 45, 44 and 43[4].

[4] The temperature sensors were positioned in the immediate vicinity of the connection between the TDR probe and the coaxial cable.

Sensor conditions

Table 9 and Table 10 summarise the list of sensors retrieved and sensor conditions, respectively. Selected photographs are provided in Figure 48. More details of the probe conditions are provided in Sakaki et al. 2016. The technical data of the TDRs are compiled in section 9.3.9.

Table 9. Sensors retrieved sampling section 42 / Instrumented section I

Dismantling section	Layer	GM (m)	Dismantling code	Installation code	Dismantling date	Date of failure	Damaged during dismantling
46	46, 45, 44, 43	64.5-65.0	S-S-46-01	WTSM2-03	02/07/2015	22/05/2003-	Yes
			S-S-46-02	WTSM2-04	01/07/2015	-	Yes
			S-S-46-03	WTSM2-05	01/07/2015	-	Yes
			S-S-46-04	WTSM2-06	01/07/2015	-	Yes
			S-S-46-05	WTSM2-07	01/07/2015	-	Yes
			S-S-46-06	WTSM2-08	30/06/2015	-	Yes
			S-S-46-07	WTSM2-09	30/06/2015	-	Yes
			S-S-46-08	WTSM2-10	30/06/2015	31/05/1997	Yes
			S-S-46-09	WTSM2-11	30/06/2015	01/10/2008	Yes
			S-S-46-10	WTSM2-12	30/06/2015	-	Yes

Table 10. Summary of sensor status and conditions

Sensor type	Sensor no.	Pre dismantling status	Sensor conditions	Cable conditions	Remark
TDR water content	WT-M2-03	no data	head missing	cut, missing	
	WT-M2-04	ok	shear up to 2 mm, coating brown	old cracks, small cracks near probe head	close to heater
	WT-M2-05	ok	small shear	cut, cracks near probe head	
	WT-M2-06	ok	small shear	cracked	
	WT-M2-07	ok	small shear, damages on coating from extraction	ok	
	WT-M2-08	ok	shear up to 1.5 mm, deep damage on coating from extraction	ok	
	WT-M2-09	suspicious	shear up to 3 mm, old long cracks on coating, coating brown	cracked near probe head	close to heater, trace of water in cracked coating
	WT-M2-10	no data	shear up to 3 mm, coating pealed	ok	
	WT-M2-11	no data	shear up to 3 mm, cuts on head	nearly disconnected	
	WT-M2-12	ok	shear up to 1 mm, coating peeled 15 cm	ok	

Cracked coating near heater (WT-M2-09)

Large shear at block joints (WT-M2-10)

Typical damage during extraction (WT-M2-11)

Typical damage during extraction (WT-M2-10)

Typical damage during extraction (WT-M2-11)

Nearly disconnected cable (WT-M2-11)

Figure 48. Selected photographs of the retrieved TDR probes

A change in colour from white to brown was seen on the coating film of the probes near the heater (WT-M2-04 and 09). The cable protection showed old cracks in half of the probes (WT-M2-04, 05, 06, 09 and 11), sensor no. 11 –that had failed in 2008– was the most damaged. Most of the probes showed shear deformation at the bentonite block interfaces, although it didn't seem to disturb the volumetric water content estimated with the TDRs that was in close agreement with the sample results, except for WT-M2-09 that had major cracks on the probe coating.

4.9 SAMPLING SECTION 47/INSTRUMENTED SECTION F2

There was only a crackmeter / fissurometer (S-S-47-1) in this bentonite slice, which belongs to instrumented section F and was dismantled on the 3rd of July 2015. The technical data of this particular sensor can be found in section 9.3.10.

The crackmeter, which had three sensors to measure the displacement in three spatial directions, was out of order from the early part of the operational phase, see Table 11. The majority of sensors of measuring section F2 were located in next sampling section.

Figure 49. Sampling section 47 after installation, the arrow indicated the location of the sensor

Figure 50. Sampling section 47 during dismantling
The crackmeter is shown inside the red circle

Table 11. Sensors retrieved sampling section 47 / Instrumented section F2
(codes 1 to 3 refer to the three sensors of the crackmeter)

Dismantling section	Layer	GM (m)	Dismantling code	Installation code	Dismantling date	Date of failure	Damaged during dismantling
47	44	11.75	S-S-47-1	3SEF2-01-F1	03/07/2015	13/07/1999	-
			S-S-47-2	3SEF2-01-F2	03/07/2015	13/07/1999	-
			S-S-47-3	3SEF2-01-F3	03/07/2015	13/07/1999	-

The metal box of the crackmeter was found filled with water and with all metal parts in an advanced state of corrosion. The sensing elements inside showed evidence of prolonged submersion in water; the cables were disintegrated in some points, with the inner wires completely rusty/corroded (see Figure 51 and Figure 52). The cable glands that used to isolate the cable input from the sensing element were no longer fixed to it.

Figure 51. S-S-47-1 / 3SEF2-01-F1 box filled with water after dismantling

Figure 52. Detail of the state of the crackmeter components (S-S-47-1 / 3SEF2-01-F1)

4.10 SAMPLING SECTION 48/INSTRUMENTED SECTION F2

The sensors from instrumented section F2 (eight psychrometers S-S-48-1 to 8/WCSF2-01 to 08, eight pore pressure sensors S-S-48-9 to 16/QSF2-01 to 08, eight thermohygrometers of the capacitive type S-S-48-17 to 24/WPSF2-01 to 08, four thermocouples S-S-48-25 to 28/TSF2-01 to 04 and two extensometers S-S-48-29&30/SBSF2-01&02) were dismantled between the 2nd and 10th of July 2015. Only 9 of the 30 sensors were still operative at the time of dismantling; see Table 12 for information.

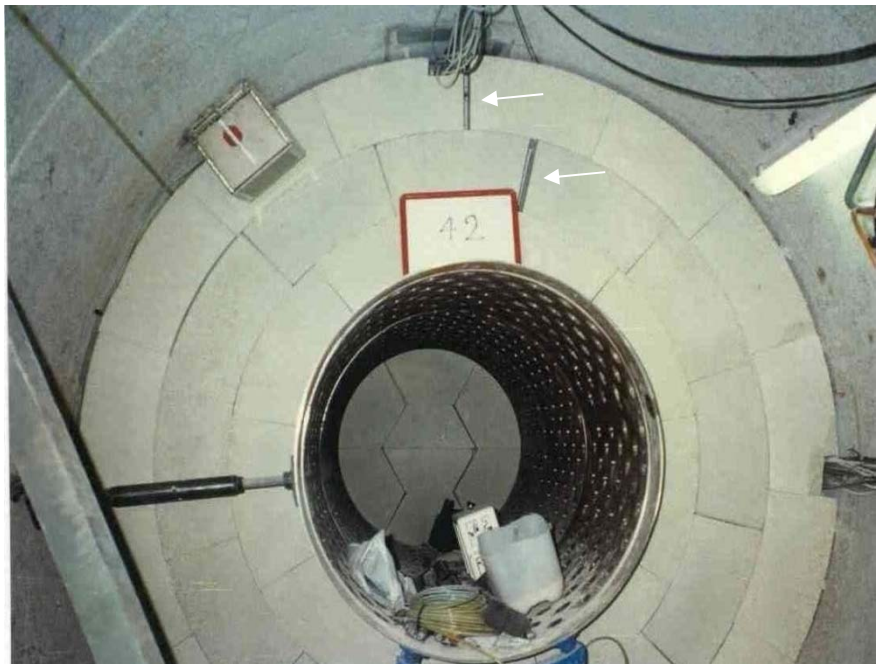

Figure 53. Sampling section 48 after installation
Gaps (see white arrows) between blocks seen at the upper part of the barrier are due to buffer construction

Figure 54. Sampling section 48 after dismantling

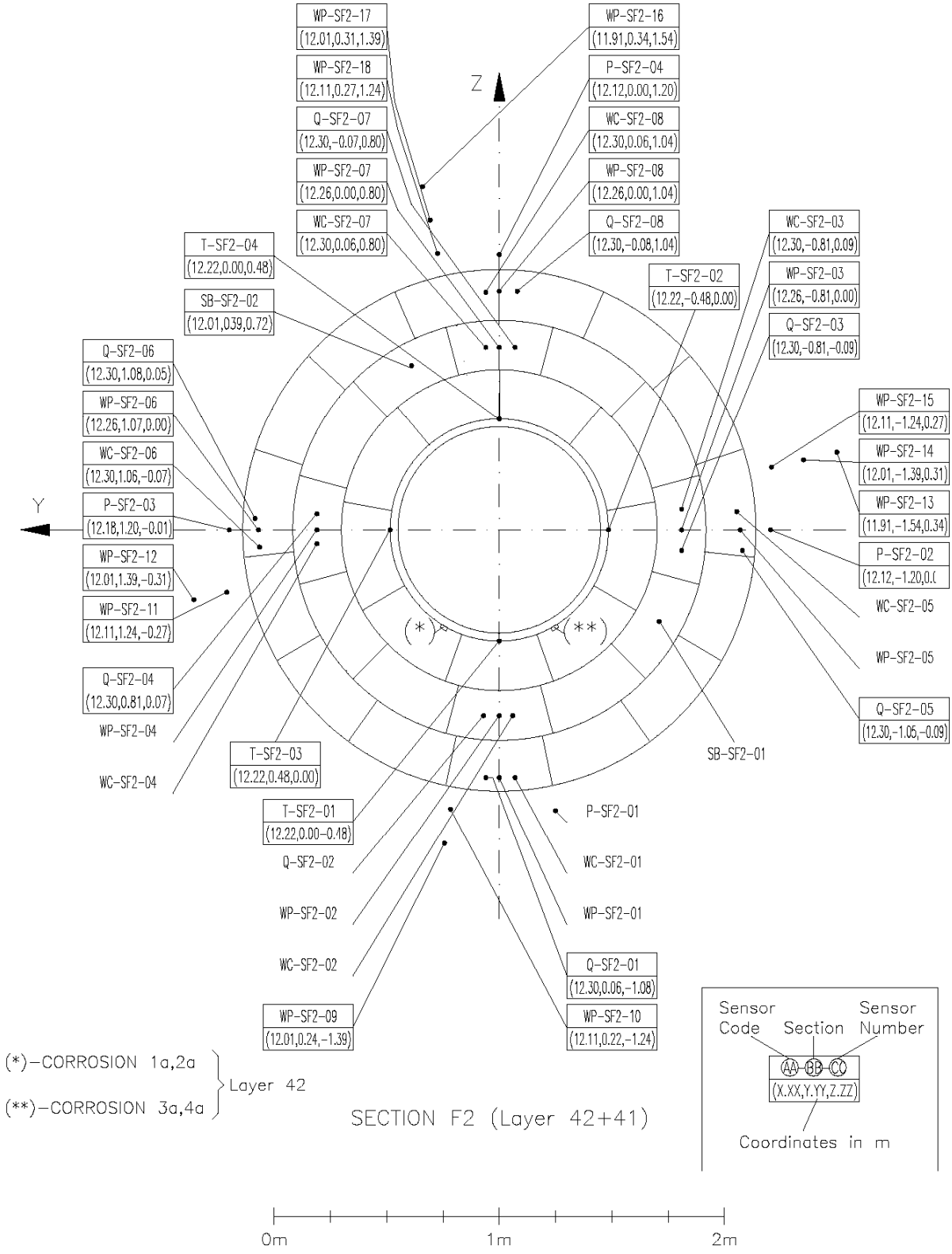

Figure 55. Sensors in sampling section 48

Table 12. Sensors retrieved sampling section 48 / Instrumented section F2

Dismantling section	Layer	GM (m)	Dismantling code	Installation code	Dismantling date	Date of failure	Damaged during dismantling
48	42	12.01	S-S-48-1	WCSF2-01	06/07/2015	16/01/1997	-
			S-S-48-2	WCSF2-02	06/07/2015	26/11/2001	Yes
			S-S-48-3	WCSF2-03	06/07/2015	26/06/2003	-
			S-S-48-4	WCSF2-04	06/07/2015	05/04/2003	Yes
			S-S-48-5	WCSF2-05	06/07/2015	15/10/1997	-
			S-S-48-6	WCSF2-06	06/07/2015	15/11/2005	-
			S-S-48-7	WCSF2-07	06/07/2015	26/03/2003	-
			S-S-48-8	WCSF2-08	06/07/2015	19/06/1999	-
			S-S-48-9	QSF2-01	07/07/2015	-	-
			S-S-48-10	QSF2-02	07/07/2015	-	Yes
			S-S-48-11	QSF2-03	07/07/2015	05/05/2005	-
			S-S-48-12	QSF2-04	07/07/2015	31/03/2009	-
			S-S-48-13	QSF2-05	06/07/2015	05/05/2006	-
			S-S-48-14	QSF2-06	06/07/2015	22/09/2004	-
			S-S-48-15	QSF2-07	03/07/2015	-	-
			S-S-48-16	QSF2-08	03/07/2015	18/06/2003	Yes
			S-S-48-17	WPSF2-01	06/07/2015	-	-
			S-S-48-18	WPSF2-02	06/07/2015	15/10/1997	-
			S-S-48-19	WPSF2-03	06/07/2015	12/07/2002	-
			S-S-48-20	WPSF2-04	06/07/2015	29/06/1998	-
			S-S-48-21	WPSF2-05	06/07/2015	23/06/1997	-
			S-S-48-22	WPSF2-06	06/07/2015	-	-
			S-S-48-23	WPSF2-07	03/07/2015	05/08/1997	-
			S-S-48-24	WPSF2-08	06/07/2015	-	-
			S-S-48-25	TSF2-01	02/07/2015*	-	Yes
			S-S-48-26	TSF2-02	02/07/2015*	-	-
			S-S-48-27	TSF2-03	02/07/2015*	31/08/2002	-
			S-S-48-28	TSF2-04	02/07/2015*	18/06/2002	-
			S-S-48-29	SBSF2-01	10/07/2015	22/02/1998	-
			S-S-48-30	SBSF2-02	10/07/2015	-	-

The capacitive thermohygrometers (WC-SF2-01 to 08, see characteristics in section 9.3.7.) had saturated during the operational phase but they were found in good condition in general, showing small signs of humidity under the plastic jacket that protected the body of the sensors.

In general, the inner part of the sensor (inner part of filter and sensing element) showed evidence of contact with water. The sensors installed at the upper part of the section were in better condition than those installed in the lower part (see Chapter 5); the damage caused by water –corrosion, degradation and disintegration of the sensing element– were larger in the lower part of the section.

Those sensors installed in the central ring showed important signs of squashing of the cable and of the thermo-retractile that covers the metal body (WC-SF2-03 and 04), especially in the sensor installed on the right (WC-SF2-04); see Figure 56 and Figure 57.

Figure 56. Detail state of sensor WC-SF2-03

Figure 57. Detail of the state of cable sensor WC-SF2-04

The cable and the cable plastic jacket were quite degraded and sometimes broken, as in sensor WC-SF2-02 (Figure 58).

Figure 58. Detail of the state of sensor WC-SF2-02 in situ after dismantling

The pore pressure sensors (Q-SF2-01 to 08, see technical data in section 9.3.3.) were found in quite good conditions. There were traces of humidity in the inner part of the filter but the intermediate zone was clean. These sensors had no visible humidity effects. Again, the cables of those sensors installed in the central ring were damaged (Q-SF2-03, Q-SF2-04 and Q-SF2-07), most probably due to the bentonite swelling.

The cables at the output of the sensor were bent in a 90° angle breaking the cable at this point in some cases (see Figure 59 Q-SF2-01, 04, 05, 07 and 08; see Figure 60). The inner wires/conductors were rusty (showed signs of rustiness), especially in those sensors with broken cables.

Figure 59. Detail of the cable conditions at the sensor's output, Q-SF2-04

Figure 60. Detail of the cable position at the sensor's output, Q-SF2-07

The psychrometers (WP-SF2-01 to 08, see characteristics in section 9.3.8.) were clearly affected by the bentonite swelling, with the protection body slightly deformed and the measuring area broken as a consequence of the cable's stretching (WP-SF2-02 and 03).

The filter was damaged and had even disappeared in some cases (WP-SF2-01, 03, 05 and 06). The cable and the protection tube were in a bad state, very damaged, with evident signs of degradation (black colour in some points). The sensors with the most significant signs of damage were those installed in the lower part and left part of the section.

Figure 61. Detail of the deformation of sensor WP-SF2-04

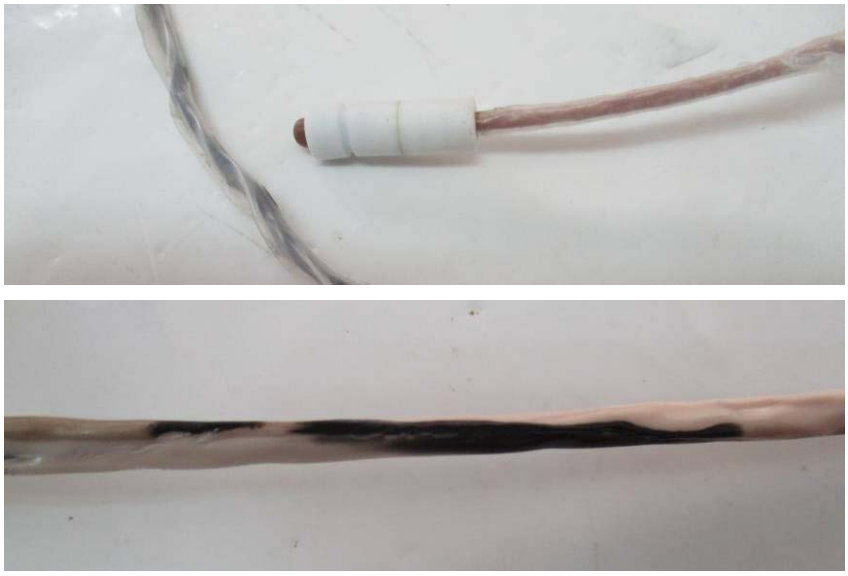

Figure 62. Detail of the state of cable sensor WP-SF2-07

Figure 63. Detail of cable stretching of WC-SF2-02 due to swelling of bentonite

The bentonite block extensometers (SBF2-01 and SBF2-02) were found slightly deformed and blocked. The body of the sensor was in good condition, but the rest of the sensor elements (anchors, screws…) were rusty. The technical data of these sensors can be found in section 9.3.5.

The cable was brown at the sensor output, probably as a consequence of corrosion. Some traces of humidity/water were found in the inner part of the cable of SBF2-01.

Figure 64. View of sensor SBF2-02 during dismantling

Figure 65. Detail of cable output from sensor SBF2-01

As mentioned in the previous sections, the effect of bentonite swelling was greater in those sensors located in the left side of the section, especially in those installed in the central ring.

As usual, the thermocouples were moved away and left in place for further calibration, see Figure 66 and Figure 67.

Figure 66. Detail of one thermocouple before being collected

Figure 67. View of a corroded dent at the end of one thermocouple

4.11 SAMPLING SECTION 51/INSTRUMENTED SECTION E2

This section corresponds to instrumented section E2. The sensors (ten thermohygrometers of the capacitive type S-S-51-1 to 10/WCSE2-01 to 10, eight pore pressure sensors S-S-51-11 to 18/QSE2-01 to 08, eight psychrometers S-S-51-19 to 26/WPSE2-01 to 08, two thermocouples S-S-51-27&28/TSE2-01 &02, two total pressure cells S-S-51-29&30/PSE2-02&05 and two extensometers S-S-51-31&32/SBSE2-01&02) were dismantled between the 9th and 13th of July 2015. See the state of sensors in

Table 13.

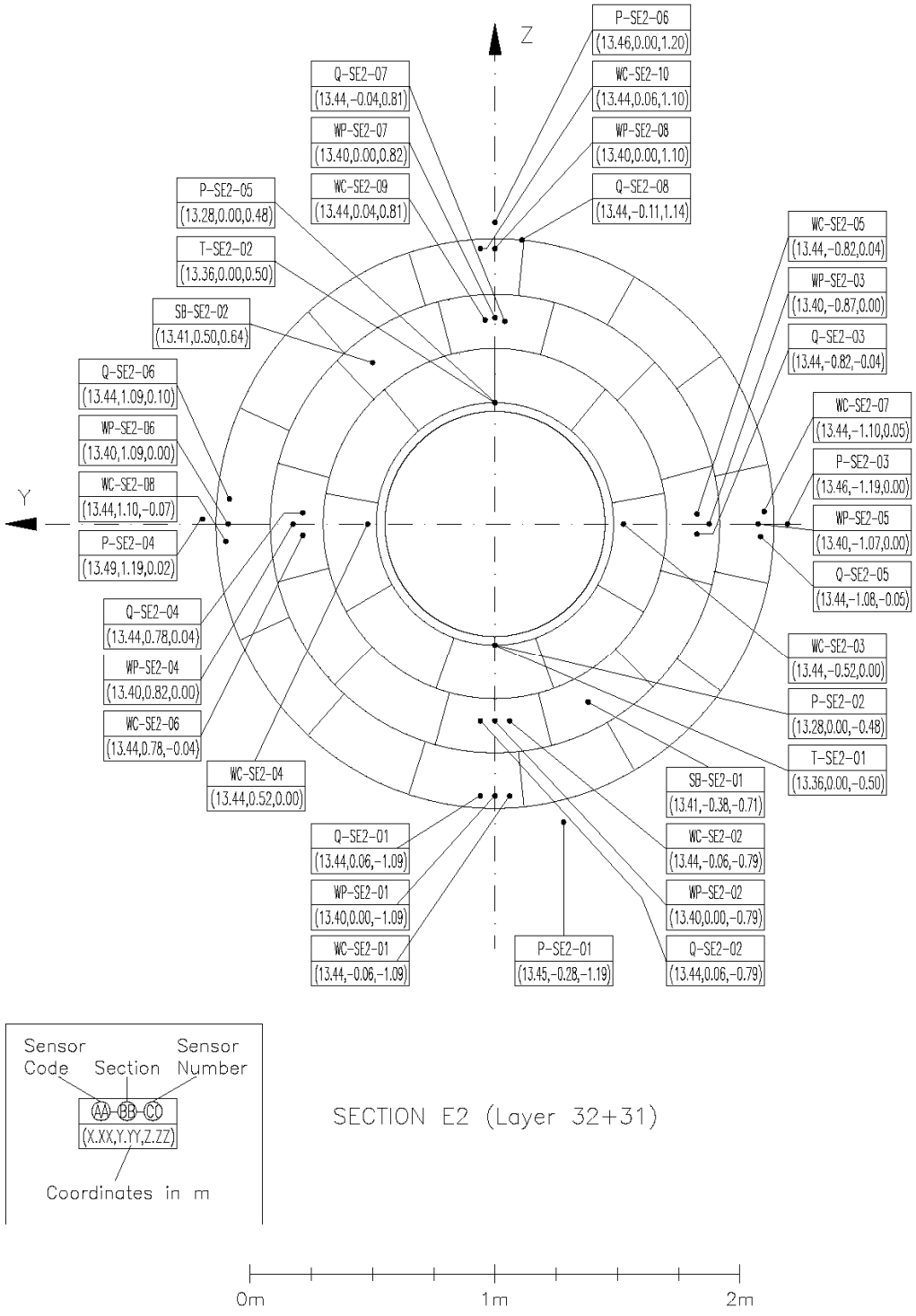

Figure 68. Sensors in sampling section 51

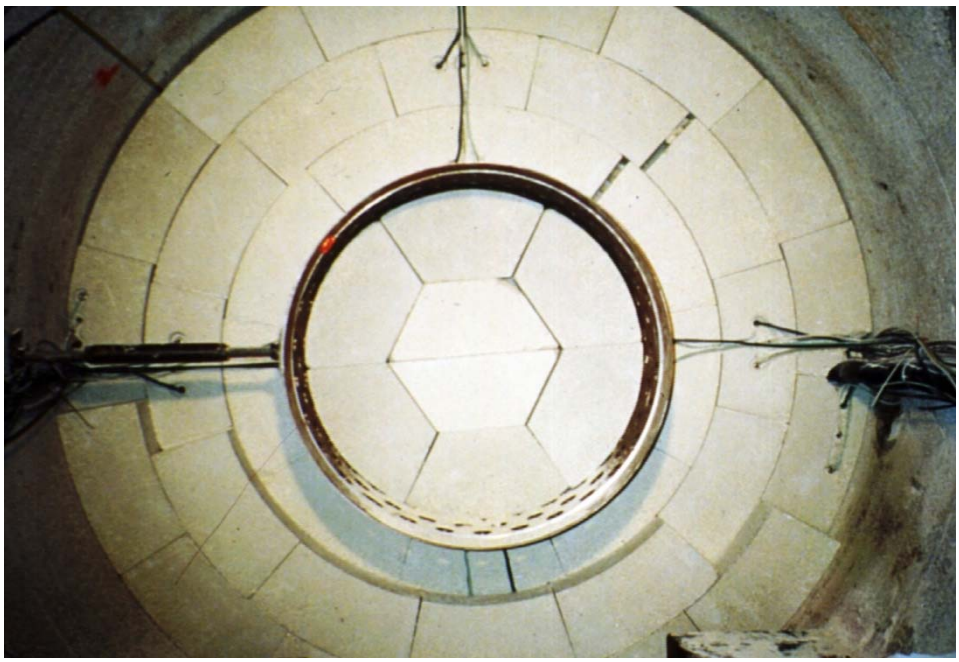

Figure 69. General view of instruments after being installed at the bentonite front

Figure 70. View of extensometers during installation inside bentonite blocks

Table 13. Sensors retrieved sampling section 51 / Instrumented section E2

Dismantling section	Layer	GM (m)	Dismantling code	Installation code	Dismantling date	Date of failure	Damaged during dismantling
51	32	13.28	S-S-51-1	WCSE2-01	13/07/2015	16/01/1997	-
			S-S-51-2	WCSE2-02	13/07/2015	16/01/1997	-
			S-S-51-3	WCSE2-03	09/07/2015	04/05/1997	-
			S-S-51-4	WCSE2-04	13/07/2015	25/07/1997	-
			S-S-51-5	WCSE2-05	10/07/2015	31/10/1997	-
			S-S-51-6	WCSE2-06	13/07/2015	16/03/1997	-
			S-S-51-7	WCSE2-07	10/07/2015	14/07/1999	-
			S-S-51-8	WCSE2-08	13/07/2015	14/10/2000	-
			S-S-51-9	WCSE2-09	10/07/2015	22/03/1999	-
			S-S-51-10	WCSE2-10	10/07/2015	28/01/2001	-
			S-S-51-11	QSE2-01	13/07/2015	-	-
			S-S-51-12	QSE2-02	13/07/2015	26/09/2014	-
			S-S-51-13	QSE2-03	10/07/2015	12/08/2009	-
			S-S-51-14	QSE2-04	13/07/2015	16/04/1999	-
			S-S-51-15	QSE2-05	13/07/2015	-	-
			S-S-51-16	QSE2-06	13/07/2015	09/11/2007	-
			S-S-51-17	QSE2-07	13/07/2015	-	-
			S-S-51-18	QSE2-08	13/07/2015	-	-
			S-S-51-19	WPSE2-01	13/07/2015	30/09/2000	-
			S-S-51-20	WPSE2-02	13/07/2015	01/04/1998	-
			S-S-51-21	WPSE2-03	13/07/2015	03/05/1997	-
			S-S-51-22	WPSE2-04	13/07/2015	01/01/1999	-
			S-S-51-23	WPSE2-05	13/07/2015	20/07/2002	-
			S-S-51-24	WPSE2-06	13/07/2015	17/07/1998	-
			S-S-51-25	WPSE2-07	10/07/2015	18/05/1997	-
			S-S-51-26	WPSE2-08	10/07/2015	04/04/2001	-
			S-S-51-27	TSE2-01	13/07/2015	-	Yes
			S-S-51-28	TSE2-02	13/07/2015	19/12/1996	Yes
			S-S-51-29	PSE2-02	13/07/2015	24/02/2005	-
			S-S-51-30	PSE2-05	13/07/2015	27/03/1997	-
			S-S-51-31	SBSE2-01	13/07/2015	13/12/1999	-
			S-S-51-32	SBSE2-02	13/07/2015	26/08/2009	-

Figure 71. Sampling section 51 during dismantling

The thermohygrometers (WC-SE2-01 to 10, see technical data in section 9.3.7.) were in quite good condition, with only a few traces of rust under the plastic jacket protecting the sensor in WC-SE2-01, 02, 07 and 08. In the case of WC-SE2-03 and 04, the sensor body was very rusty; see Figure 72. The effect was smaller for WC-SE2-05 and 06.

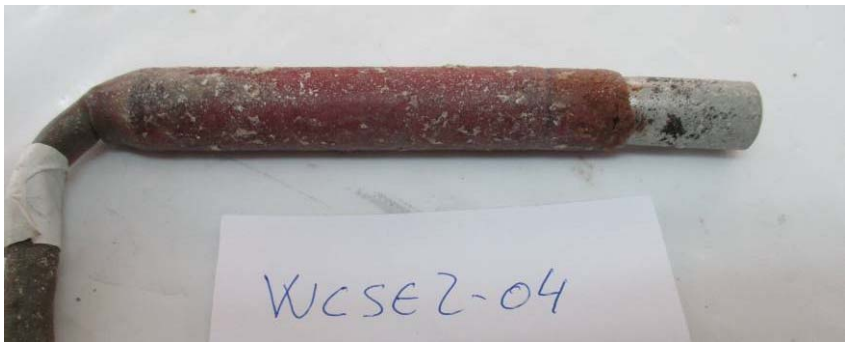

Figure 72. Detail of thermo-retractile with rust from sensor WC-SE2-04

The sensing element and inner side of the filter were damaged in almost all sensors; it was disintegrated in the case of sensors WC-SE2-03, 05 and 10 and to a smaller extent in sensors 04 and 06; see Figure 73. Sensor WC-SE2-07 was recovered with no filter, and bentonite was found in the measuring element. The rest of sensors were dirty and rusty, but without important damage.

Figure 73. Detail of the state of sensing element sensor WC-SE2-05

The cables of those sensors located in the central ring showed important/significant damage, as well as those installed in contact with the rock. The cable and its thermo-retractile protection were quite degraded, as seen in previous dismantled sections, see Figure 74.

Figure 74. Detail of the squashed cable sensor WC-SE2-10

The pore pressure sensors (QSE2-01 to 08, see technical data in section 9.3.3.) did not show anything remarkable. The external appearance was good and there were only small traces of humidity inside the filter and in the sensing element. Some rust traces were observed in sensor QSE2-03, whereas the cables of sensors QSE2-01 and 04 were broken just at the base of the sensors as in previous sections; see Figure 75.

Figure 75. Detail of broken cable, sensor QSE2-04

Sensor QSE2-08 was slightly deformed as a consequence of bentonite swelling, Figure 76.

Figure 76. Detail of sensor QSE2-08 deformation

The case of the psychrometers (WPSE2-01 to 08, see technical data in section 9.3.8.) was similar to previous sections. In general, they were slightly deformed (see Figure 77), with the filters appearing broken in the case of sensors 01, 03, 04, 05, 06 and 07. The cable and the protection tube were both quite damaged; the colour of the cable had turned black; see Figure 78.

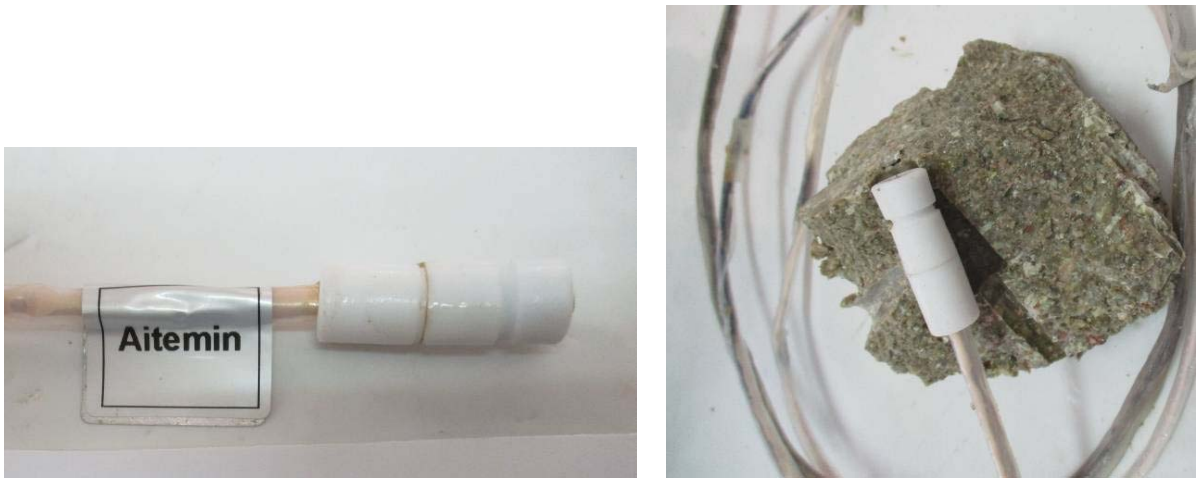

Figure 77. Detail of psychrometers' protection slightly deformed by bentonite's swelling (left S-S-51-19 / WPSE2-01; right S-S-51-23 / WPSE2-05)

Figure 78. Detail of cable sensor WP-SE2-07

The transducer of total pressure cells PSE2-02 and 05 was found deformed, as if they had been exposed to a great stress, see Figure 79. The technical data of these sensors can be found in section 9.3.2. (GEOKON 4580-2-6MPa NATM type).

Figure 79. Detail of deformation of sensor PSE2-02

In the case of PSE2-05 the body of the sensor appeared stretched, with the tightness joint damaged; a mercury leak was detected in this joint (see Figure 80).

Figure 80. Detail of sensor PSE2-05 with the joints sealed due to the mercury leak

The extensometers (SB-E2-01 and SB-E2-02, see technical data in section 9.3.5.), were slightly deformed as a consequence of bentonite swelling; see Figure 81. There were traces of rust in the vicinity of the sensor's body. Sensor SB-E2-02 was blocked.

Figure 81. Detail of deformation of sensor SB-E2-02

Figure 82. Detail of the state of the cable (sensor SB-E2-02)

Again, the thermocouples were moved to the rock walls in order to be checked later, see Figure 83.

Figure 83. Detail of some sensors before being retrieved and located below the liner where thermocouple T-SE2-01 can be seen close to the total pressure cell P-SE2-02

4.12 SAMPLING SECTION 54/INSTRUMENTED SECTION D2

There were three extensometers S-S-54-14 to 16 / SHSD2-01 to 03 and thirteen thermocouples S-S-54-1 to 13 / T-D2-01 13 in this section; in principle many of them were operative before dismantling. The extensometers (see Table 15) were sent to Tecnalia (Madina 2016) for further analysis and the thermocouples were left in place for further calibration (see Figure 85).

Table 14. Sensors retrieved sampling section 54 / Instrumented section D2

Dismantling section	Dismantling code	Installation code	Dismantling date	Date of failure	Damaged during dismantling
54	S-S-54-1	TSD2-01	17/07/2015*	-	-
	S-S-54-2	TSD2-02	17/07/2015*	-	-
	S-S-54-3	TSD2-03	17/07/2015*	11/08/2013	-
	S-S-54-4	TSD2-04	17/07/2015*	12/08/2000	-
	S-S-54-5	TSD2-05	17/07/2015*	-	-
	S-S-54-6	TSD2-06	17/07/2015*	-	Probably
	S-S-54-7	TSD2-07	17/07/2015*		-
	S-S-54-8	TSD2-08	17/07/2015*	-	-
	S-S-54-9	TSD2-09	17/07/2015*	-	-
	S-S-54-10	TSD2-10	17/07/2015*	-	-
	S-S-54-11	TSD2-11	17/07/2015*	-	-
	S-S-54-12	TSD2-12	17/07/2015*	16/06/2003	-
	S-S-54-13	TSD2-13	17/07/2015*	-	Probably
	S-S-54-14	SHSD2-01	20/07/2015	17/01/2005	-
	S-S-54-15	SHSD2-02	20/07/2015	-	-
	S-S-54-16	SHSD2-03	21/07/2015	18/06/2001	-

Table 15 lists the sensors that were sent to TECNALIA.

Table 15. List of sensors sent to TECNALIA

Dismantling section	Dismantling code	Installation code
54	S-S-54-14	SHSD2-01
	S-S-54-15	SHSD2-02
	S-S-54-16	SHSD2-03

The technical data of the thermocouples can be found in section 9.3.1; those of the extensometers in section 9.3.4.

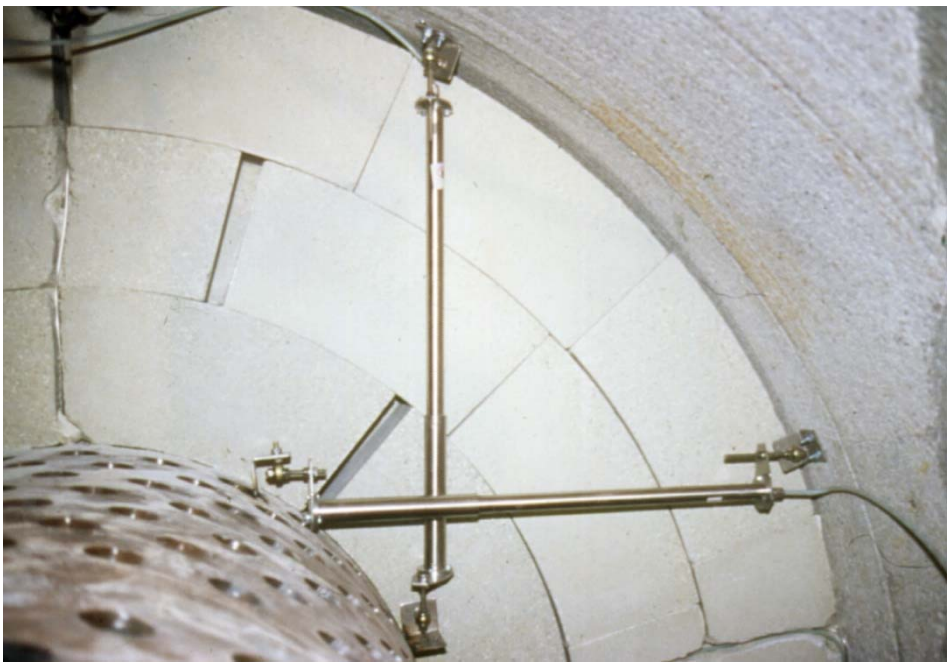

Figure 84. View of extensometers after being installed

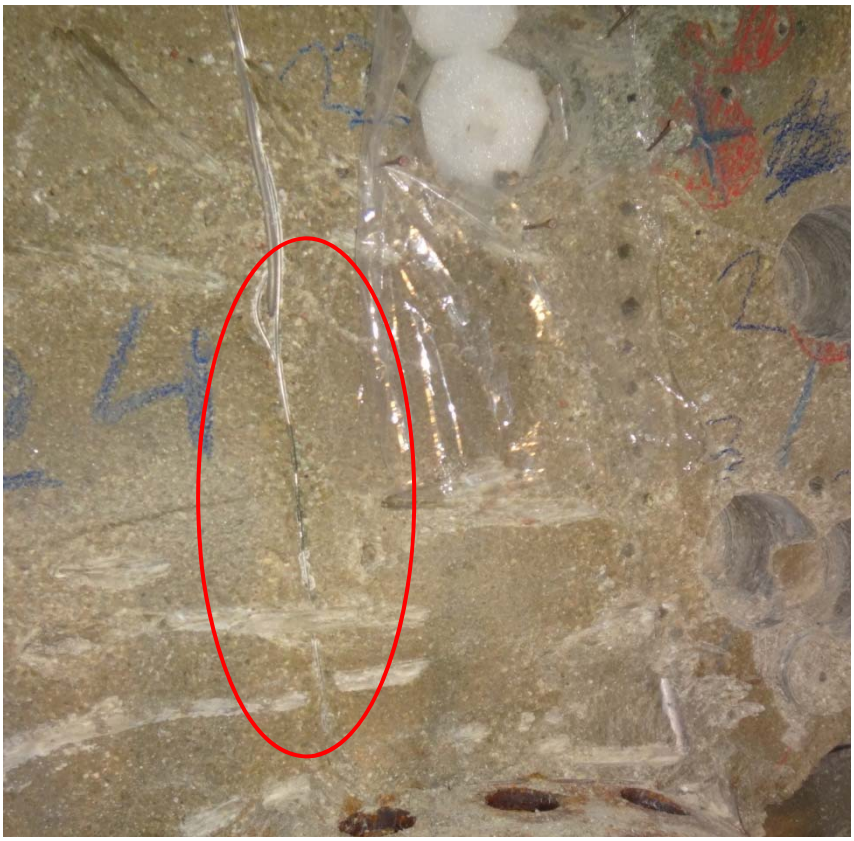

Figure 85. Detail of thermocouples T-SD2-12 and 11 running towards the liner where some rust (black colour) can be seen in T-SD2-11

4.13 SAMPLING SECTION 62/INSTRUMENTED SECTION B2

There were nine thermocouples in this section, T-SB2-01 to 09 / S-S-62-1 to 9. All of them – which were in principle operative– were left in place for further calibration. The technical data of the thermocouples can be found in section 9.3.1.

Table 16. Sensors retrieved sampling section 62 / Instrumented section B2

Dismantling section	Dismantling code	Installation code	Dismantling date	Date of failure	Damaged during dismantling
62	S-S-62-1	TSB2-01	04/08/2015*	-	-
	S-S-62-2	TSB2-02	04/08/2015*	-	-
	S-S-62-3	TSB2-03	04/08/2015*	-	-
	S-S-62-4	TSB2-04	04/08/2015*	-	-
	S-S-62-5	TSB2-05	04/08/2015*	19/12/1996	-
	S-S-62-6	TSB2-06	04/08/2015*	-	-
	S-S-62-7	TSB2-07	04/08/2015*	-	-
	S-S-62-8	TSB2-08	04/08/2015*	-	Probably
	S-S-62-9	TSB2-09	04/08/2015*	-	-

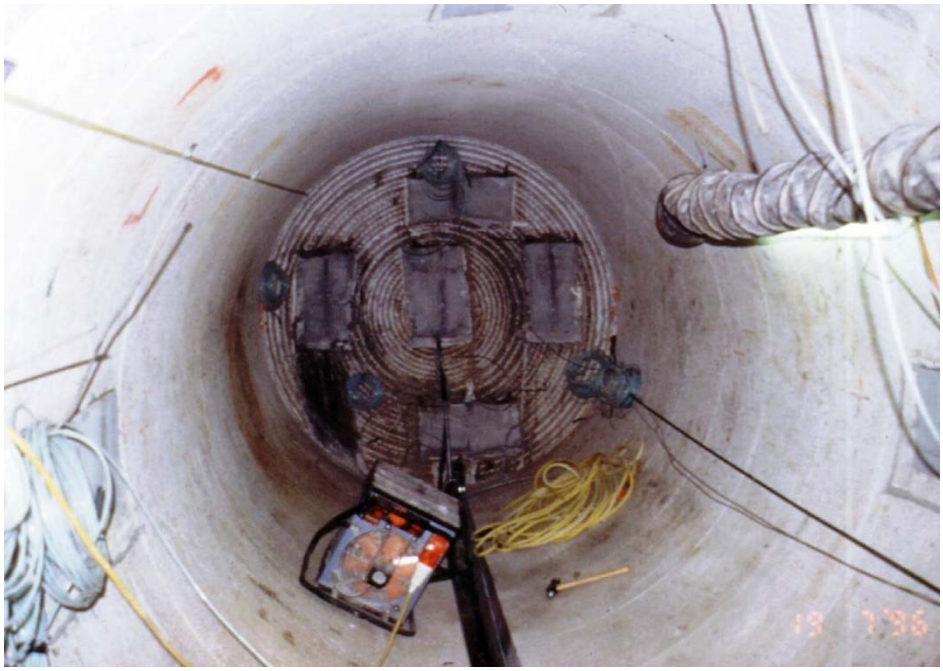

Figure 86. View of the back of the gallery with the total pressure cells embedded in rock and the thermocouples at the rock surface

5 POST DISMANTLING ANALYSIS OF SENSORS

A general synthesis of the state of the sensors according to their type is given in this section.

5.1 VIBRATING WIRE SENSORS

The vibrating wire type sensors –total pressure cells, pore pressure sensors and extensometers– manufactured by Geokon Inc. were quite robust and many of them remained operative during the complete operational phase (18 years), up to 60% of pore pressure sensors, up to 50% of the total pressure cells, 25% of the bentonite block extensometers and 14% of the heater ones (see Table 17). However, only some pore pressure sensors were found functioning during the verification made at the laboratory (see chapter 6.1).

5.1.1 Mechanical effects

The mechanical effects caused by the swelling of bentonite were not significant in these sensors, with the exception of the extensometers placed in vicinity of the heaters and the bentonite blocks, there deformations were such that they prevented the correct functioning of the sensor. This deformation was the cause of failure in almost all the cases. The mechanical effects witnessed in the pore pressure sensors did not affect their performance significantly. With regard to the total pressure cells, the transducers of these cells in section E2 showed important mechanical effects and both cells failed during the experiment. In general, the sensor cables had become more fragile after functioning in these circumstances over an extensive time period; they lost the initial flexibility favouring breakdown in case of smashing or pulling.

5.1.2 Corrosion and tightness

The effects of corrosion were almost negligible in these sensors. The body of the sensors, made of stainless steel 316L, remained in good condition. A corrosion study on three heater extensometers (see Table 15) was made by Tecnalia (Madina 2016), which indicates that the corrosion damage observed on these sensors is located on the carbon steel components for anchoring the sensors to the rock and to the liner. The corrosion damage observed in the stainless steel components of the anchoring devices is attributed to the corrosion of carbon or low alloyed steel particles/residues from the welding process and no signs of localized or generalized corrosion were observed on the 316 stainless steel tubes sensors. Further investigations are reported in Wersin et al. 2016.

The sensors remained water tight and the electronics were not in direct contact with free water. The wires did not suffer any rusting process, apart from those whose cable jacket was broken.

A disassembly was performed on one sensor of each type, focussing on those that failed during the test or presented a worse than general status, in order to determine the principal weak spots.

Total pressure cells

These sensors have a joint (O-ring seal) to guarantee the water tightness of the transducer at the cable entry and to avoid any mercury leaks. This seal withstood the long duration of the test and the conditions of the experiment. However, in case the sensor was deformed as a consequence of bentonite swelling, the sealing could be lost and mercury did leak, as was the case for PSE2-05. Nevertheless, in general, the sensors remained watertight, with a minimal presence of rust in the inner wires and only evident/visible in those sensors whose cable was previously damaged.

Figure 87. Total pressure cell close-up of a disassembled damaged sensor

Pore pressure sensors

These sensors were made of a metallic cylinder with a membrane and a filter on one side and the transition to cable/wire on the opposite end. Both ends were sealed by means of O-rings and the interior was empty; no resin filled the body.

Sensor QSH-02 was disassembled –the body was cut longitudinally to observe the interior part– and the presence of rust inside the chamber was observed (see Figure 88), originating in the measuring membrane. However, the quantity of rust was negligible considering the duration of the experiment and the fact that there was no effect on the sensor's electronics. It can be therefore stated that these sensors were watertight and robust.

Figure 88. Pore pressure sensor QSH-02 after being cut longitudinally, close-up of disassembled parts

Figure 89. Detail of pore pressure sensor QSH-02 close-up

Displacement sensors or extensometers

These sensors are made of a cylinder that houses the sensing element, and which moves along another cylinder that acts as protection as well, preserving water tightness by means of several O-rings. The transition sensor's electronics-vibrating wire was encapsulated with resin. Again, the body of one sensor (SHSG-02) was cut longitudinally to inspect the interior (Figure 90).

Figure 90. Extensometer close-up of disassembled parts

From the visual inspection, it can be concluded that the main problem for these sensors was the deformation caused by bentonite swelling. When the tubes were slightly bent the movement was limited and finally blocked. As a consequence of this deformation the O-rings may lose their seal, allowing water or bentonite to enter although in small amounts only.

Therefore, the main cause of failure for these sensors was a mechanical defect. They can be called delicate, probably due to their long size.

Survival rate for vibrating wire sensors

The survival rate, i.e. the sensors still operative at the time of dismantling, of the vibrating wire sensors is synthesised in Table 17.

Table 17. Survival rate of vibrating wire sensors

Sensor type	Total number of sensors	Number survived	Survival rate	General remark
Total pressure cells	6	3	50%	
Pore pressure	28	17	60%	Only some were operative at the laboratory
Heater displacement	7	1	14%	
Bentonite block displacement	4	1	25%	
Total	**45**	**22**	**48.9%**	

5.2 CAPACITIVE TYPE RELATIVE HUMIDITY SENSORS

These sensors (manufactured by ROTRONIC) turned out to be quite robust, as they remained functional and survived significantly longer than their life expectations (only six months according to manufacturer at the beginning) in an experiment such as this. Note that although all sensors failed during the test due to flooding they were capable to track the increase of saturation of the bentonite up to their upper range (100% RH).

The rate of failure/saturation was high during the first year (8 units) and then it was of 2-3 units per year only until 2002. Just after the partial dismantling the rate raised up to 8 units again (2003) and the last sensor lasted until 2005. These sensors were not checked or calibrated by the manufacturer this time as it was done after the partial dismantling (García-Siñeriz et al. 2006).

5.2.1 Mechanical effects

The mechanical defects in these sensors were seen mostly in the cable, which was protected with thermo-shrinkage tubing at the vicinity of the sensor body. The body of the sensors, made of stainless steel, was resistant to the bentonite swelling and only some filters broke; however, the thermo-shrinkage tubing and the cables did suffer from being crushed by the bentonite.

5.2.2 Corrosion

This seems to be the weak point of these sensors. In general, the corrosion and rusting took place in the sensing element (inside the chamber isolated from the bentonite thanks to a metallic filter) and the cable. There was evidence of the presence of water inside the filters and in direct contact with the sensing element, causing the oxidation or even destruction in the worst cases.

There were clear signs of decomposition of the cable and its protection made of thermo-shrinkage tubing; their mechanical properties were deeply affected.

5.2.3 Water tightness

The body of the capacitive relative humidity sensor WCSH-09 was cut longitudinally to examine the inner part (Figure 91). As a result, it can be stated that these sensors lost their water tightness during the operation. The water reached the sensing element entering by the filter or by the connecting point of filter and capsule. This connection was protected by thermo-shrinkage tubing but the protection did not prove effective enough.

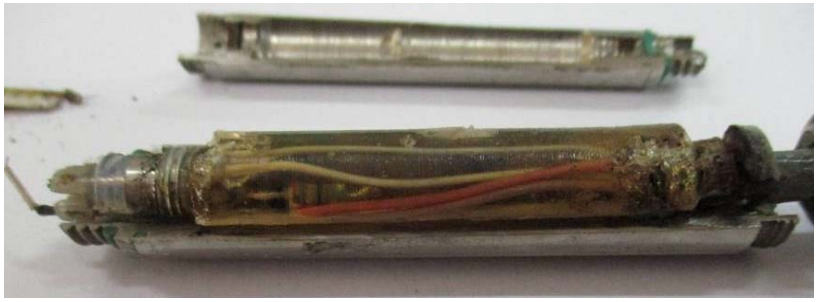

Figure 91. Capacitive relative humidity sensor WCSH-09 exploded view

The transition from electronics to wire was made inside the metallic capsule, which was encapsulated with resin. However, as the transition was directly connected to the sensing element, the water entered through the conductors/wires, causing the corrosion of the metallic wires.

Table 18. Survival rate capacitive relative humidity sensors

Sensor type	Total number of sensors	Number survived	Survival rate	General remark
Water content	31	0	0%	All sensors reached the saturation during the operational phase and they survived much longer than expected (one up to 2005)

5.3 PSYCHROMETERS

As expected, these sensors were fragile and too delicate for the media in which they were used.

5.3.1 Mechanical effects

Most of the sensors were damaged or harmed as a consequence of the bentonite swelling; the Teflon® protection provided to the sensing element appeared damaged in most of them. The rate of broken sensors was very high but it is difficult to say, taking into account their fragility, if the damage –such as breaking the ceramic filter– was caused or not by the dismantling operations. On the other hand, the tube that protected the cable was quite damaged as a consequence of bentonite swelling and subsequent crushing, causing it to break at several points.

A possible explanation for the failure of some sensors was that when the cable was stretched (by bentonite swelling) the joint with the sensing head could break.

5.3.2 Corrosion and chemical attack

One of the most clear visual effects on these sensors was that the originally white cable (made of PVC and protected with a tubing of Teflon) turned black, with variable extent and length depending on the sensor.

The results of the previous dismantling made in 2002 (García-Siñeriz et al. 2006), stated that this colour change of the cable started at the point of contact with the rock, and that combined with the presence of water it caused some kind of corrosion or chemical attack. Therefore, the sensors in the worst conditions in 2002 were those located in the lower cables' channel, where the amount of water was higher. This view was confirmed during this final dismantling.

This phenomenon could be a consequence of the alkalinity of the rock when in contact with the tubing (fluorides) protecting the cable combined with prolonged exposure to higher humidity and temperature. The effect is bigger with higher humidity and temperature.

A viscous substance was detected in the ceramic filter; see Figure 92. This might be silicone or an adhesive after decomposition and the phenomenon seems to be related to temperature.

Figure 92. Viscous substance in psychrometer

5.3.3 Water tightness

The psychrometers were not watertight at all. In fact, they were not specially protected to prevent the entrance of water.

Table 19. Survival rate psychrometers

Sensor type	Total number of sensors	Number survived	Survival rate	General remark
Psychrometer	24	5	20.8%	The apparent surviving ones were very corroded and contaminated (see chapter 6.3)

5.4 THERMOCOUPLES

The thermocouples were robust, and they confirmed their long life expectancy in an experiment with conditions such as those in the FEBEX experiment. As can be seen in chapter 9, these sensors were manufactured using two different types of metal, Inconel 600 for those in close contact with the liners of the heaters and SS304 for the rest, although those installed in the middle bentonite ring were further protected with Teflon tubing covering the last 2 m in length of the thermocouple.

5.4.1 Mechanical effects

The state of conservation of these sensors was quite good, apart from those mechanically damaged during the dismantling operations.

5.4.2 Corrosion

The thermocouples did not show any signs of relevant corrosion this time (see chapter 5.3.2). The exception was for those located in contact with the liner (made of Inconel 600) and the corrosion was minor.

5.4.3 Water tightness

These sensors remained sufficiently watertight.

5.4.4 Survival rate

The survival rate depending on the type of sensor (metal and additional protection if any) is given in Table 20.

Table 20. Survival rate for thermocouples

Sensor type	Total number of sensors	Number survived	Survival rate	General remark
Inconel 600	21	10	47.62%	Their performance was better than expected after the partial dismantling.
SS304 with Teflon	17	13	76.47%	
SS304	16	16	100%	
Total	**54**	**39**	**72.22%**	

The survival rate seems to be much higher for sensors made of SS304 but, as the working conditions were probably more difficult in the positions closer to the heaters (higher temperature) probably influencing their performance, the result is not conclusive.

5.5 TDRS

The key findings about the status of TDRs located in Section 46 are as summarized below.

- The surface of the coating film of the probes near the heater (WT-M2-04 and 09) was more discoloured (brown) than on other probes.
- WT-M2-09, which kept showing an increase in water content, had major cracks on the surface coating. The copper electrodes showed some corrosion-like stains. The unrealistic increase in the water content readings was presumably caused by water intruding inside the coating film.
- Some of the probes (WT-M2-04, 05, 06, 09 and 11) had old cracks on the cable protection. Probe no. 11 showed the most damage on the co-axial cable and this probe failed in 2004. Minor damages or water intrusion into the outer shield of the co-axial did not seem to cause significant effects on the TDR signals.
- Most of the probes showed shear deformation at the bentonite block interfaces (every 12.5 cm along the probe length). The deformation ranged from very slight to as much as ~3 mm. The surface coating seemed to have sufficient resistance against the shearing.
- The majority of the damage to the probes seemed to be caused by the power chisel during the removal of bentonite blocks under difficult conditions. The damage was so severe that re-calibration could not be performed.
- The volumetric water content estimated with the TDR probes showed a close agreement with the sample results with an exception of probe 09 which had major cracks on the probe coating.

The survival rates of the TDR probes and temperature sensors are summarized in Table 21.

Table 21. Survival rate of TDRs

Sensor type	Total number of sensors	Number survived	Survival rate	General remark
TDR	10	7	70%	TDR body looked intact, cable and connection seemed less durable
Temperature	10	4	40%	

6 POST DISMANTLING VERIFICATION

All the sensors that remained operative after the dismantling operation were verified in order to determine their reliability and correct functioning after more than 18 years of operation.

6.1 VIBRATING WIRE SENSORS

For this verification the initial reading, which is the value given by the sensor immediately after being installed, was taken into account as reference; this reading was taken in state condition during the visual inspection of the sensors.

6.1.1 Total pressure cells

Six cells were dismantled and three of them failed during the operational phase. One of the surviving ones (P-SG-01) remained attached to the bottom part of the dummy canister inside the liner and not visible (see Figure 93) and P-SI-01 remained attached to heater#2 (see Figure 94). Therefore, from all the dismantled total pressure cells only S-S-36-2/ P-SP-01 was found operative for verification at the laboratory. The verification was performed in a press at the laboratory, in conditions of stable humidity and temperature, applying different pressures along the measuring range of the sensor. The results are shown in Table 22 and Figure 96.

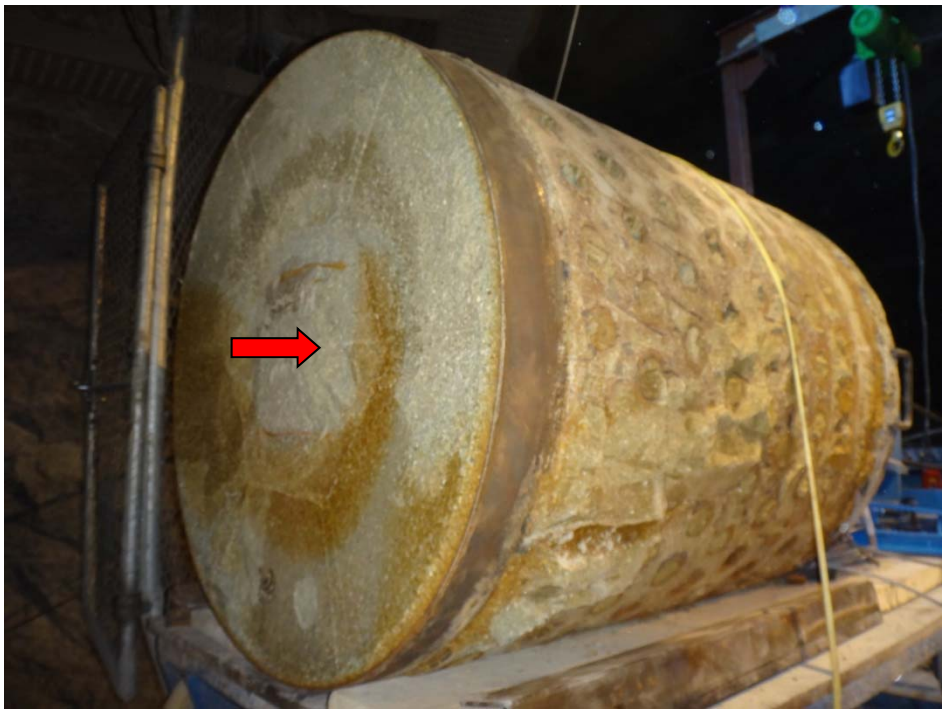

Figure 93. Position of P-SG-01 in dummy canister

Figure 94. P-SI-01 at the Heater surface

Figure 95. Detail of damage in P-SI-01 after extraction

Table 22. Results of verification of total pressure cell (dg=digits)

		Set point (MPa)					
Sensor	**Temp**	**0**	**1**	**2**	**3**	**4**	**5**
S-S-36-2/ P-SP-01	27 ºC	7906.6 dg	7512.1 dg	7118 dg	6401.8 dg	5727.3 dg	5085.7 dg

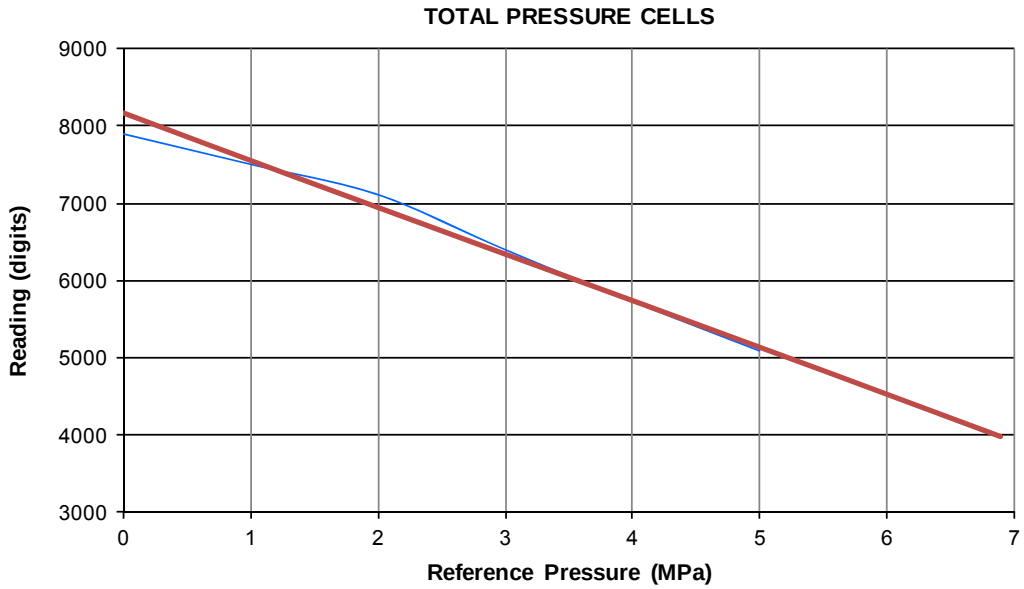

Figure 96. Plot of the results of the verification of total pressure cell S-S-36-2 / P-SP-01 (reference in red colour and readings in blue colour)

6.1.2 Pore pressure sensors

The verification of the surviving pore pressure sensors was done inside a hydrostatic pressure chamber in conditions of controlled temperature, applying different pressures along the range of the sensor and comparing the values registered by the sensors. Some sensors that failed during the operational phase were found operative after dismantling, as for instance QSH-05 or QSF2-03 to 06 and it can be concluded the problem was the cable.

The results are shown in Table 23.

Table 23. Results of verification of pore pressure sensors

		Temp	Set Point					
Sensor		ºC	0 MPa	1 MPa	2 MPa	3 MPa	4 MPa	4.5 MPa
S-S-41-1	QSH-01	0	0	1.1856	1.97735	2.9421	3.9932	4.3431
S-S-41-3	QSH-03	11.9	0	1.2696	2.2589	3.2616	4.2609	4.8768
S-S-41-4	QSH-04	22.2	0	0.7545	1.7006	2.6814	3.6883	4.3267
S-S-41-5	QSH-05	22.1	0	1.2796	2.6449	3.8084	4.9979	6.2401
S-S-41-6	QSH-06	21.9	Cable was cut too close to the sensor body during dismantling					
S-S-41-7	QSH-07	24.4	0	2.6100	3.5900	4.6080	5.5188	6.0854
S-S-41-8	QSH-08	28.7	0	0.7679	1.5508	2.2462	3.144	3.5242
S-S-41-10	QSH-10	-1.1	0	1.1897	2.2057	3.1936	4.2707	4.7342
S-S-41-11	QSH-11	24.6	0	1.3074	2.2826	3.3438	4.2993	4.8863
S-S-41-12	QSH-12	23.1	0	1.5250	2.5994	3.6331	4.6012	5.1366
S-S-48-9	QSF2-01	Cable was cut too close to the sensor body during dismantling						
S-S-48-10	QSF2-02	Cable was cut too close to the sensor body during dismantling						

Sensor		Temp	Set Point					
		ºC	0 MPa	1 MPa	2 MPa	3 MPa	4 MPa	4.5 MPa
S-S-48-11	QSF2-03	21.2	0	0.8784	1.6400	2.1817	3.5854	4.1049
S-S-48-12	QSF2-04	26.2	0	1.0059	1.4331	2.4834	3.4007	3.8645
S-S-48-13	QSF2-05	23.1	0	0.7358	1.4953	2.5924	3.9368	4.1431
S-S-48-14	QSF2-06	21	0	1.1896	2.1925	3.2132	4.16912	4.7449
S-S-48-15	QSF2-07	20.7	0	0.9203	1.6402	2.5483	3.4316	3.9930
S-S-48-16	QSF2-08	23.9	0	1.5083	2.7754	3.7942	4.7834	5.2850
S-S-51-11	QSE2-01	23.5	0	1.0967	2.2361	3.1023	4.1076	4.2871
S-S-51-12	QSE2-02	20.8	0	1.2016	2.4158	3.3015	4.219	4.8096
S-S-51-13	QSE2-03	23.1	0	1.1164	2.1625	3.0402	4.5274	4.5836
S-S-51-14	QSE2-04	Cable was cut too close to the sensor body during dismantling						
S-S-51-15	QSE2-05	21.5	0	1.2225	2.1855	3.2816	4.2464	4.8025
S-S-51-16	QSE2-06	23.3	0	0.9761	2.1436	3.1048	4.1348	4.6139
S-S-51-17	QSE2-07	23.2	0	0.77984	1.6585	2.4133	3.4214	3.9035
S-S-51-18	QSE2-08	23	0	1.1449	2.2482	3.0838	4.0131	4.4302

QSH-02 and QSH-09 were not functioning when checked at laboratory.

The results are also plotted in Figure 97; a reference curve of the ideal response is added in red , to compare with the recorded verification reading. As can be seen, they showed an average deviation below 10% except for QSH-07, which had a higher error. Sensor QSH-05 also had a larger deviation, but only above 4 MPa. These results, after 18 years of operation, can be considered as excellent. Temperature sensors of QSH-01 and QSH-10 were broken.

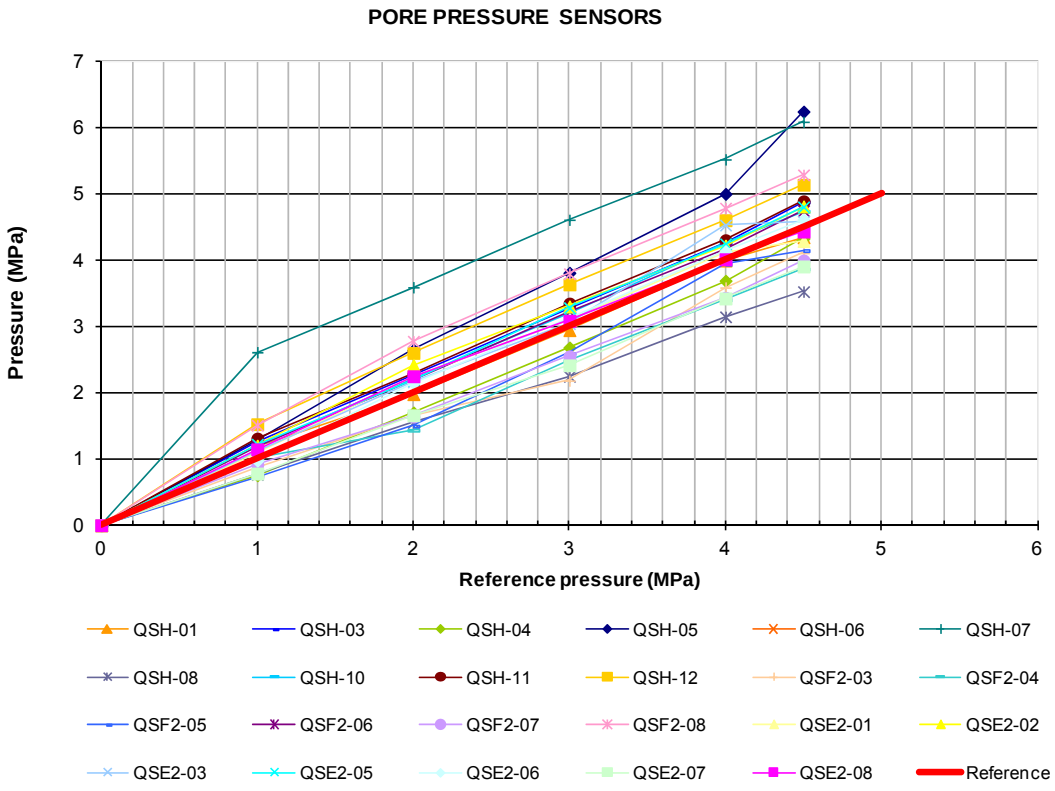

Figure 97. Results of the verification of pore pressure sensors

6.1.3 Displacement sensors / extensometers

Seven heater extensometers were retrieved and four bentonite block ones. Three heater extensometers were sent to Tecnalia (Madina 2016) and the remaining four were found defective during the operational phase but one could be tested at the laboratory (SHSG-01). Regarding the bentonite block extensometers, only one remained operative (SBSF2-02) but another one could be verified at the laboratory (SBSE2-01). For their verification they were extended up to known lengths, along the measuring range, measuring the output in conditions of stable humidity and controlled temperature.

The results are shown in Table 24.

Table 24. Results of verification of displacement sensors

Sensor		T during checks (ºC)	Set Point (cm)						
			0	1	3	5	7	9	10
S-S-38-01	SHSG-01	28.1	0	1.527	2.5108	4.4837	6.4668	8.4066	10.2929
S-S-48-30	SBSF2-02	26.0	0	1.0107	2.7586	5.0276	6.9479	8.8737	9.7103
S-S-51-31	SBSE2-01	24.3	0	0.3194	1.6835	3.6664	5.6999	7.5388	8.1282

The results are plotted in Figure 98, Figure 99 and Figure 100. The ideal response or reference was included as a red line for comparison with the verification performance.

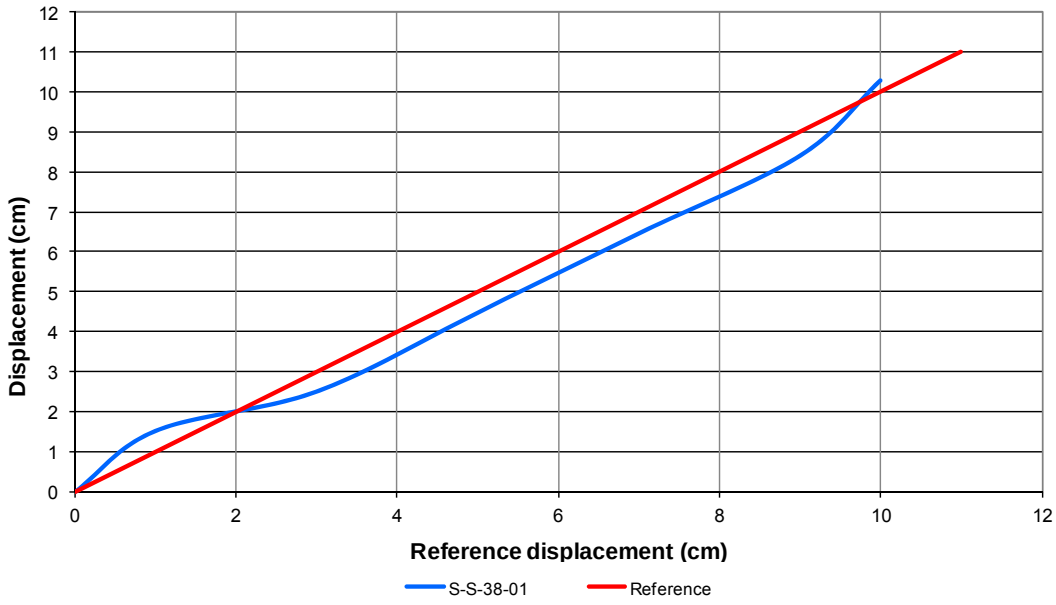

Figure 98. Results of the verification of displacement sensor S-S-38-01 / SHSG-01

A maximum deviation of 0.59 cm was recorded for sensor S-S-38-01 / SHSG-01 see Figure 98.

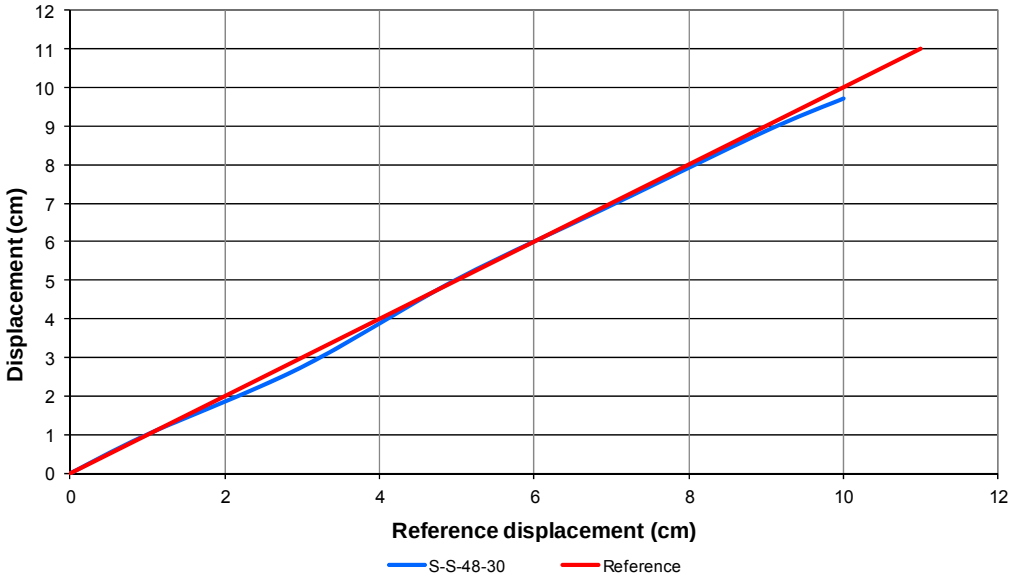

Figure 99. Results of the verification of displacement sensor S-S-48-30 / SBSF2-02

A maximum deviation for sensor of 0.29 cm was recorded for S-S-48-30 / SBSF2-02, see Figure 99.

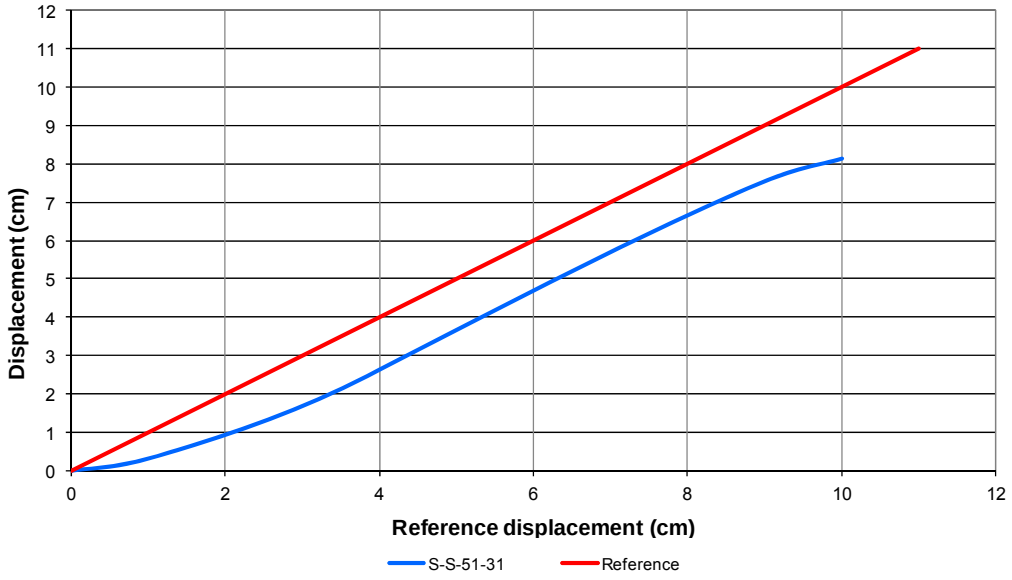

Figure 100. Results of the verification of displacement sensor S-S-51-31 / SBSE2-01

Finally, a maximum deviation of 1.88 cm is seen for sensor S-S-51-31 / SBSE2-01 (Figure 100.

The deviation average was around 18% but there is a clear offset which, if considered, would give much better results.

The maximum deviation of 1.88 cm was given by sensor S-S-51-31 but this is the sensor with the dubious results during the operational phase. In general, the performance of these sensors could be considered satisfactory given the long operational time, the working conditions and the potential effects of the dismantling operation.

6.2 CAPACITIVE RELATIVE HUMIDITY SENSORS

It was not possible to verify these sensors because as soon as the cables are cut the calibration of the electronics is lost, and they could only be verified by the manufacturer in their workshop. However, all of them reached the full saturation during the operation (see section 5.2).

6.3 PSYCHROMETERS

Due to the fragility of these sensors, the majority of the sensors that were still operative before dismantling were damaged during the dismantling process. Therefore, only those that showed a good enough aspect (a total of 8) were verified to determine their real status. A reading unit PSYPRO from WESCOR was used, as well as three saline standard solutions (of known concentration):

- SS-120: water potential -250 kPa,
- SS-121: water potential -750 kPa,
- SS-122: water potential -2500 kPa.

For their verification, the psychrometers were introduced in a humidity chamber and after sufficient stabilization time measurements started along their range.

The curves obtained by the different sensors are shown in the following figures.

Sensor WP-SF2-03 (faulty during the test):

The graphs are coincident for the three standard solutions, i.e. it is not functioning:

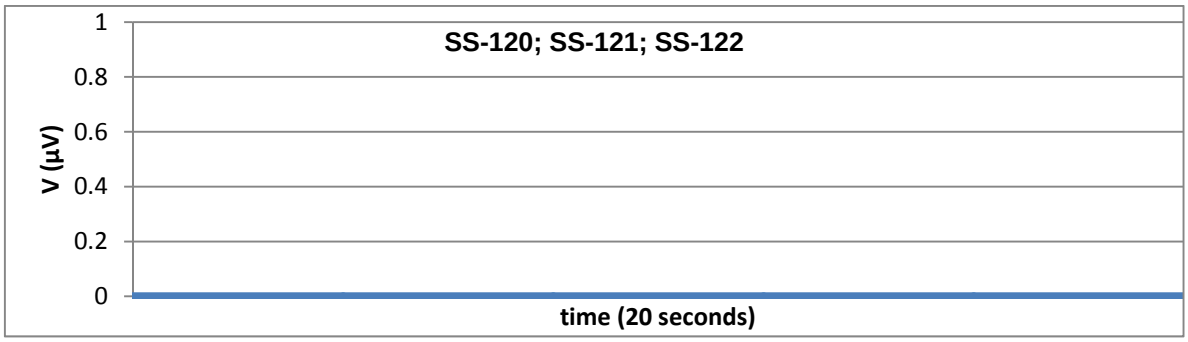

Figure 101. Verification curve for psychrometer WC-SF02-03

Sensor WP-SF2-04 (faulty during the test):

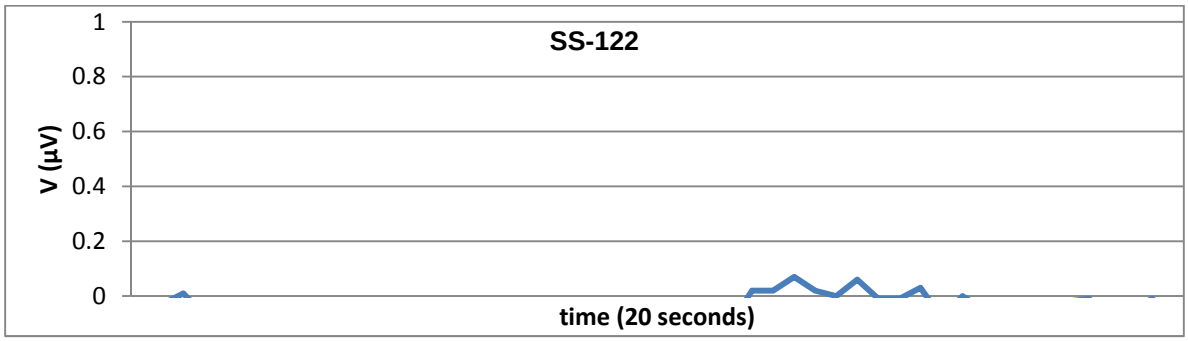

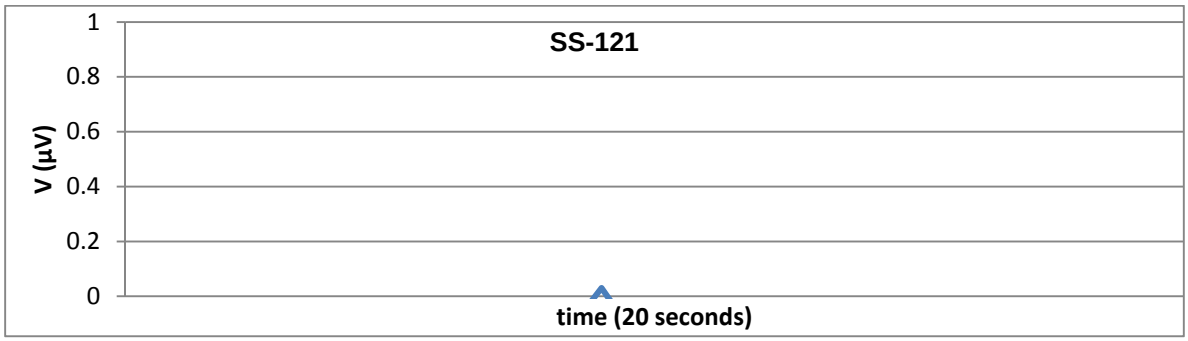

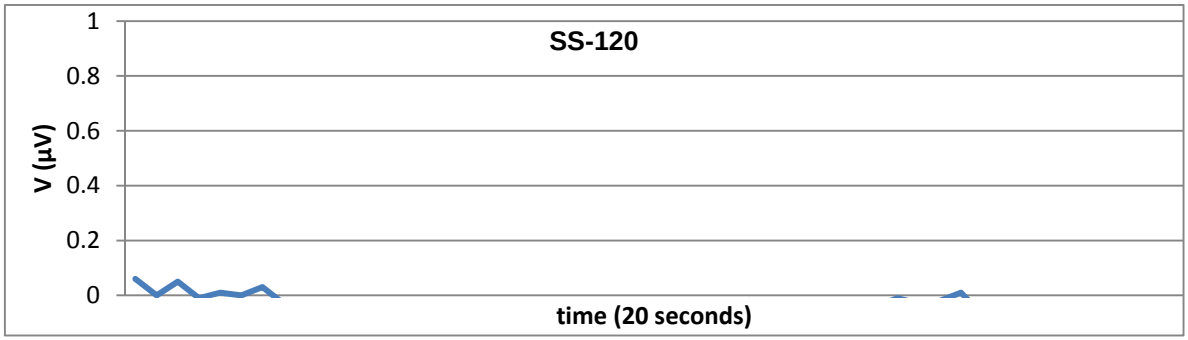

Figure 102. Verification curves for psychrometer WP-SF2-04

Sensor WP-SF2-05 (faulty during the test):

The graphs are coincident for the three standard solutions:

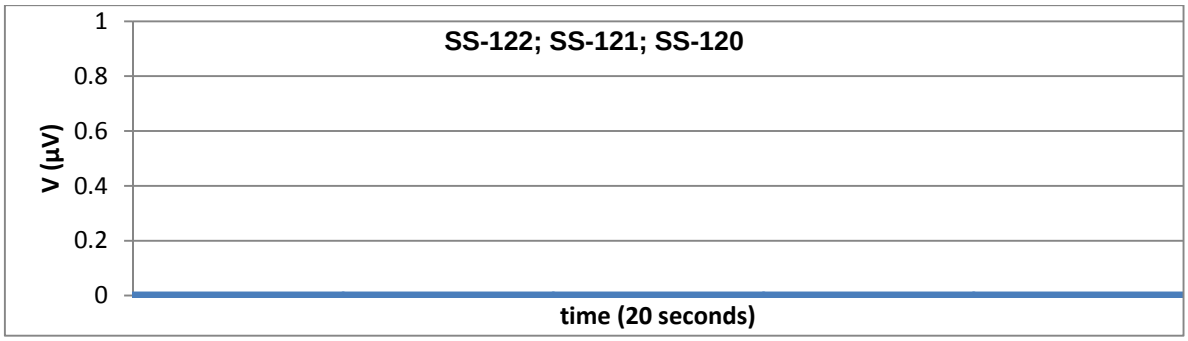

Figure 103. Verification curves for psychrometer WP-SF2-05

Sensor WP-SF2-07 (faulty during the test):

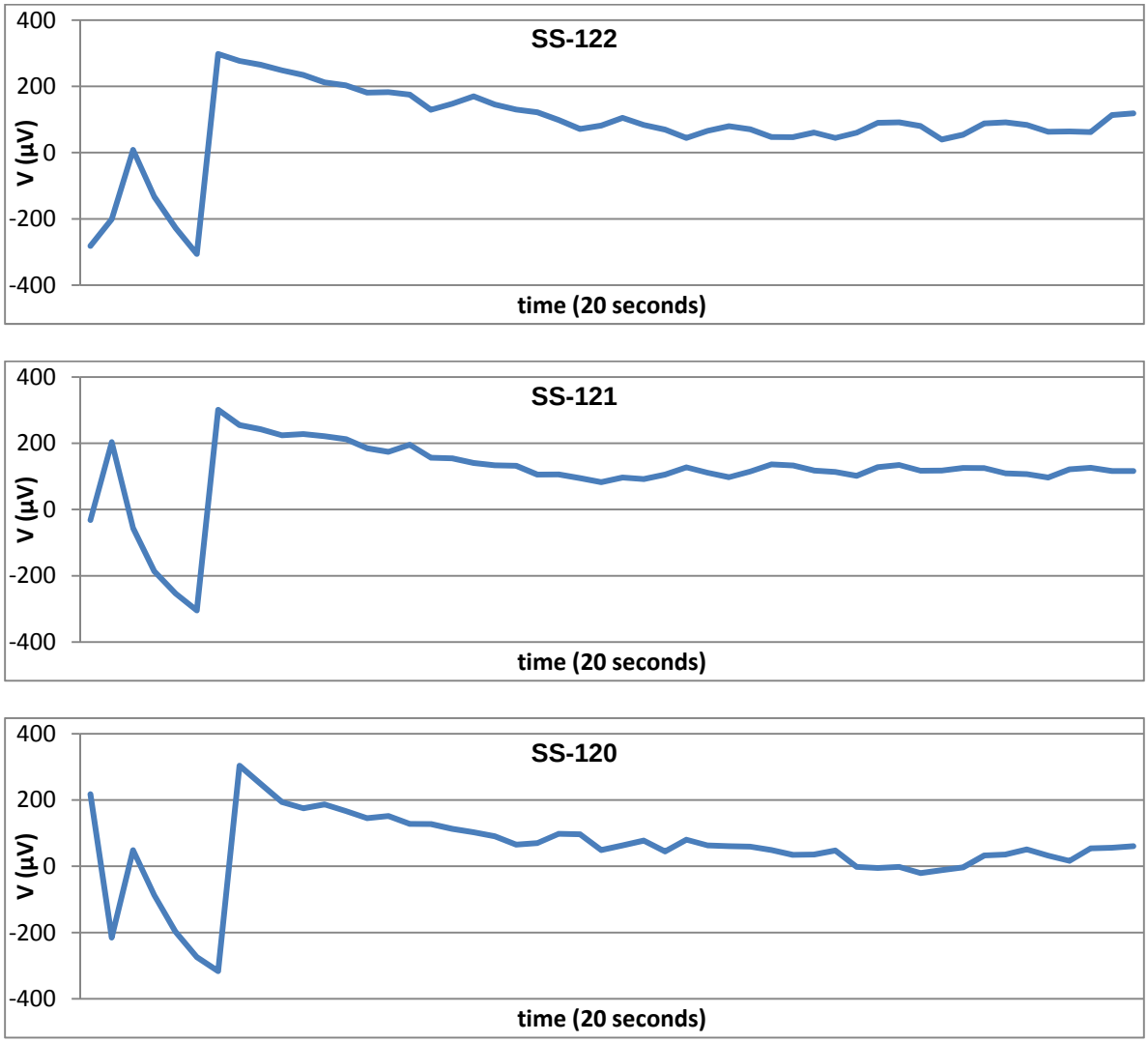

Figure 104. Verification curves for psychrometer WP-SF2-07

Sensor WP-SE2-02 (faulty during the test):

The graphs are coincident for the three standard solutions:

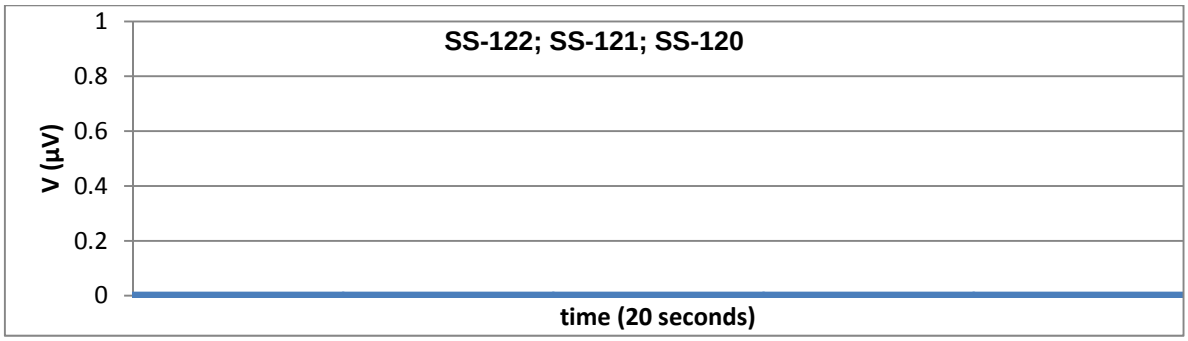

Figure 105. Verification curves for psychrometer WP-SE2-02

Sensor WP-SE2-04 (faulty during the test):

The graphs are coincident for the three standard solutions:

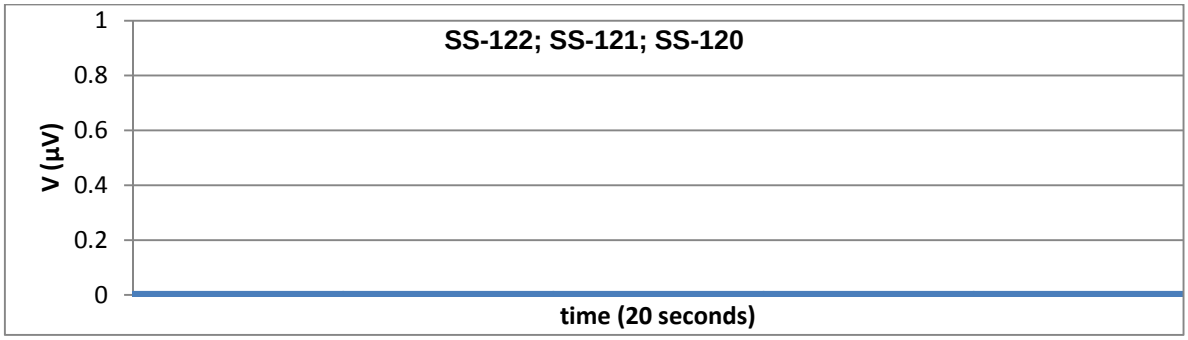

Figure 106. Verification curves for psychrometer WP-SE2-04

Sensor WP-SE2-05 (faulty during the test):

The graphs are coincident for the three standard solutions:

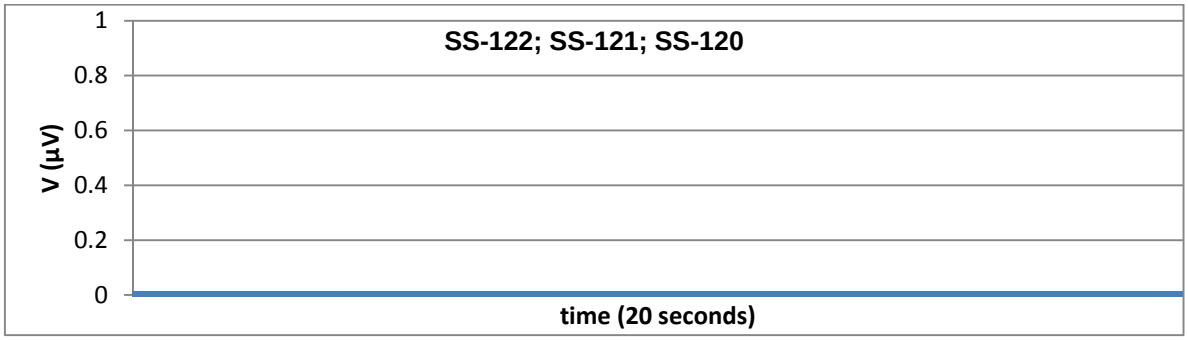

Figure 107. Verification curves for psychrometer WP-SE2-05

Sensor WP-SE2-08 (faulty during the test):

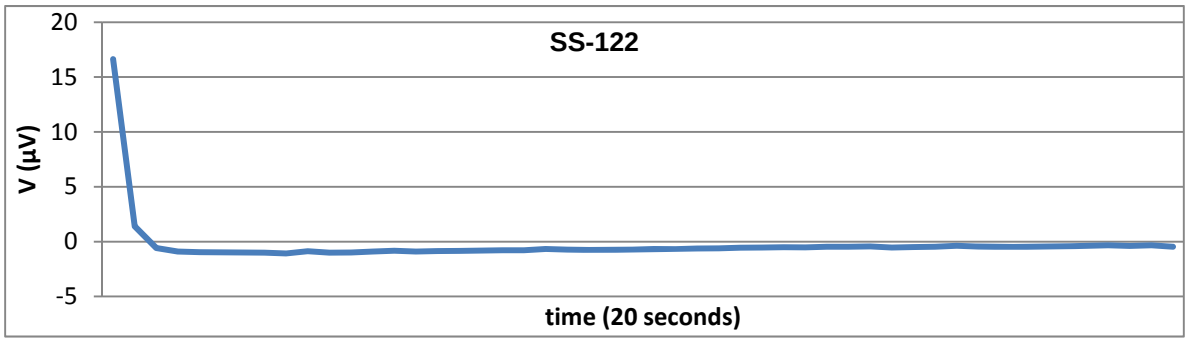

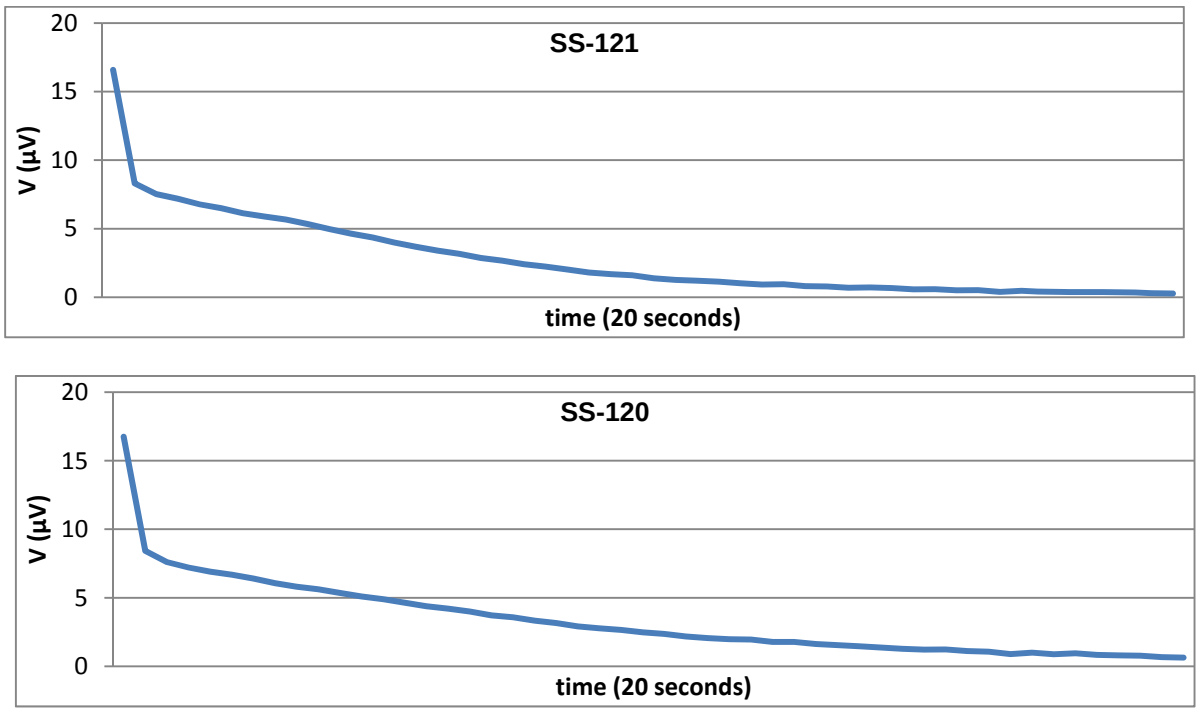

Figure 108. Verification curves for psychrometer WP-SE2-08

The obtained results show that none of the checked sensors can be considered as reliable. As it had already been observed in the previous dismantling operation (García-Siñeriz et al. 2006), the heating-cooling cycles of the sensing elements of the sensors, to which they are subject for the continuous reading, may have damaged the sensor, causing its failure and accelerating the contamination of the chamber with salts coming from the bentonite. The signal of a contaminated sensor looks like the graph at the right hand of Figure 109.

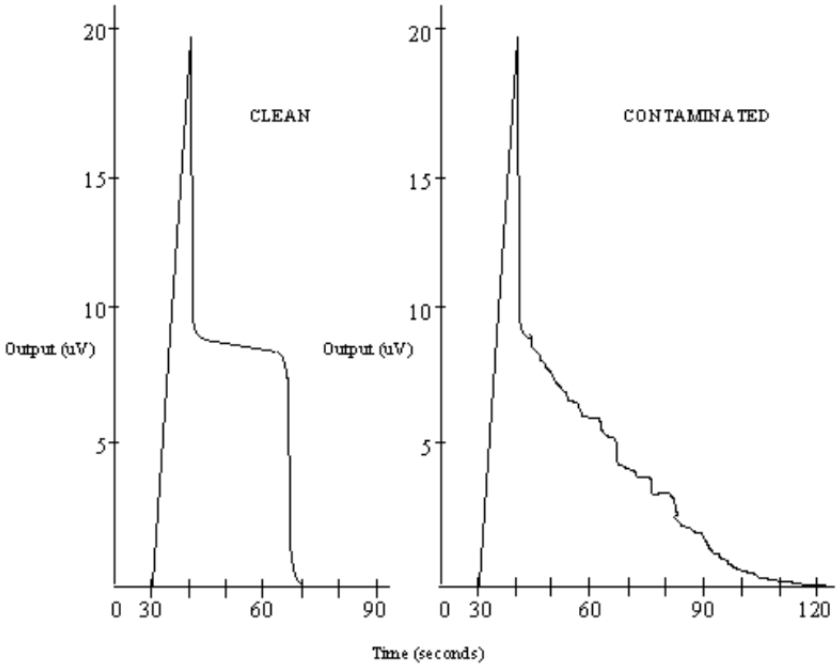

Figure 109. Output signal for clean and contaminated psychrometer (from sensor's manual)

6.4 THERMOCOUPLES

The thermocouples were verified in situ as can be seen in Figure 110.

Figure 110. Thermocouples in place for calibration (left) and equipment for in situ calibration (right)

They were introduced in a dry oven with a reference probe and there were three different verifications, depending on the position of the thermocouples with respect to the heater. Those sensors that were closer to the heater –internal ring– were tested at higher temperatures (20 ºC, 80 ºC, 100 ºC and 80 ºC), those in the middle point at 20 ºC, 60 ºC, 80 ºC and 60 ºC and those closer to the rock –in the external ring– were tested at 20 ºC or 30 ºC, 40 ºC, 60 ºC and 40 ºC; in the three cases the readings of the sensors taken manually with a calibration sensor were compared to their readings in the data acquisition system and the last reading at lower temperature was made to check they were able to detect a temperature decrease after an increase (hysteresis). See Table 25, Table 26 and Table 27 for more details.

The data shown are the available data, in some cases the sensor was not checked at a certain temperature as it did not correspond to its position in the buffer.

Table 25. Calibration of sensors in external ring at 20 ºC, 40 ºC, 60 ºC and 40 ºC

All of them made of SS304

Sensors section G

	Reference T (ºC)			
Sensors	**20.2**	**40.52**	**59.9**	**40.13**
T-SG-01	Sensor cut during dismantling operation			
T-SG-09	19.9	40.1	59.4	39.8
T-SG-10	20.1	40.2	59.2	39.7
T-SG-13	15.3	Wrong readings, probably damaged during dismantling		

Sensors section I

	Reference T (ºC)			
Sensors	**29**	**40.1**	**59.4**	**40.1**
T-SI-01	Sensor cut during dismantling operation			
T-SI-09	27.4	39.6	58.5	39.9
T-SI-10	28.3	39.1	58	39.4
T-SI-13	27.7	38.2	56.8	34.9

Sensors section D2

	Reference T (ºC)					
Sensors	**30.3**	**30**	**40.1**	**60.6**	**59.4**	**40.3**
T-D2-01	-	29.4	38.1		59.1	39.3
T-D2-09	29.8	-	39.1	59.1		39.1
T-D2-10	29.4		39.1	58.8		39.6
T-D2-13	-	16.1	Wrong readings, probably damaged during dismantling			

Sensors section B2

	Reference T (ºC)				
Sensors	**30.6**	**30.5**	**40.4**	**59.9**	**40.6**
T-SB2-01	30.1	-	39.7	58.8	40.2
T-SB2-06	-	29.8	39.6	58.7	39.9
T-SB2-07	30	-	39.5	58.7	39.5
T-SB2-09	29.9	-	39.7	58.8	40.3

Figure 111 shows the calibration results of sensors installed in external ring giving a valid signal after dismantling.

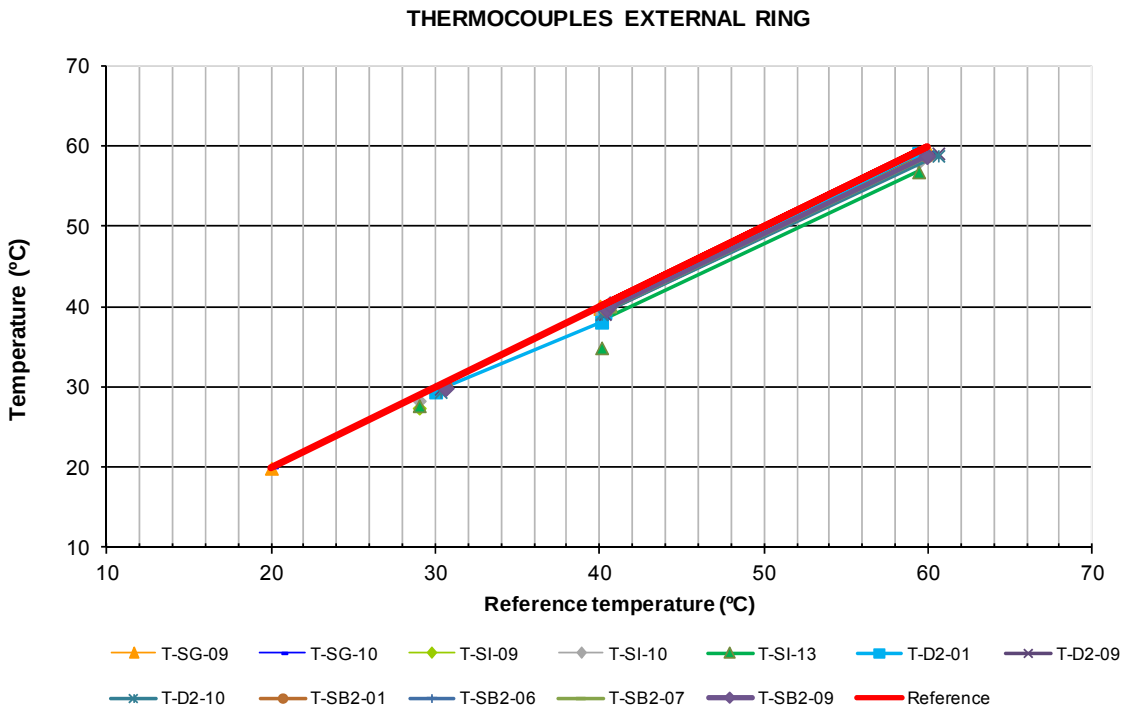

Figure 111. Results calibration thermocouples external ring

Table 26. Calibration of sensors in middle ring at 20 ºC, 60 ºC, 80 ºC and 60 ºC
All of them made of SS304 and with Teflon tubing at the last 2 m.

Sensors section G

	Reference T (ºC)			
Sensors	**20.2**	**59.9**	**80.2**	**60**
T-SG-02	2.4	N.R.[5]	N.R.	N.R.
T-SG-07	14.6	N.R.	N.R.	N.R.
T-SG-08	N.R. (Date of failure 23/04/2004)			
T-SG-12	N.R. (Date of failure 12/06/2003)			

Sensors section I

	Reference T (ºC)				
Sensors	**29**	**59.4**	**60.1**	**80.1**	**60**
T-SI-02	Sensor cut during dismantling operation				
T-SI-07	29.7	-	57.4	77.5	58
T-SI-08	28.4	58.3	-	79.2	59.4
T-SI-12	28.5	-	56.5	75.3	57

Sensors section D2

	Reference T (ºC)					
Sensors	**30.3**	**30.4**	**60.6**	**59.4**	**80.1**	**60**
T-D2-02	-	29.5	-	58.8	79.5	59.3
T-D2-07	30.1	-	59.1	-	79.1	59
T-D2-08	29.9	-	58.6	-	78	56.5
T-D2-12	N.R. (Date of failure 16/06/2003)					

Figure 112 shows the calibration results of sensors installed in middle ring giving a valid signal after dismantling.

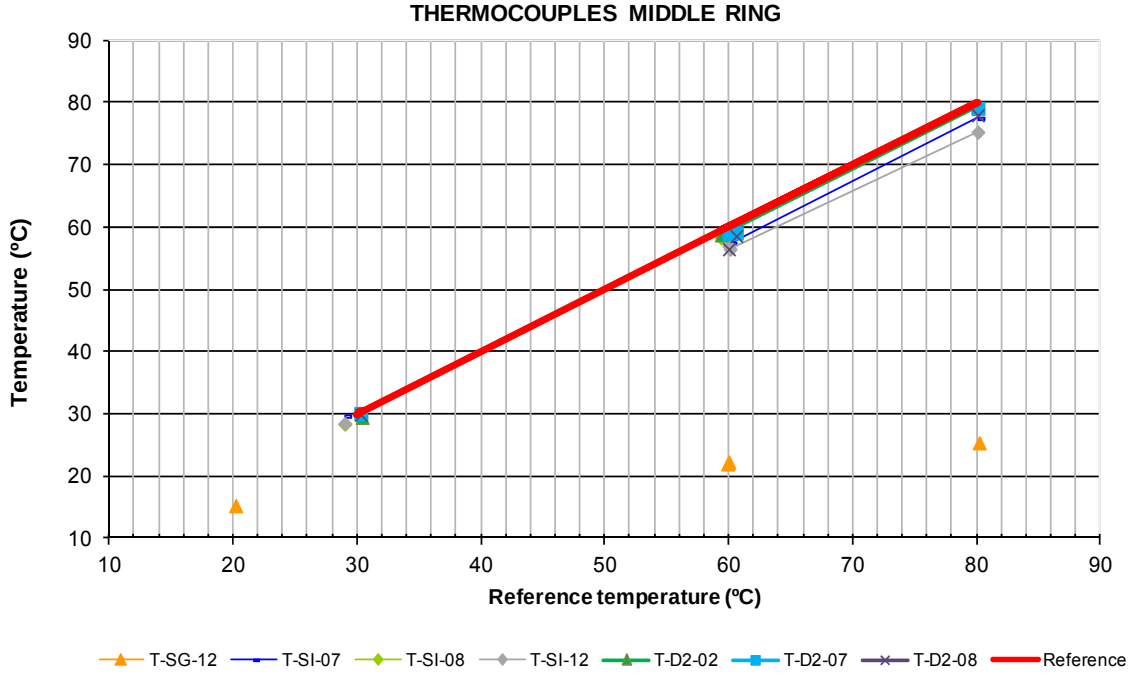

Figure 112. Results calibration thermocouples middle ring

[5] N.R. No response. probably damaged during dismantling

Table 27. Calibration of sensors in inner ring at 20 ºC, 80 ºC, 100 ºC and 80 ºC

All of them made in Inconel 600 except those at SB2 that are of SS304 and protected with Teflon (last 2 m).

Sensors section G

	Reference T (ºC)			
Sensors	**20.2**	**80.2**	**100.1**	**79.99**
T-SG-03	Sensor lost during dismantling			
T-SG-04	N.R. (Date of failure 6/06/2003)			
T-SG-05	N.R. (Date of failure 10/06/2003)			
T-SG-06	N.R. (Date of failure 10/02/2008)			
T-SG-11	20	79.3	97.6	78.1

Sensors section I

	Reference T (ºC)			
Sensors	**29**	**80**	**100**	**80**
T-SI-03	Sensor cut during dismantling operation			
T-SI-04	N.R. (Date of failure 19/12/1996)			
T-SI-05	No coherent values, probably damaged during dismantling			
T-SI-06	No coherent values, probably damaged during dismantling			
T-SI-11	N.R. (Date of failure 11/06/2003)			

Sensors section F2

	Reference T (ºC)			
Sensors	**30**	**80.05**	**98.8**	**79.9**
T-SF2-01	Cable cut during dismantling operation			
T-SF2-02	29.6	77.8	97	78.1
T-SF2-03	N.R. (Date of failure 31/08/2002)			
T-SF2-04	N.R. (Date of failure 18/06/2002)			

Sensors section D2

	Reference T (ºC)					
Sensors	**30.3**	**30.4**	**80.1**	**80**	**100.5**	**80.4**
T-D2-03	N.R. (Date of failure 01/08/2013)					
T-D2-04	N.R. (Date of failure 12/08/2000)					
T-D2-05		29.6	77.9		96.5	78
T-D2-06	No coherent values, probably damaged during dismantling					
T-D2-11		29.1		78	96.4	78.2

Sensors section B2

	Reference T (ºC)			
Sensors	**30.5**	**80.6**	**100**	**80**
T-SB2-02	29.8	76.6	94.7	76
T-SB2-03	29.9	78.6	97.3	77.9
T-SB2-04	29.8	78.9	97.7	78.3
T-SB2-05	N.R. (Date of failure 19/12/1996)			
T-SB2-08	No coherent values, probably damaged during dismantling			

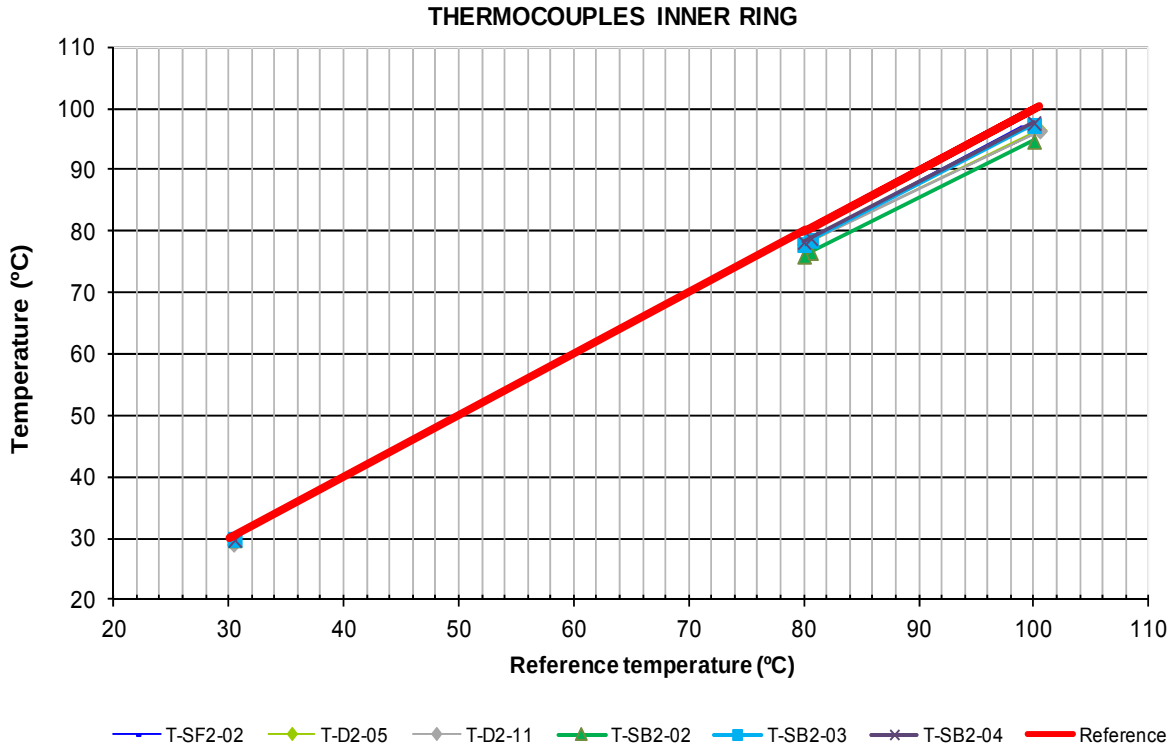

Figure 113. Results calibration thermocouples inner ring

General comments:

Unfortunately, some thermocouples did not show any response to temperature changes (N.R.) probably these were damaged during the dismantling operations.

The surviving thermocouples kept providing reliable enough readings with errors below 5.3% of the reference.

6.5 TDRS

Figure 114 shows the comparison of the TDR-measured volumetric water content (VWC) and those of the samples taken in the vicinity of the probes. More details of the verification of the data are given in Sakaki et al. 2016. Although the circled TDR-measured VWC was overestimated possibly due to water intrusion via cracked probe coating, the rest showed a good agreement with the sample results.

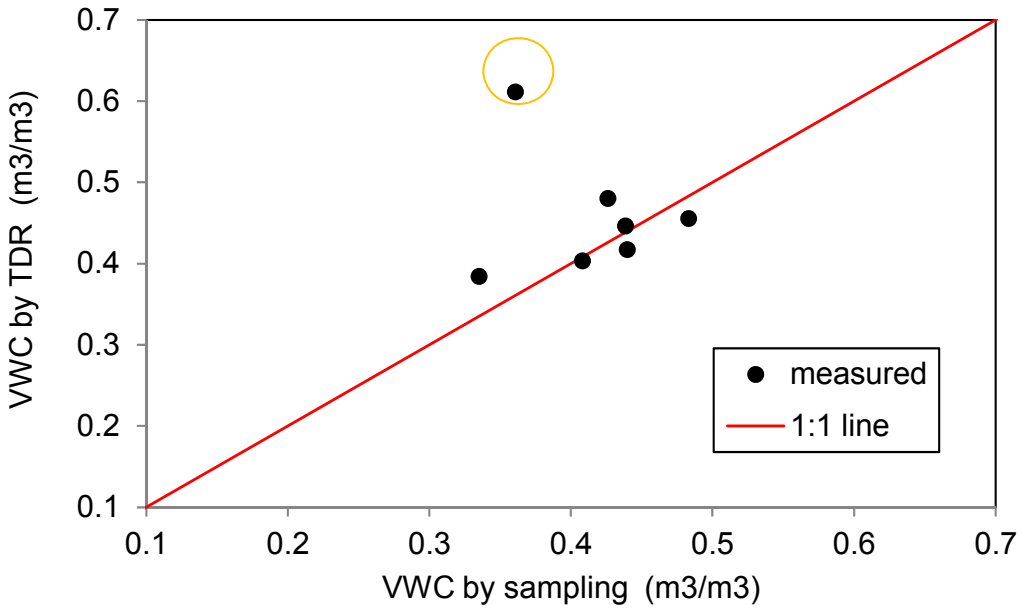

Figure 114. Comparison of TDR-measured volumetric water content and those from samples

Note: The TDR data are those taken on or before 24th June 2015 just before the samples were collected and temperature had dropped. The VWC by sampling was calculated using the lab results by Plötze 2016 (AN 16-464) assuming bentonite grain density of 2.7 Mg/m^3.

7 CONCLUSIONS, COMMENTS AND RECOMMENDATIONS

7.1 CONDITIONS AND CAUSES OF FAILURE

From the 176 sampled sensors, 108 were out of order before the dismantling operation and taking into account that for 28 relative humidity sensors the reason was that they reached the full saturation, it can be stated that only 80 effectively failed during the operational phase (Table 1). From these, 20 more were damaged during dismantling and thus only 60 remained operative for post- experimental verification.

The conditions imposed on the sensors during the operational phase are given in Table 29 and Table 30. It can be stated that they were exposed to demanding conditions by the combination of temperature, pressure and high water contents over a long period of time.

Post mortem analysis of the broken sensors allowed discerning different types of reasons for failing (see Table 28). Although sensor failure is the result of a combination of factors caused by the surrounding media (thermal field, pressure developed by the barrier, corrosion and water exposure, etc) it can be concluded that 16 sensors were flooded (water into the electronics of the sensor), 26 were damaged due to mechanical effects and up to 36 failed due to defects in the cable.

Table 28. Types of failure for retrieved sensors

Type	Total No.	Out of order	Saturated	Flooded	Mechanical	Cable
S Plug	4	0				
P Kulite	2	2		2		
WC Vaisala	3	3				3
3S	3	3		3		
WT	10	1				1
WC Rotronic	31	31	20	11		
WP	24	19	8			11
P Geokon	6	3			3	
SH Geokon	7	6			6	
SB Geokon	4	3			3	
Q Geokon	28	23				23
T	54	14			14	
Total	**176**	**108**	**28**	**16**	**26**	**38**

Table 29. Maximal temperature, pressure and humidity conditions in sections (gallery and plug)

Dismantling section	Max. Temperature (ºC)	Max. Pressure (MPa)	Max. Relative Humidity (%)	Comments
32	17	Atmospheric	84%	Gallery conditions
34	<36	<0.1 MPa	N/A	Concrete plug

Table 30. Maximal temperature, pressure and humidity conditions in sections (bentonite)*

	Outer ring			Intermediate ring			Inner ring			Centre		
Dismantling section	Max. Temp. (ºC)	Max. Pressure (MPa)	Max. Relative Humidity (%)	Max. Temp. (ºC)	Max. Pressure (MPa)	Max. Relative Humidity (%)	Max. Temp. (ºC)	Max. Pressure (MPa)	Max. Relative Humidity (%)	Max. Temp. (ºC)	Max. Pressure (MPa)	Max. Relative Humidity (%)
36					6.24							
37			<98			<88			<72			
38	44		100	60		100	84		100	100	6.13	
41			100			<96			100			<52
42	46		100	64	2.23	100	98	1.11	100		2.23	
46				68			88					
47-48		>6.6	100	76	>2	100	100		<69			
51		>5	100		>3	<78	100		<30			
54	36			56			88			100		
62	23			23	5.7		23			23		

*Empty cell means data not available

7.2 CONCLUSION AND COMMENTS

This report focused on the analysis of sensors that were installed in the bentonite buffer after more than 18 years of operation under challenging conditions. The sensors installed in the rock were left in place. The results and conclusions gathered now complement those obtained after the first partial dismantling made in 2002 (García-Siñeriz J.L. et al. 2006).

The conclusions about the performance of the installed sensors are of great importance because the information provided by them is used to improve the understanding of the THM processes. In fact, the database created so far is being used to validate the existing modelling codes. For some sensors the results from the laboratory verification revealed large offsets at the end (e.g. S-S-51-31/SB-SE2-01 or S-S-48-12/QSH-04) but there is no indication as to when these data became unreliable during the operational phase.

From the 176 sensors retrieved, 108 (61.36%) were out of order prior to the dismantling operation (see Table 1 and section 7.1). However, taking into consideration that 28 capacitive sensors and psychrometers reached 100% RH during the operational phase (15.9% of the total of sensors and 25.9% of the failed ones), they should be considered as fully saturated sensors and not failed ones. This leaves the real number of broken sensors at 80 (45.45% of the total) which is a very good rate after 18 years of operation.

As during the partial dismantling operation, all sensors and cables were found in good contact with the bentonite and those close to the rock walls or the liner were very much pressed towards them. No noticeable changes in the location of sensors were found due to the bentonite swelling and no movement of the heater was registered.

The mechanical effects of the bentonite swelling on some sensors were clearly visible, as similarly observed in 2002, in particular close to rigid surfaces or when the sensor was present in several bentonite blocks. For instance, some capacitive type humidity sensors, psychrometers and TDRs showed squashed cables (but still operative) and bent, broken or loose filters. The ceramic filter of the psychrometers' measuring head was found broken and/or separated from the cable in some cases. The metallic body of the transducer of some total pressure cells was found crushed and the tube of several extensometers was bent due to the bentonite swelling. In general, sensors looked in better shape than the ones retrieved during the first dismantling operation (García-Siñeriz et al. 2006) with regard to corrosion, sensor failure and there were no signs of bacteria attack (see Madina 2016), except for the crackmeter. However, further bacteria analyses are currently on the way.

There was less damage from the dismantling operation than in the previous dismantling in 2002, so it can be concluded that the dismantling procedure was better controlled.

The sensor's performance is analysed qualitatively and quantitatively based on the measurements recorded during the operational lifetime, from the dismantling operation and the verification process:

- Temperature sensors (thermocouples): data obtained seemed to be accurate enough according to the verification made on site and when compared with measurements from temperature sensors incorporated in other instruments. According to verification

data, the behaviour of temperature sensors was acceptable (error below 5.3%). The number of surviving sensors was 72.2% but some were damaged during dismantling.

- Humidity sensors (capacitive type, psychrometers and TDRs): in general, the readings provided by one sensor type matched quite well with the others. Capacitive type sensors have widely surpassed the initially expected operative lifetime of six months, many of the initially installed sensors lasted more than five years (12 of 31) and the last one was operative until 2005 (almost nine years). As checked after the partial dismantling made in 2002 (five years of operation), the readings provided by these sensors were accurate and, given their wide range, the data obtained from them is very useful to track the hydration process of the bentonite buffer that starts from low water contents and is sufficiently slow.. Psychrometers, installed with no significant mechanical protection, proved to be very fragile for the bentonite buffer environment: only five out of the 24 psychrometers dismantled remained operative in principle, but they were damaged during dismantling so it was not possible to check their final accuracy. They also seemed to be very sensitive to contamination, which may come from the salts in the bentonite. However, recorded data from those installed in the outer buffer ring (which reached humidities within the measuring range, above 95% RH) seem to be accurate enough and they match with the capacitive ones. On the other hand, the psychrometers in the granite gave reasonable readings (very low suction) and seem to be less affected by salt contamination. TDRs installed in the bentonite buffer also proved to be quite fragile for such an environment; although 9 out of 10 remained operative, all of them were somehow damaged during dismantling.
- Total pressure cells: in general, their behaviour has been good for all the sensors based on the vibrating wire technique. Three sensors out of six recovered were out of order during operation, in many cases the reason for malfunctioning was the cable that was damaged most probably during operation. Another difficulty came from the weakness of the embedded thermistor, which failed in some sensors. The thermistor is used for temperature compensation of the vibrating wire signal.
- Pore pressure sensors: only 11 sensors out of 28 showed problems during operation and in many sensors the problem was due to the cable or the data recording unit, up to 22 units were functioning in the laboratory. These sensors were by far the best surviving ones but provided in general very low readings, showing positive values only in the most humid parts, located at the outer part of the buffer, especially at the right hand side.
- Heater displacement sensors: only one of the seven installed sensors remained operative but they were damaged by corrosion in the anchoring pieces only. The major problem was related with the tube of the sensors that was bent in several cases blocking the displacement. The verification results obtained at the laboratory indicated that the offset was big for the same reason. Therefore, the confidence on the readings obtained from these sensors is very low.
- Displacement sensors for bentonite blocks: only one of the four installed sensors remained operative at the end of the operational phase. The same performance is seen as for the displacement sensor in the heater area with regard to corrosion and mechanical integrity. Results from calibration indicate they suffer mechanically

(blocked frequently) and those still operative showed an error below 18% of the reference value. These displacement transducers, installed “floating” in specific bentonite blocks in the intermediate ring of the buffer, gave very small length variations (in the range of 1-2 mm). However, the general trend was, at the sensors in the upper left part, to a small but fast expansion at the beginning of the experiment, followed by a slow contraction that changed smoothly to an expansion movement, especially for those at the upper left side. These trends were less clear in sensor recordings in the lower right part.

- The crackmeter: as had already happened with similar prototypes provided by G3S and dismantled in 2002, it failed quite soon due to the complete flooding and the damage of the associated electronics.

A qualitative analysis of the sensor performance can also be made according to the measuring method:

a) The vibrating wire type sensors –total pressure cells, pore pressure sensors and extensometers– that came with a large previous experience working in a similar environment (surface or underground civil constructions or similar experiments in European URLs) were quite robust and most of them remained operative. The reason is they were well designed and built: appropriate materials (SS steel and tough plastics) and correct isolation at the cable entry. However, the cable entry was the weakest point and several sensors showed damaged cables at this point, most probably due to the loss of flexibility of plastics with time combined with the differential movements cable/metal body. For these sensors corrosion effects were only significant in standard carbon steel pieces (attachments to rock or liner) or when two different metals were in contact or close to each other: e.g. sensors made in stainless steel with the liner made of carbon steel.

b) Some prototypes of new sensors (sensors used for the first time in this kind of experiments) proved to be not properly designed and implemented, as the crackmeter, which was flooded from the very beginning.

c) All sensors that measure in a chamber isolated from the buffer by means of a filter (capacitive sensors, pore pressure sensors and psychrometers) were damaged over time, after being flooded, due to the salts deposition and/or the intrusion of bentonite. Some filters turned out to be not strong enough to withstand the bentonite pressure, in particular those made of ceramics. In particular the psychrometers demonstrated to be quite weak mechanically, both the sensing head and the cable. However, many of them surpassed the initial estimations of operational lifetime provided by the manufacturers (maximum 6 months). In this regard, the capacitive sensors performed best, although the cable was not strong enough. Furthermore, the isolation between the measuring chamber and the sensor electronics was defective and thus the water reached the conductors inside the cable and migrated up to the electronics beyond the concrete plug.

d) Long body sensors, extensometers and TDRs showed clear deformations due to the bentonite swelling making them inoperative with time.

e) In general, the plastic material used for the cables were not good enough; many of them were significantly degraded, lost their initial properties and were damaged.

As a main conclusion, it can be stated that the performance of the installed sensors was really good and much better than initially expected providing valuable information about the THM parameters during more than 18 years. A major reason for sensor failure was when the cable was cut at the body entrance due to the swelling pressure of the bentonite and the mechanical deformation of the sensor body. The effects of corrosion were in general negligible and not a relevant cause of malfunctioning. Sensors having a measuring chamber isolated from bentonite with a sintered filter are prone to suffer of corrosion after being flooded. The calibration results for the surviving sensors indicate that many of them remained accurate enough which shows that the recorded data can be trusted.

7.3 RECOMMENDATIONS

The use of well-designed and proven sensors and, if feasible, the use of passive measuring methods (for instance the vibrating wire technique) demonstrated to be the best choice. The failure rate for the so called “experimental sensors” (those used first time) could be minimised for future experiences in similar conditions, by avoiding the use of fragile ceramic or metallic filters and weak plastic parts (or if not avoided they should be at least well protected mechanically). The use of corrosion resistant metals (for instance AISI 316L), or if not possible, the use of non-corrosive external protections will help to extend the lifetime of several components. In particular the plastics proved to be the weakest point in all cases both when used as a component of the sensor housing or of the cables. The cables should be routed to provide the required flexibility when differential movements between the sensor body and cable happen. To minimise the mechanical effects on the sensor bodies they shouldn’t be too long and the junctions between bentonite layers should be avoided too.

Thanks to the partial dismantling carried out significant information was obtained about the real status of the sensors after more than 18 years of “in situ” operation, in conditions similar to those of a HLW repository except for radiation. The confidence on the recorded data has increased significantly, as the results from verified-calibrated sensors showed negligible or very low drift for most of them.

Information gathered from the sensor performance should be used to improve the design of the sensors and get better ones for future monitoring in similar conditions. In particular, the results are of relevance for the currently running H2020 project Modern2020. They will help to update the state of art and can be used as reference for the new developments being carried out in WP3.

8 REFERENCES

Bárcena I. & García-Siñeriz J.L. (2015)a: FEBEX-DP (GTS) Full Dismantling Sampling Plan. Nagra Arbeitsbericht NAB 15-014.

Bárcena I. & García-Siñeriz J.L. (2015)b. FEBEX-DP (GTS) Full Dismantling Test Plan. Nagra Arbeitsbericht NAB 15-015.

Fuentes-Cantillana J.L. & García-Siñeriz J.L (AITEMIN). (1998)b "FEBEX Full-scale Engineered Barriers Experiment in Crystalline Host Rock. FINAL DESIGN AND INSTALLATION OF THE "IN SITU" TEST AT GRIMSEL". ENRESA Technical Report 12/98.

Fuentes-Cantillana J.L., García-Siñeriz J.L., Franco J.J., Obis J., Pérez A. (AITEMIN); Jullien F. (ANDRA); Alberdi J., Barcala J.M., Campos R., Cuevas J., Fernández A.M., Gamero E., García M., Gómez P., Hernández A., Illera A., Martín P.L., Melón A.M., Missana T., Ortuno F., Pardillo J., Rivas P., Turrero M. J., Villar M.V., Mingarro M., Pelayo M. (CIEMAT); Caballero E., Cuadros J., Huertas F., Huertas F.J., Jiménez de Cisneros C., Linares J. (CSIC-Zaidín); Bazargan-Sabet B., Ghoreychi M. (G.3S); Jockwer N., Wieczorek K. (GRS); Kickmaier W., Marschall P. (NAGRA); Martínez M.A. (SGS Tecnos, S.A.); Carretero P., Dai Z., Delgado J., Juncosa R., Molinero J., Ruiz A., Samper J., Vázquez A. (ULC); Alonso E., Carrera J., Gens A., García-Molina A. J., Guimera J., Guimaraes L.do N., Lloret A., Martínez L., Olivella S., Pintado X., Sánchez M. (UPC-DIT); Elorza F.J., Borregón J.L., Canamon I., Rodriguez Pons – Esparver R. (UPM); Fariña P. (DM Iberia, S.A.) and Farias J. (Geocontrol, S.A.) were the technical editors of this report under the direction of Huertas F. (ENRESA) 2000: FEBEX full-scale engineered barriers experiment for a deep geological repository for high level radioactive waste in crystalline host rock FINAL REPORT. ENRESA, Technical Report 1/2000.

García-Siñeriz J.L., Bárcena I, Fernández P. A., and Sanz F.J. (AITEMIN) Addendum to [5] "Post-mortem Analysis: Instruments", December 2006. ENRESA Technical Report 05-4/2006.

García-Siñeriz J.L., Abós H., Martínez V. and De la Rosa C. (AITEMIN), Mäder U. (University of Bern) and Kober F. (NAGRA) (2016): "FEBEX-DP Dismantling of the heater 2 at the FEBEX "in situ" test. NAB 16-011Nagra, Wettingen.

Huertas F. (ENRESA); Fariñas P. (DM Iberia S.A.); Farias J. and García-Siñeriz J.L. (AITEMIN); Villar M.V., Fernández A.M. and Martín P.L (CIEMAT); Elorza F.J (UPM); Gens A., Sánchez M. and Lloret A. (UPC-DIT); Samper J. (UDC) and Martínez M.A. (SGS Technos S.A.). (2006) "Full-scale Engineered Barriers Experiment. UPDATED FINAL REPORT 1994-2004" December 2006. ENRESA, Technical Report 05-0/2006 [5].

Martínez V., Abós H. and García-Siñeriz J-L. (AITEMIN) (2016) FEBEX/FEBEX-DP: Final sensors data report. AN 16-019. March 2016.

Plötze, M. (2016): FEBEX-DP – Bentonite Characterization (ETH) AN 16 – 464.

Rey M., Bárcena I. & García-Siñeriz J.L. (2015): Full Dismantling Sampling Plan. Rev. 5. AITEMIN May 2015.

Sakaki, T. et al. FEBEX-DP Post-mortem analysis: TDR. NAB 16-021, Nagra, Wettingen. April 2016. AN 16-170, Nagra, Wettingen. April 2016.

Madina, V. (2016): Corrosion study of FEBEX-DP components. Nagra Arbeitsbericht NAB 16-054.

Wersin, P., Giroud, N., Kober, F. (2016): FEBEX-DP Corrosion Report. Nagra Arbeitsbericht NAB 16-016.

9 INSTRUMENTATION

9.1 INTRODUCTION

This annex is intended to provide the basic technical information about the instrumentation that was dismantled from FEBEX "in-situ" experiment.

9.2 SENSOR CODES

All sensors were coded as described below and the relevant codes for the dismantling are highlighted in bold font at tables.

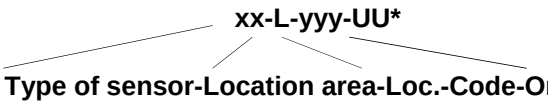

*Hyphen used to separate the codes could be removed to simplify the sensor description.

"xx" - TYPE OF SENSORS

T	**Temperature thermocouple**
P	**Total pressure**
Q	**Pore Pressure (bentonite)** or Hydraulic Pressure (borehole)
SH	**Heater displacement**
SB	**Bentonite block displacement**
S	**Displacement (general)**
3S	**Crackmeter/Fissurometer**
PP	Packer pressure
IT	Bentonite clinometer
GP	Gas pressure
GF	Gas flux
WC	**Water content (capacitive)**
WP	**Water content (psychrometer)**
WT	**Water content (TDR)**
AP	Absolute atmospheric pressure*
A	Anemometer*
V	Voltage meter*
C	Current meter*
Ω	Isolation meter*

*Not installed inside the test

"L" - TYPE OF LOCATION

A	service Area
B	Borehole (granite)
S	**Section (bentonite)**
H	**Heaters**
P	Power regulation unit (heaters)
R	spaRe

"yyy" - LOCATION CODE. This is the instrumented section in the FEBEX drift, where the sensor was placed, and it was: U, O, P, Q, G, H, I, R, S, M2, F2, E2, T, D2, L1 and B2 (updated after the partial dismantling made in 2002).

"UU" - ORDER NUMBER. This was given by the sensors installation sequence of each type of sensor in every specific section.

9.3 CHARACTERISTICS OF SENSORS

9.3.1 Temperature within the buffer and at the heater's surface (T code)

These sensors were located within the bentonite buffer and at the heater surface, having an operating temperature of up to 100 ºC. All of them were thermocouples type T class 1. Some sensors were manufactured by Watlow Gordon (UK) and the remaining ones by Cableries de Lens (FR). Their characteristics are given below (Table 31, 32, 33 and 34).

Table 31. Characteristics of thermocouples (Inconel 600)

Manufacturer	Watlow Gordon
Model	Type T
Measuring Principle	Thermocouple
Range	-200 ºC to 350 ºC
Accuracy	Class 1, 0.5 ºC
Dimensions	Ø 3 mm, length variable
Casing	INCONEL 600
Cable	Mineral insulated and transition to Teflon/PVC jacketed cable beyond the concrete plug
Cable protection	Not required
Cable output protection	Totally tight due to the mineral insulation

Table 32. List of thermocouples made of Inconel 600

SECTION	CODE
SD2	TSD2-03, 04, 05, 06, 11
SE2	TSE2-01, 02
SF2	TSF2-01 to 04
SI	TSI-03, 04, 05, 06, 11
SG	TSG-03, 04, 05, 06, 11
*SF1**	*TSF1-01 to 04*
*SE1**	*TSE1-01, 02*
*SD1**	*TSD1-03, 04, 05, 06, 11*

**Dismantled in 2002*

Table 33. Characteristics of thermocouples (AISI 304)

Manufacturer	Cableries de Lens
Model	Type T
Measuring Principle	Thermocouple
Range	-200 ºC to 350 ºC
Accuracy	Class 1, 0.5 ºC
Dimensions	Ø 3 mm, length variable
Casing	AISI 304
Cable	Mineral insulated and transition to Teflon/PVC jacketed cable beyond the concrete plug
Cable protection	Few were provided with Teflon jacket at the last 2 m (see table below)
Cable output protection	Totally tight due to the mineral insulation

Table 34. Thermocouples protected with Teflon

SECTION	CODE
SB2	TSB2-02, 03, 04, 05, 08
SD2	TSD2-02, 07, 08, 12
SI	TSI-02, 07, 08, 12
SG	TSG-02, 07, 08, 12
*SD1**	*TSD1-02, 07, 08, 12*
*SB1**	*TSB1-02, 03, 04, 05, 08*

**Dismantled in 2002*

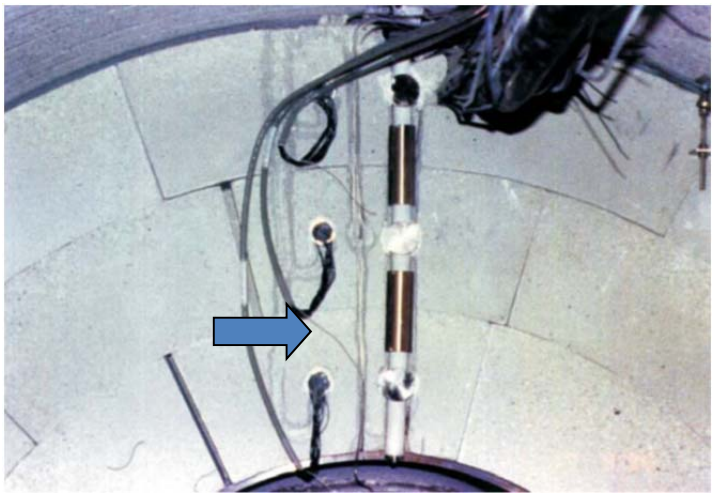

Figure 115: Example of installed thermocouples

9.3.2 Total Pressure cells (P code)

These are Geokon N.A.T.M. (New Australian Tunnelling Method) shotcrete stress cells model 4580-2, which consists of two rectangular steel plates welded together around the periphery, with a de-aired fluid occupying the space between the plates. When the sensor is installed on a rigid surface it registers load on one side of the cell. This model was selected to measure total pressure at bentonite/rock wall or bentonite/liner interfaces. The internal fluid is connected to a vibrating wire type pressure transducer. The technical details of the sensor are summarised in Table 35.

Table 35. Characteristics of total pressure cell Geokon 4580-2

Manufacturer	GEOKON
Model	4580-2-6MPa NATM stress cell custom made
Measurement principle	Vibrating Wire
Range	0 to 6 MPa
Over range capacity	150 % F.S. (max)
Excitation	1400-3500 Hz
Output	2000-3000 Hz
Resolution	1.5 KPa
Fluid	Mercury
Precision	0.5% F.S.
Thermal Effect on Zero	0.025% F.S./ºC
Temperature compensation	Thermistor YSI 44005, range -80 to 150ºC, accuracy ±0.5 ºC
Weight	2 kg
Calibration	Linear formula vs. digits and temperature
Case material	AISI 316 Stainless steel
Operating Temperature	0 ºC to 150 ºC
Dimensions	150 x 250 x 6 (mm)
Pinch tube	1 meter
Cable	4 Cu wires 0.25 mm^2, PTFE jacketed. Halar jacketed cable. Outer diameter 6 mm. Operating Temperature: 0 -125 ºC
Cable connection	Gas tight
Sensor protection	Concrete

Figure 116. Installed NATM stress cell

Three additional total pressure sensors (PSP-01, 02 and PSG-01) were installed within the bentonite buffer during the partial dismantling and all of them were vibrating wire type too from GEOKON but model 4810. This “Fat Back” Pressure Cell is intended to measure contact earth pressures on the surface of concrete or steel structures. The cell has an extra thick backplate to minimize any point loading effects. ‘Ears’ on the cell help to hold the cell to concrete forms or to retaining walls during installation. The technical details of the sensor are summarised in Table 36.

Table 36. Characteristics of total pressure cell Geokon 4810-7

Manufacturer	GEOKON
Model	4810-7
Measurement principle	Vibrating Wire
Range	0 to 7 MPa
Over range capacity	150% F.S. (max)
Excitation	1400-3500 Hz
Output	2000-3000 Hz
Resolution	0.025% F.S.
Fluid	Oil
Accuracy	0.1% F.S. with polynomial expression
Temperature compensation	Thermistor YSI 44005, range -80 to 150ºC, accuracy ±0.5 ºC
Weight	2.3 kg
Calibration	Polynomial formula vs digits and temperature
Case material	AISI 316 Stainless steel
Operating Temperature	0 ºC to 80 ºC
Dimensions	230 mm OD
Cable	4 Cu twisted wires, PUR jacketed. Outer diameter 0.125”. Operating Temperature: 0 to 80 ºC
Cable connection	Gas tight

Figure 117: “Fat Back” Pressure Cell

Two total pressure sensors (PSO-01 and 02) were installed between both sections of the new concrete plug after the partial dismantling. They were solid state silicon pressure transducer (4-active semiconductor strain gages) coupled to a fluid filled diaphragm from KULITE (US). The technical details of the sensor are summarised in Table 37.

Table 37. Characteristics of total pressure cell kulite 0234

Manufacturer	KULITE
Model	0234 (special version)
Measurement principle	4-active semiconductor strain gages
Range	80 Bar
Over range capacity	200% F.S. (max)
Excitation	10 V
Output	0-100 mV
Resolution	Infinitesimal
Fluid	Silicone
Accuracy	Less than 1% F.S.
Weight	250 g
Case material	AISI 316 Stainless steel
Operating Temperature	0 ºC to 150 ºC
Dimensions	O.D. 55 mm, 17 mm thick
Cable	4 wires, Teflon insulation
Cable connection	Gas tight epoxy potted

Figure 118. KULITE pressure cell

9.3.3 Pore pressure sensors (Q code)

These are vibrating wire Geokon pore pressure sensors model 4500 HT-5, which are high temperature piezometers designed to monitor downhole pressures and temperatures in oil recovery systems and geothermal applications, where the temperature may be as high as 250°C. The technical details of the sensor are summarised in Table 38.

Table 38. Characteristics of pore pressure sensors Geokon 4500 HT-5

Manufacturer	GEOKON
Model	4500 HT-5 piezometer
Measurement principle	Vibrating Wire
Range	0 to 5 MPa
Over range capacity	200 % F.S. (max.)
Output	1400-3500 Hz
Resolution	1.25 KPa
Precision	0.5% F.S.
Thermal Effect on Zero	0.02% F.S./ºC
Temperature compensation	Thermistor YSI 44005, range -80 to 150ºC, accuracy ±0.5 ºC
Calibration	Linear formula vs digits and temperature
Weight	0,12 kg
Case material	AISI 316 Stainless steel
Operating Temperature	0 ºC to 150 ºC
Dimensions	Ø25.4x127 (mm)
Filter	Ceramic 2 microns
Cable	4 Cu wires 0.25 mm^2, PTFE jacketed. Halar jacketed cable. Outer diameter 6 mm. Operating Temperature: 0 -125 ºC
Cable connection	Gas tight
Sensor protection	None

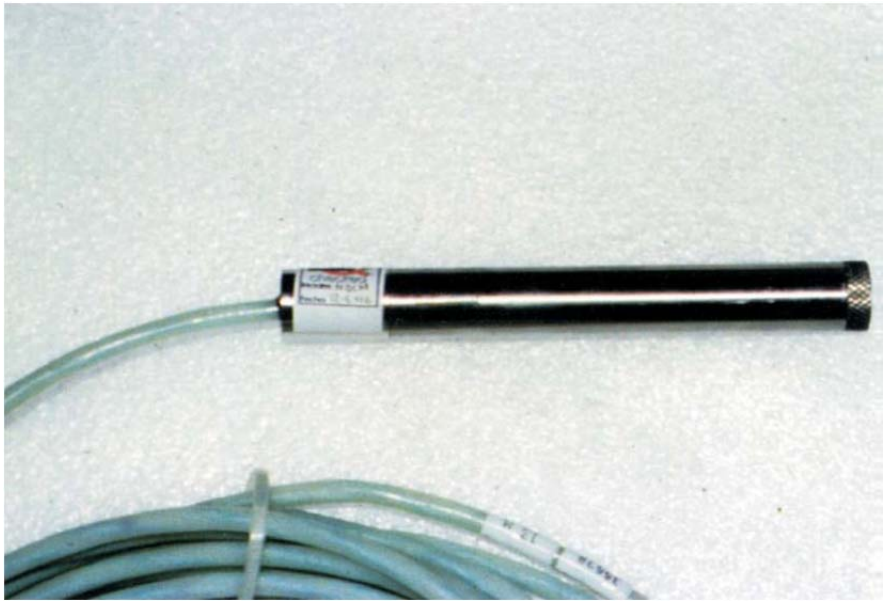

Figure 119. Installed piezometer 4500 HT

9.3.4 Heater extensometers (SH code)

These are Geokon vibrating wire deformation meters model 4430 provided with flanged ends and designed to measure longitudinal deformation in dams and embankments. It can also be grouted or held in place by hydraulic anchors to measure deformations in boreholes. This sensor was selected for measuring the movements of the heaters with respect to the rock walls. The technical details of the sensor are summarised in Table 39.

Table 39. Characteristics of heater extensometers Geokon 4430

Manufacturer	GEOKON
Model	4430 deformation meter
Measurement principle	Vibrating Wire
Range	0 to 150 mm
Output	1400-3500 Hz
Resolution	0.02 mm.
Precision	0.2% F.S.
Thermal Effect on Zero	0.03% - ½ F.S./ºC
Temperature compensation	Thermistor YSI 44005, range -80 to 150ºC, accuracy ±0.5 ºC
Calibration	Linear formula vs digits and temperature
Case material	AISI 316 Stainless steel
Operating Temperature	0 ºC to 150 ºC
Dimensions	Ø50 x 400 (mm)
Cable	4 Cu wires 0.25 mm^2, PTFE jacketed. Halar jacketed cable. Outer diameter 6 mm. Operating Temperature: 0 -125 ºC
Cable connection	Gas tight
Sensor protection	None

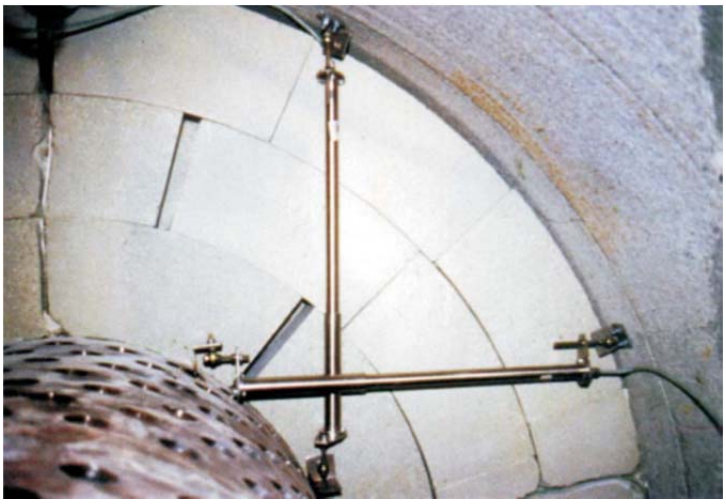

Figure 120. Installed heater extensometers 4430

9.3.5 Bentonite extensometers (SB code)

These are the same Geokon vibrating wire deformation meters model 4430 as in the previous case (SH code) but with a shorter range. The technical details of the sensor are summarised in Table 40.

Table 40. Characteristics of bentonite extensometers Geokon 4430

Manufacturer	GEOKON
Model	4430 deformation meter
Measurement principle	Vibrating Wire
Range	0 to 100 mm
Output	1400-3500 Hz
Resolution	0.02 mm.
Precision	0.2% F.S.
Thermal Effect on Zero	0.03% - ½ F.S./ºC
Temperature compensation	Thermistor YSI 44005, range -80 to 150ºC, accuracy ±0.5 ºC
Case material	AISI 316 Stainless steel
Calibration	Linear formula vs digits and temperature
Operating Temperature	0 ºC to 150 ºC
Dimensions	Ø50x440 (mm)
Cable	4 Cu wires 0.25 mm^2, PTFE jacketed. Halar jacketed cable. Outer diameter 6 mm. Operating Temperature: 0 -125 ºC
Cable connection	Gas tight
Sensor protection	None
End plates	Provided with end plates to confine a bentonite block

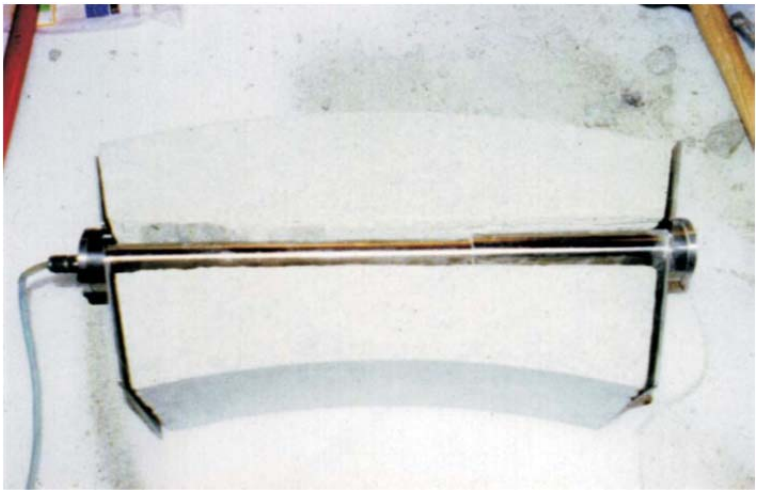

Figure 121. Installed bentonite deformation meter 4430

9.3.6 Plug extensometers (SP code)

These sensors were heavy-duty DC operated gauge heads allowing a good performance in environments containing moisture, dirt, and fluid contaminants that need to be installed in the accessible surface of the concrete plug. They were installed after the partial dismantling. These gage heads were spring loaded LVDTs (Linear Variable Differential Transformers) with precision linear bearings and internal conditioning electronics. The technical details of the sensor are summarised in Table 41.

Table 41. Characteristics of plug extensometers Schaevitz GDC-121-500

Manufacturer	SCHAEVITZ
Model	GDC-121-500
Measurement principle	LVDT
Range	±0.5”
Output	±10 V
Repeatability	6 microns
Stability	0.125% of FSO after warm up
Non-linearity	±0.25% of FR, maximum
Case material	AISI 400 Series stainless steel
Operating Temperature	0 °C to 70 °C
Dimensions	Ø19 x150 (mm)
Cable connection	6-pin MS type connector (MIL-C-5015)
Sensor protection	IP68 to 1,000 PSI [70 bars] with use of proper mating connector plug

Figure 122. Installed LVDT plug extensometer

9.3.7 Water content (capacitive) and temperature in the buffer (Code WC)

These sensors were installed within the bentonite blocks to measure the natural wetting process. The sensor used was a special relative humidity (RH) sensor from ROTRONIC (CH) and provided by ANDRA. This sensor provides both relative humidity and temperature readings. The conditioning electronic board was located beyond the concrete plug. The sensing element was mechanically protected with a stainless steel filter. The main features are in Table 42.

Table 42. Characteristics of relative humidity sensors Rotronic

Manufacturer/Model	ROTRONIC AG/ Special for ANDRA based on model I-420T22WFC1FxxT
Measurement principle	Capacitive
Relative humidity range	0 % to 100% R.H. (not condensing)
Temperature range	0 ºC to 100 ºC (PT100)
Operating Temperature range	-55 ºC to 125 ºC
Output from conditioning electronics	4-20 mA (R.H) & 4-20mA (ºC)
Accuracy	±1% RH between 0 to 80% and 1.5% above Better than ±0.5ºC
Dimensions	Diameter: 15 mm; Length: 125 mm
Head casing material	SS304 with sintered stainless steel filter 316L, 5 microns
Cable	PUR jacketed, range -55 to 120 ºC. Up to 100 m in length
Nº of wires	5 + screen, Polyester jacketed
Diameter of cable	5 mm
Cable protection	3 m of thermo-retractable INSULSITE HFT-333 and Epoxy
Electronics: Temperature range	-20 ºC to 50 ºC

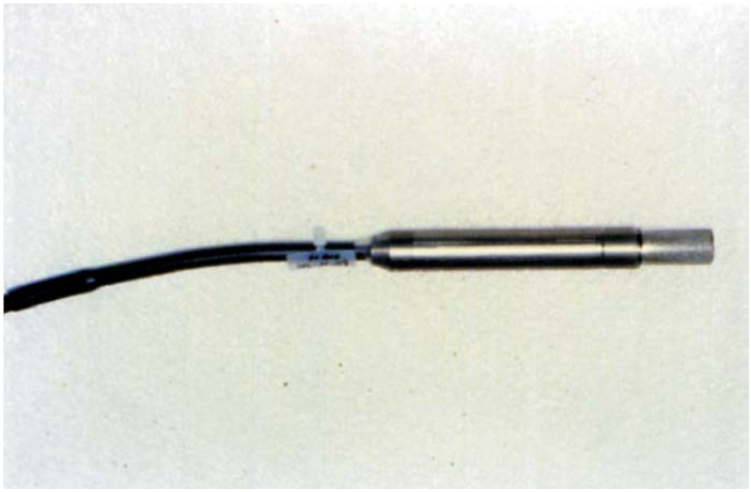

Figure 123. Installed Rotronic sensor

Additional RH sensors were installed within the bentonite buffer during the partial dismantling, three directly within the buffer (WCSQ-01, 02 and 03) and some more within the so called instrumented pipes. All of them were made by Vaisala Oyj (FI) with the characteristics given in Table 43.

Table 43. Characteristics of relative humidity sensors Vaisala HMP237

Manufacturer/Model	VAISALA/ HMP237
Measurement principle	Capacitive + Pt 100 RTD 1/3 Class B IEC 751
Relative humidity range	0 % to 100 % R.H. (not condensing)
Temperature range	0 ºC to 180 ºC
Operating Temperature range	-40 to +180 °C
Output from conditioning electronics	4-20 mA (R.H.) & 4-20 mA (ºC)
Accuracy	±1 %RH (0...90 %RH) ±2 %RH (90...100 %RH) Better than ±0.1ºC
Dimensions	Diameter: 13.5 mm; Length: 64 mm
Head casing material	SS316 with sintered filter, stainless steel, 5 microns, Ø 13.5 mm
Cable	PUR jacketed, range -55 to 120 ºC.
Nº of wires	Coaxial + screen
Length and diameter of cable	10 m and 5.5 mm
Electronics: Temperature range	0 ºC to 50 ºC

Figure 124: HR sensor and conditioning electronics

9.3.8 Water content (suction) and temperature in the buffer (Code WP)

In thermocouple psychrometry, the temperature depression of the sensing (wet) junction that is measured relative to the reference (dry) junction varies as a function of the relative humidity of air surrounding the sensing junction. A thermocouple is a double junction of two dissimilar metals. When the two junctions are subject to different temperatures, they generate a voltage difference (Seebeck effect). One junction of the thermocouple is suspended in a thin-walled porous ceramic or stainless screen cup in contact with the material, while another is embedded in an insulated plug to measure the ambient temperature at the same location.

Wescor Psychrometers were used to measure within a relative range of 95.5 to 99.96% RH that means suction from 6200 to 50 kPa. They can be measured using the dew-point or psychrometric methods (first one is more sensible) and their accuracy is around ±3%. Thermocouple psychrometers are very sensitive to fluctuations of environmental temperature. The main features are in Table 44.

Table 44. Characteristics of psychrometers Wescor PST-55

Manufacturer/Model	WESCOR /type PST-55
Temperature range	-200/350 °C
Humidity range	95 % RH to 99.96 % RH
Suction range	50 to 6200 kPa
Output signal	Two analogue outputs (µV). 0.47 µV/bar
Filter	Ceramic filter
Probe material	Teflon-vinyl
Cable connection	Welded and epoxy sealed
Nº of wires	1 cable with 3 conductors, PVC insulation
Diameter of cable	3.8 mm
Body dimensions*	Diameter 16 mm, length 124 mm
Cable protection	Teflon tubing 4 mm O.D.
Measuring method	Psychrometric
Conditioning electronics	Campbell CR7
External electronic unit operating temperature range	-40/45 °C

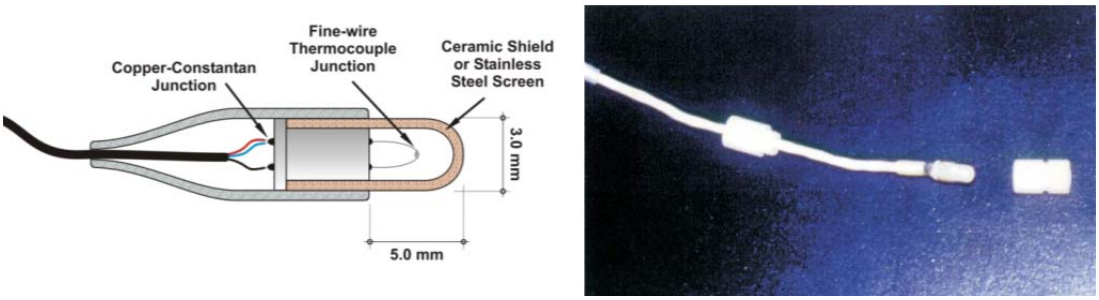

Figure 125. Wescor sensor

9.3.9 Volumetric water content (Code WT)

These sensors estimate water content by measuring the bulk permittivity (or dielectric constant), which determines the velocity of an electromagnetic wave or pulse through the measured material. The relationship between the permittivity and the water content depends on the electromagnetic wave frequency sent by the specific monitoring device and usually requires a specific calibration. They use empirically-calibrated relationships between volumetric water content and the sensor output signal (time, frequency, impedance, wave phase). In principle a TDR could cover the whole range of volumetric content in the bentonite buffer with accuracy depending on the calibration made.

Table 45. Characteristics of TDR water content sensors

Manufacturer/ Model	Eddi Meier + Partner AG/Febex-bentonite
Range	All volumetric water content
Accuracy	Depending on calibration
Temperature range	0 to 100 °C (operation)
Output	Reflectograms
Output temperature	PTC Siemens KTY 10-62, range 0 to 150 ºC, accuracy 0.5 %
Sensor dimensions	500 mm x 22 mm (L x Ø)
Case material	Two copper foils of 470 mm x 10 mm x 0.6 mm (L x W x T) on PTFE rod of 20 mm OD coated with polyolefin shrinkable tube
TDR Cable	Coax RG213
PTC cable	RG108 (75 Ohm, twisted-pair cable) 6 mm OD
Cable connection	Epoxy potted output
Cable protection	Shrinkable sleeve from metre
Conditioning electronics	Based on Tektronix 1502C TDR cable tester + CR10 data logger

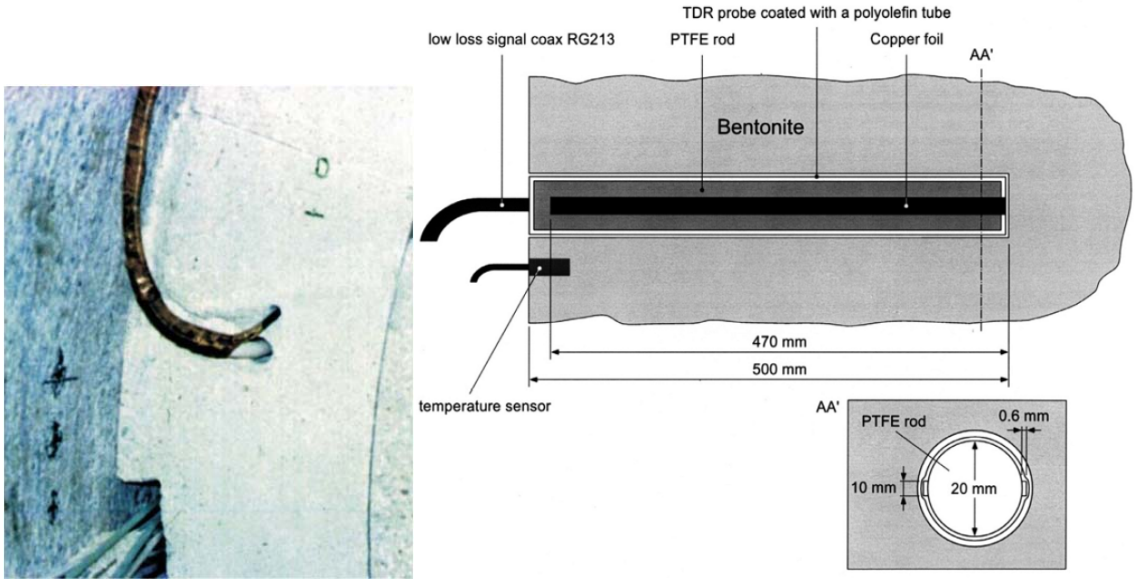

Figure 126. Installed bentonite TDR and PTC

9.3.10 Crackmeter (Code 3S)

A tri-axial crackmeter of high resolution, provided by G.3S (FR) was installed in an existing granite fracture in the zone near the centre of Heater #2. It was intended to measure the possible displacement of the edges of the fracture as a result of thermal effects or swelling of the bentonite.

Table 46. Characteristics of Crack meter G.3S

Manufacturer/ Model	G.3S / Fisurometer (3 x LVDT sensors)
Displacement sensors	RDP D5/100 AW
Range	±2.5 mm, displacement on X, Y and Z.
Accuracy	Better than 0.3%
Temperature range	-20 to 125 ºC, temperature calibration 24 to 74 °C
Conditioning electronics	3xRDP-S7AC, Included in the case
Output	±2.5 V
Output temperature	PT 100
Sensor dimensions	66 +12.5 mm x 9.5 mm (L x Ø)
Case dimensions	220 x 200 x 200 mm
LVDT supports material	SS316
Case material	Steel E24
Cable	16 wires of 0.34 mm^2 Hytrel jacketed + screen. Cable jacket in PUR+ECTFE with 9.1 mm OD
Cable connection	Welded and cable gland

Figure 127. Installed LVDT sensors

Figure 128. Installation details